5-2014

Multi-cycle Boiling Water Reactor Fuel Cycle Optimization

Keith Everette Ottinger
University of Tennessee - Knoxville, kottinge@utk.edu

To the Graduate Council:

I am submitting herewith a dissertation written by Keith Everette Ottinger entitled "Multi-cycle Boiling Water Reactor Fuel Cycle Optimization." I have examined the final electronic copy of this dissertation for form and content and recommend that it be accepted in partial fulfillment of the requirements for the degree of Doctor of Philosophy, with a major in Nuclear Engineering.

G. Ivan Maldonado, Major Professor

We have read this dissertation and recommend its acceptance:

Arthur E. Ruggles, Ronald E. Pevey, James A. Ostrowski

Accepted for the Council:

Carolyn R. Hodges

Vice Provost and Dean of the Graduate School

(Original signatures are on file with official student records.)

Multi-cycle Boiling Water Reactor Fuel Cycle Optimization

A Dissertation Presented for the
Doctor of Philosophy
Degree
The University of Tennessee, Knoxville

Keith Everette Ottinger
May 2014

ABSTRACT

A multi-cycle nuclear fuel cycle optimization code, BWROPT (Boiling Water Reactor OPTimization), has been developed. BWROPT uses the Parallel Simulated Annealing (PSA) algorithm to solve the coupled out-of-core and in-core optimization problems. There are two depletion methods used for the in-core optimization: the Haling depletion and a Control Rod Pattern (CRP) search. The result of this optimization is the optimum new fuel inventory and the core loading pattern for the first cycle considered in the optimization. Several changes were made to the optimization algorithm with respect to other nuclear fuel cycle optimization codes that use PSA. Instead of using constant sampling probabilities for the solution perturbation types throughout the optimization, as is usually done, the sampling probabilities can be varied to get a better solution and/or decrease runtime. Also, the new fuel types available for use can be sorted into an array based on any parameter so that each parameter can be incremented or decremented. In addition several evaluations were performed to test the CRP search option.

Using the variable sampling probabilities was found to produce slightly better results in less time than the standard method of having constant sampling probabilities. Performing ordered and random sampling of the new fuel types using the new fuel type array was found to yield slightly better solutions on average than random sampling alone, but with a somewhat higher runtime. Using variable length Markov chains for optimizations in which a CRP search is performed for the first cycle and the Haling depletion is used for the remaining cycles was found to increase CPU utilization by 33%. Starting the CRP search with the CRP determined for the previous solution was found to be better than starting the CRP search with all of the rods fully withdrawn. Using the CRP search in an optimization was slow and produced inferior results compared to using the Haling depletion, indicating the need for more work in this area.

TABLE OF CONTENTS

LIST OF TABLES

LIST OF FIGURES

LIST OF ABBREVIATIONS

AAE	Assembly average exposure
ARO	All rods out
BOC	Beginning of cycle
BP	Burnable poison
BWR	Boiling water reactor
CCC	Control cell core
CPR	Critical power ratio
CPU	Central processing unit
CR	Control rod
CRP	Control rod pattern
CS	Cooling step
CVC	Conventional core
EOC	End of cycle
EPRI	Electric power research institute
EXP	Exposure
FCC	Fuel cycle cost
GWD	Gigawatt day
HEM	Homogeneous equilibrium mixture
HPD	Haling power distribution
LP	Loading pattern
OF	Objective function
MTU	Metric ton uranium
MTHM	Metric ton heavy metal
PB2	Peach Bottom 2
PSA	Parallel simulated annealing
PWR	Pressurized water reactor
ROI	Region of influence
RPF	Relative power fraction
RSICC	Radiation safety information computational center
SA	Simulated annealing
SWU	Separative work unit
T2N	Triton to NESTLE

Chapter 1 Introduction

The efficient and safe operation of nuclear power reactors has been a high priority ever since the first reactor was built. This concern has led to much effort being exhausted optimizing the fuel cycles of nuclear reactors. Traditionally, the task of fuel cycle optimization has been split into two parts, out-of-core and in-core. In the out-of-core step the size and approximate enrichment of the new fuel batches are determined so that the cycle energy demand can be met for many (typically 5 or more) additional cycles. Out-of-core optimization also includes the selection of previously exposed fuel assemblies to be used in the next cycle. In-core optimization determines the design of the new fuel batches, the location of each fuel bundle, and the operating strategy, which for Boiling Water Reactors (BWRs) entails the determination of control rod positions, rod sequence exchanges (blade selection and duration of sequence), and core flow during each sequence. [1, 2]

Though the out-of-core and in-core optimizations are generally done separately they are inherently coupled and in recent years there have been efforts to combine the out-of-core and in-core optimizations, particularly for Pressurized Water Reactors (PWRs). The coupled optimization takes all of the variables and constraints into account at the same time and, thus, should be able to produce better results than the individual "decoupled" optimizations. However, because the out-of-core optimization is multi-cycle in nature the coupled optimization requires solving the in-core optimization for several cycles at the same time. If a high fidelity core simulator is used this requirement makes the coupled optimization very computationally intensive necessitating the use of parallel programming and computer architectures. [2]

In this work the development of a new computer code, BWROPT (Boiling Water Reactor OPTimization), is described. BWROPT uses the popular Parallel Simulated Annealing (PSA) algorithm [3] to solve the combined out-of-core and in-core fuel cycle optimization problem.

In Chapter 2 a literature review of existing fuel cycle optimization codes is presented. The information gathered in the literature was used as the starting point for the development of a new BWR fuel cycle optimization code described in Chapter 3. Chapter 4 describes the model and test cases used to evaluate BWROPT, and in Chapter 5 the results of these evaluations are given. In the final chapter conclusions and future work applicable to this research are discussed.

Chapter 2 Literature Review

Many computer codes have been developed to improve the efficiency and safety of nuclear power reactors. In the next section the features of several well-known and respected BWR fuel cycle optimization codes are discussed. This is followed by discussions of multi-cycle fuel cycle optimization codes and control rod pattern search algorithms.

2.1 BWR Fuel Cycle Optimization Codes

2.1.1 FORMOSA-B

FORMOSA-B, a code developed at North Carolina State University (NCSU), was an early BWR in-core fuel cycle optimization code that originally used the Simulated Annealing (SA) [4] optimization algorithm [5]. The initial version optimized the fuel assembly Loading Pattern (LP) for a single cycle using the following constraints: Linear Heat Generation Rate (LHGR), Average Planar LHGR (APLHGR), Critical Power Ratio (CPR), Cold ShutDown Margin (CSDM), octant power tilt, node discharge burnup, assembly discharge burnup, region average discharge burnup, region/batch power sharing, and End Of Cycle (EOC) k_{eff}. One interesting feature of the alogirthm was the use of adaptive penalty functions for constraint violations that increase the weighting of the the constraints as the algorithm approaches convergnce. Later the ability to perform Control Rod Pattern (CRP) optimization using heuristic rules (experience-based constraints that are applied to reduce the runtime of the optimization or improve solution quality) was added to the code. When combined CRP-LP optimization is performed the CRP is updated after a user-specified number of LP samples have occurred. The

number of iterations allowed for the CRP optimization to find a new CRP is limited so that the code does not spend too long looking for an acceptable CRP when one may not exist. [5, 6] FORMOSA-B was recently updated to use PSA with OpenMP parallel communication, which significantly reduced runtime while producing results comparable to the nonparallel version [7].

2.1.2 ePrometheus

The ePrometheus code, developed at Global Nuclear Fuel (GNF), is another in-core optimization code for BWRs. The decision variables used in ePrometheus are: exposed fuel loading pattern, fresh bundle design, control blade placements, core flow, and control blade sequence exchange times. The constraints considered and their units and dimensions used in the Objective Function (OF) calculation are listed in Table 2.1. A Tabu search [8] based algorithm is used to perform the optimization and cases are run on a computational server in parallel. The first step in the algorithm is generating a response surface from perturbation calculations of each variable in the current solution. This response surface is then used to estimate the OF of all solutions in the neighborhood of the current solution (reachable by changing any single variable in the current solution) that are not tabu (require a variable change that has been used within a user specified number of iterations). The solutions with the highest estimated OFs are then evaluated with a core simulator to determine the actual best solution. The process of finding new best solutions via estimation of OFs with the response surface and core simulator evaluations is repeated for a user specified number of iterations or until no new solution is found at which point the response surface is updated and the optimization continues. The stopping criterion for the algorithm is a user specified number of response surface updates. [9, 10]

Table 2.1 List of constraints available in the GNF ePrometheus optimization code [9].

Number	Constraint	Units	Dimension
1	> Minimum cycle length	MWD/sT	0
2	< Maximum average MAPRAT over the cycle	none	0
3	< Maximum average MFLPD over the cycle	none	0
4	< Maximum average MFLCPR over the cycle	none	0
5	< Maximum hot excess slope throughout the cycle	%/(MWD/sT)	0
6	> Minimum hot excess at 200 MWD/sT	%	0
7	< Eigenvalue tolerance at EOC above target	none	0
8	> Eigenvalue tolerance at EOC below target	none	0
9	< Eigenvalue tolerance above target throughout cycle	none	1
10	> Eigenvalue tolerance below target throughout cycle	none	1
11	> Minimum flow value throughout cycle	%	1
12	< Maximum flow value throughout cycle	%	1
13	< Maximum hot excess throughout cycle	%	1
14	< Maximum SLCS margin throughout cycle	%	1
15	> Minimum core average void fraction throughout cycle	none	1
16	< Maximum core average void fraction throughout cycle	none	1
17	> Minimum axial void tilt throughout cycle	none	1
18	< Maximum axial void tilt throughout cycle	none	1
19	> Minimum axial power tilt throughout cycle	none	1
20	< Maximum axial power tilt throughout cycle	none	1
21	> Minimum axial power peak throughout cycle	none	2
22	< Maximum axial power peak throughout cycle	none	2
23	< Maximum cold shutdown margin	%	3
24	< Maximum integrated power	none	3
25	< Maximum MFLCPR throughout cycle	none	3
26	< Maximum MAPRAT throughout cycle	none	4
27	< Maximum MFLPD throughout cycle	none	4
28	< Maximum NEXRAT at EOC	none	4
29	< Maximum bundle average exposure at EOC	MWD/sT	2
30	< Maximum number of unique pin types	none	0
31	> Minimum fresh U^{235} efficiency	(MWD/sT)/(kg-U^{235})	0

2.1.3 OCOTH

OCOTH, created by Ortiz et al. [11], also solves the in-core optimization problem for BWRs. The code uses an iterative process reminiscent of that used in FORMOSA-B. A flow chart of OCOTH is provided in Figure 2.1 below. OCOTH starts by using RENOR, a recurrent neural network, to determine an initial optimized LP based on Haling's principle, which states: the minimum power peaking achievable for any given EOC state is attainable only by having a constant power profile throughout the cycle [12]. The neural network is an empirical model created by fitting LP data from other cycles [13]. After the initial LP is created an optimum CRP

is calculated for this LP using Azcatl-CRP [14], an ant colony code [15], which performs a heuristic search in which good solutions are reinforced and bad solutions are forgotten. Another LP generation code, RECOPIA, uses a genetic algorithm to determine an optimum LP based on the CRP generated in the previous step. Genetic algorithms like the ant colony algorithm reinforce good changes while discarding bad changes but use an evolution like algorithm [16]. The process of finding optimum CRPs and LPs is iterated until a stopping criterion is met. The CRP generation and LP design with RECOPIA have their own OF which each use some of the following constraints: Beginning Of Cycle (BOC) Cold ShutDown Margin, keff, axial power distribution, CPR, LHGR, power density, and hot excess reactivity. [11]

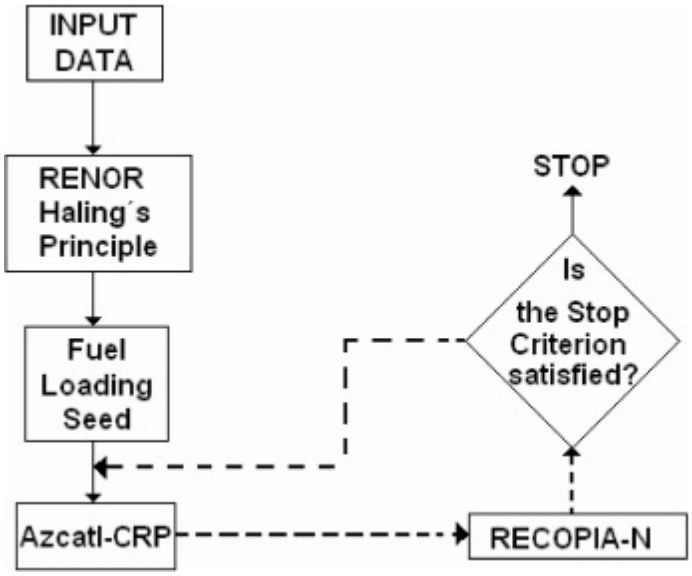

Figure 2.1 – OCOTH flow chart [11].

2.2 Multi-cycle Fuel Cycle Optimization Codes

Several multi-cycle fuel cycle optimization codes have been developed for PWRs but the author knows of none for BWRs. One early example of a PWR multi-cycle code was developed

by Yamamoto et al. [17] to solve the in-core optimization for two successive cycles using SA and a simplified core simulator to reduce runtime. The OCEON-P code, developed at NCSU, solves the out-of-core problem for multiple cycles using the PSA algorithm and SIMULATE 3 core simulator. OCEON-P also has some in-core optimization elements such as LP selection from multiple user specified LPs. One interesting feature of OCEON-P is that after each cycle simulation is run the code estimates the OF, and if it appears unlikely the solution will be accepted rejects it avoiding the simulation of the remaining cycles. [18, 19, 20] Studsvik's multi-cycle PWR fuel cycle optimization code, COPERNICUS, solves both the out-of-core and in-core problems simultaneously. Like OCEON-P, COPERNICUS uses the PSA algorithm and SIMULATE-3 core simulator. [2]

2.3 Control Rod Pattern Search Algorithms

The Control Rods (CRs) in a BWR are used to control the reactivity and power shape of the reactor. A CRP defines the position/movement of each CR at every point in a cycle. Actual CRPs used in operating reactors are still created by engineers with years of experience; however, there have been many studies of developing long-term CRPs with computer programs. Long-term CRPs are much coarser than actual CRPs and consist of the CR positions at BOC, EOC, and at user specified depletion steps. For example, an 11 GWD/MTU cycle with a user input depletion step of 2 GWD/MTU would entail CRPs be generated at the following depletions: 0, 2, 4, 6, 8, 10, and 11 GWD/MTU. The purpose of long-term CRPs is to serve as an aid in developing an actual CRP and/or to determine the feasibility of a LP by determining the feasibility of generating a CRP that would eliminate constraint violations for the LP.

There are two main strategies for control rod movement in BWR operation: ConVentional Core (CVC) and Control Cell Core (CCC). In CVC operation the Control Rods (CRs) in the core are divided into two groups A and B which are divided into subgroups 1 and 2. This creates a total of four groups which are arranged in the reactor core according to the pattern shown in Figure 2.2. During normal reactor operation only one of these groups is used at a time and they are generally alternated throughout the cycle in the following order: A1, B2, A2, B1, A1, … (starting group can vary). In CCC operation a single CR group is selected and used for reactivity control throughout the entire cycle. [21, 6]

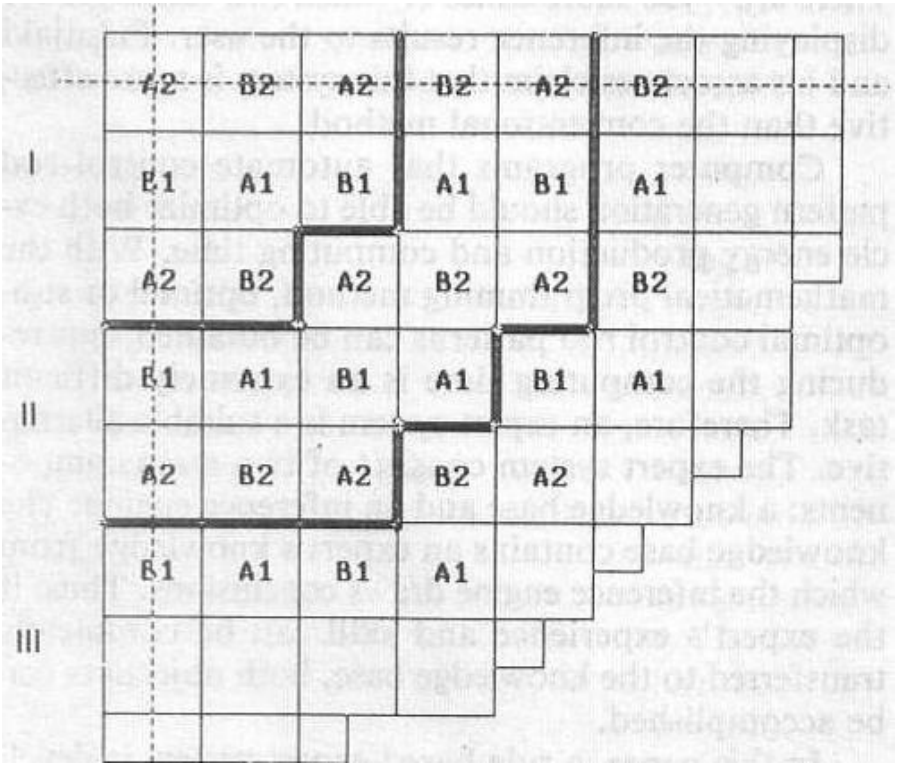

Figure 2.2 - Arrangement of CVC Control Rod Groups in a Quarter Reactor Core (Each CR Box Covers a 2x2 Grid of Assemblies) [21].

Typical computer programs that generate long-term CRPs rely on heuristic rules. These programs can be divided into two categories: indirect, which try to find a CRP that approximates

a target power distribution, and direct, which try to eliminate constraint violations and maximize core life without fitting a target power distribution. Often the target power distribution used for indirect CRP searches is the Haling Power Distribution (HPD), the power distribution obtained using Haling's principle, or a modified version of the HPD. [22] Direct CRP search algorithms often consider the power shape through constraints summary statistics such as thermal limits or power peaking or by attempting to maximize the cycle length. Because only about a quarter of the CRs are used at once it is common to define a Region Of Influence (ROI) for each CR as shown in Figure 2.3. Control rods in BWRs are referred to as "cruciform" because their radial cross section is shaped like a plus sign and they are inserted between fuel bundles so their "blades" directly border four assemblies. These neighboring assemblies are the most affected by the CR, followed by the assemblies face adjacent to these, and the least affected are the corner adjacent assemblies. This definition of the ROI allows each of the four CVC groups to cover the entire core with the exception of some of the edge assemblies which typically do not require CR insertions during normal operation. This, however, does not guarantee that constraint violation can be eliminated everywhere in the core with only one CVC group. [21, 6]

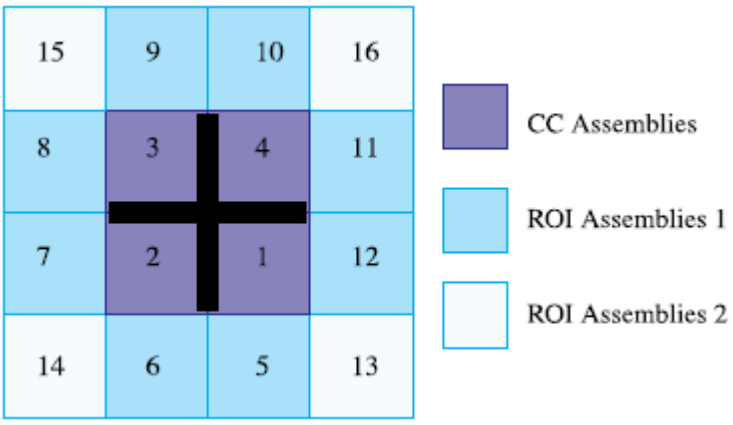

Figure 2.3 – Location of Regions of Influence for a CR [6].

Chapter 3 Optimization Algorithm

In this chapter the optimization algorithm for BWROPT; a new, multi-cycle, out-of-core and in-core, BWR fuel cycle optimization code; is described. BWROPT is written in FORTRAN and the parallel communication is done with MPI enabling the code to run on large clusters which reduce runtimes and/or allow for more exhaustive searches. In BWROPT the new fuel inventory (including total new assemblies, batch size, and batch design), LP, and CRP are varied simultaneously to find a near optimum new fuel inventory, and corresponding LP and CRP combination(s). The optimization algorithm used is PSA which is described in detail in the next section. This is followed by a description of the depletion methods used for evaluating LPs including CRP search and some new features not found in similar optimizations.

3.1 Parallel Simulated Annealing

3.1.1 Introduction

Parallel simulated annealing is a generic term used to described multi-process versions of the SA algorithm developed by Kirkpatrick et al [4] which itself is based on the Metropolis algorithm [23]. The name simulated annealing is an analogy to annealing in metallurgy, in which metal is heated to a very high temperature and then cooled slowly. The heating breaks down the initial structure of the metal and the slow cooling allows for defects in the metal to be corrected producing a low energy state final product. In SA an effective temperature variable is used to control the speed of convergence of the algorithm. The PSA implementation used in this research is PSA by mixing of states developed by Chu et al [3] as described by Kropaczek [24] with some variations. A flow chart of the algorithm is included below as Figure 3.1.

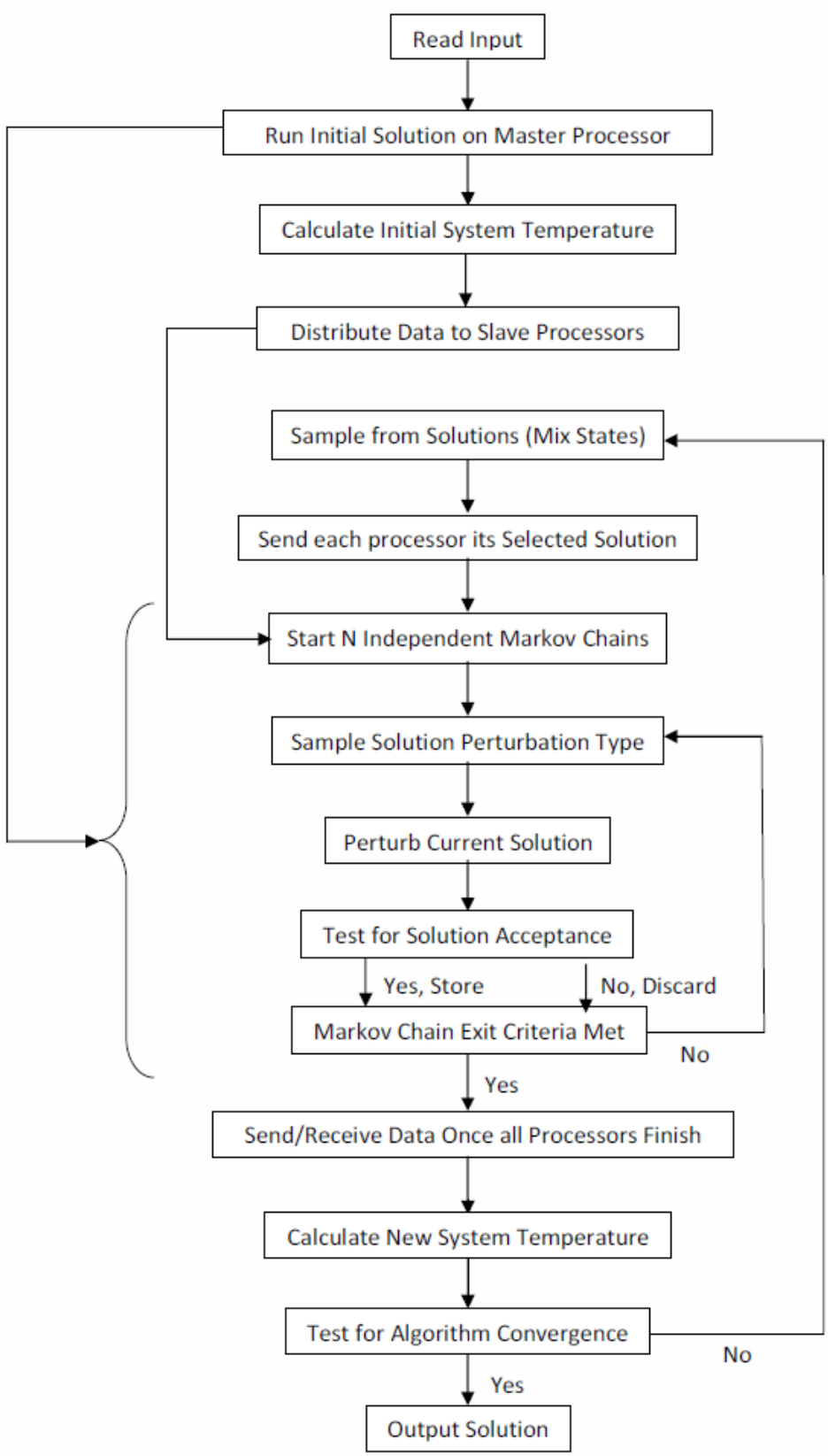

Figure 3.1 – Flow chart of PSA by mixing of states algorithm as implemented in BWROPT.

3.1.2 Initialization

The PSA algorithm starts by running an initialization to determine the standard deviation of the OF. The initialization consists of generating a series of solutions (a "solution" constitutes all the information necessary to generate the input file(s) for each cycle being optimized) by randomly changing the previous solution, analyzing the new solutions with a core simulator (the computer code, NESTLE, [25] developed at NCSU and currently maintained by UTK and ORNL is herein used), and calculating the OF of each solution. This series of solutions constitutes a Markov chain because each solution depends only on the previous solution and random numbers. The methods for changing the solution are described latter in section 3.1.3.

The objective function, defined as C in Equation 3.1 below, is based on the Fuel Cycle Cost (FCC) and constraint violations for each cycle in the optimization.

$$C = \sum_{n=1}^{N} wf_n D_n FCC_n + wT \sum_{i=1}^{I} w_{i,n} P_{i,n} \qquad 3.1$$

$$wT = 1 + (wt_{input} - 1)\ \ 1 - \frac{T}{T_0}$$

where,

N = number of cycles considered in optimization
I = number of constraints considered in optimization
FCC_n = fuel cycle cost for cycle n
D_n = discount factor used to weight cycle n FCC in levelized FCC calculation
wf_n = FCC weight for cycle n
$w_{i,n}$ = weight for constraint i in cycle n
wt_{input} = optional weight used to increase the effective constraint weights as T decreases (≥ 1), default=1 (weigthting is not temperature dependent)
T = Current simulated annealing temperature
T_0 = Initial simulated annealing temperature

$$P_{i,n} = \begin{cases} \text{relative error of constraint i in cycle n} & \text{if constraint i is violated in cycle n} \\ 0 & \text{otherwise} \end{cases}$$

Once all of the solutions for the initialization have been evaluated the standard deviation of the solutions' OFs is used to calculate the initial temperature of the search algorithm using Equation 3.2. The user input value of α is one of two variables used to control the thoroughness of the optimization with larger values giving a higher initial temperature and, thus, a more thorough search. It should be noted that the "temperature" variable herein discussed characterizes the state of the simulated annealing algorithm and has no connection to actual operational temperatures.

$$T_0 = \alpha\, \sigma_0 \qquad 3.2$$

where,

α = initialization parameter (> 0)
σ_0 = standard deviation of C for the initialization.

3.1.3 Fuel Cycle Cost Calculation

In BWROPT the cost of each new fuel assembly type can either be specified or the user can supply the necessary data and the cost will be calculated using the simple compound interest formula in Equation 3.3. The five fuel cost components used in the cost calculation are uranium ore, ore conversion, enrichment, fabrication, and burnable poison. The amount of uranium ore that needs to be purchased and converted depends on the enrichment of the individual fuel pins in the assembly. There are also losses in during the fabrication and conversion processes which affect the amount of ore required. Therefore, the user must specify the distribution of enrichment for the pins in each lattice of the assemblies and the losses for each step of the production process. The enrichment cost is determined by the number of Separative Work Units (SWUs) required to produce the desired enrichment from natural uranium. The fabrication cost is calculated as a fixed cost per assembly independent of the assembly design. If an assembly

contains burnable poisons (typically gadolinium for BWRs) the user must specify the amount with the enrichment data so the cost of the burnable poisons can be calculated based on the mass present in the assembly.

$$Assembly\ Cost = \sum_{i=1}^{5} \left(1 + \frac{R}{12}\right)^{T_i} C_i \qquad 3.3$$

where,

R = annual interest rate
C_i = cost of fuel component i
T_i = time in months before start of cycle that fuel component i must be paid for

3.1.4 Constraints

In Table 3.1 each of the constraints available in BWROPT are described including when in the cycle they are evaluated. The constraints currently available are: k_{eff}, 2D and 3D Relative Power Fraction (RPF), node exposure, and Assembly Average Exposure (AAE). These constraints were selected because of their importance for safe operation and regulatory compliance and/or ease of calculation. BWROPT uses the NESTLE [25, 26] reactor core simulator to determine the values of the constraints for each solution generated. Other constraints, whose values the NESTLE code can calculate and write to the output file, can be added to the OF calculation relatively easily.

Table 3.1 – Table of constraint descriptions, limit directions, and exposure points for which the limits are evaluated.

Constraint	Description	Limit Direction	Exposure Points
Min/Max k_{eff}	k_{eff} measures the neutron multiplication factor (criticality) of the reactor. In order for the reactor to maintain power and operate at steady state it is necessary for k_{eff} to be very close to 1 at all times.	<,>	All
Max RPF (2D and 3D)	Relative power fraction is a parameter easy to calculate which measures the extent to which the flux is peaked. At full power a highly peaked flux is likely to violate thermal margins and thus RPF can be used as an approximate thermal limit.	>	All
Max Node Exposure	Exposure to a high neutron flux and high temperature environment degrades many materials including nuclear fuel. This limit tries to ensure the most exposed part of the fuel does not challenge thermal mechanical limits due to localized overexposure within a harsh environment.	>	EOC
Max AAE	Assembly average exposure is another exposure limit which also tries to ensure thermal mechanical limits are not challenged due to overexposure.	>	EOC

3.1.5 Solution Change Types

The core LP is determined by a LP operator (see Figure 3.2) which specifies the locations of the old and new fuel assemblies, with positive or negative numbers, respectively. The LP operator also specifies the rank of the old fuel locations, which is used to assign old assemblies to locations. The new fuel assemblies are also ranked (-1 through the number of new assemblies) but these rankings are not used in the generation of the actual LP. In Figure 3.2 the new fuel ranks have been replaced with the fuel type because the fuel type specifies the new fuel LP, this is true because each new fuel bundle in a fresh batch is identical at BOC. The ranking for the old assemblies is performed after each cycle is analyzed for use in the next cycle. The user can rank the fuel based on EOC assembly reactivity (k_{inf}) or AAE. If k_{inf} is selected the ranking is descending and if AAE is used the ranking is ascending. If change types requiring the

new fuel ranking are selected the new fuel is also sorted after each cycle evaluation but the rankings are used for the same cycle. The new fuel sorting uses the same parameter as the old fuel sorting but the assemblies are ranked in the opposite direction.

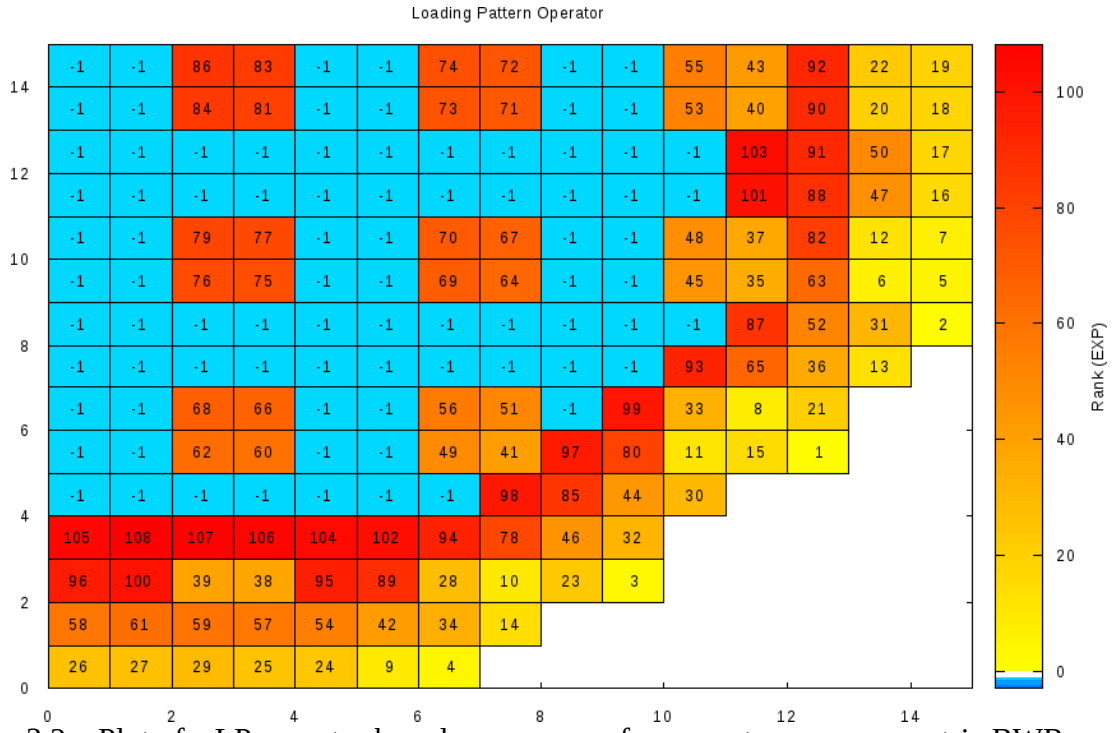

Figure 3.2 – Plot of a LP operator based on exposure for a quarter core symmetric BWR.

There are currently 10 solution change types available in BWROPT for the user to select from. All of the change types act by changing the LP operator and/or the fuel type map if the new fuel LP is being changed. Some of the change types perform similar functions but use different methods; for these the user can select the one or more they think will work best for their optimization. The only limitations placed on the exchanges are that the user can specify certain core locations as old fuel only and the maximum number of new fuel types. The available change types are listed below along with a description of each. Examples of the change types are included after the list.

1. Exchange 2 old assemblies – The ranks of two old fuel locations are exchanged (fuel type is not tracked for old locations).
2. Exchange an old and new assembly – The ranks and types of an old and new location are exchanged (the old location is sampled from only the locations allowed to be new locations).
3. Exchange 2 new assemblies – The ranks and types of two new fuel locations are exchanged (the types must be different).
4. Change region size I – The region size (number of new fuel assemblies) is increased or decreased by one (50 % chance of each) by randomly selecting the locations to alter.
5. Change region size II – The region size is increased or decreased by one (50 % chance of each) by changing the rank 1 old assembly to the rank -1 new assembly or vice versa, respectively. (This should on average be the region size change with the highest probability of acceptance)
6. Change new assembly type I – The type of a new fuel assembly is changed to another randomly selected type if no batch of this fuel type exists one is created.
7. Change new assembly type II – The type of a new fuel assembly is changed to one of the adjacent types in the new fuel array by incrementing or decrementing the index of one of the dimensions in the array if no batch of the selected type exists one is created. (Selecting the new type from the adjacent new types will have a higher average acceptance probability than random sampling if the fuel type array is constructed appropriately)
8. Change batch fuel type I – The fuel type of all the assemblies in a batch (all new fuel assemblies of a given type) is changed to another randomly selected fuel type.
9. Change batch fuel type II – The fuel type of all the assemblies in a batch is changed to another fuel type selected by incrementing or decrementing the index of one of the dimensions in the new fuel type array.
10. Change the number of batches – The new type of half of the assemblies in a batch is changed to another new type (a new batch is created if necessary) or all of the assemblies in a batch are changed to a different type.

For simplicity a 4 by 4 LP operator was used to demonstrate the different solution change types. Fuel shuffling (change types 1, 2, and 3) is demonstrated in Figure 3.3, 3.4, and Figure 3.5, respectively. In Figure 3.6 change type 4 is demonstrated by showing both an increase and decrease in the number of new fuel assemblies. Change type 5 is not demonstrated because it is the same as change type 4 except the selection of the location to be changed is different. Assembly new fuel type sampling (change type 6) is demonstrated in Figure 3.7; because change

type 7 is the same except for the new type selection it is not shown. Batch type selection (change type 8) is shown in Figure 3.8. Since change type 9 is very similar to change type 8 it is not shown. New fuel batch splitting and combining (change type 10) is shown in Figure 3.9.

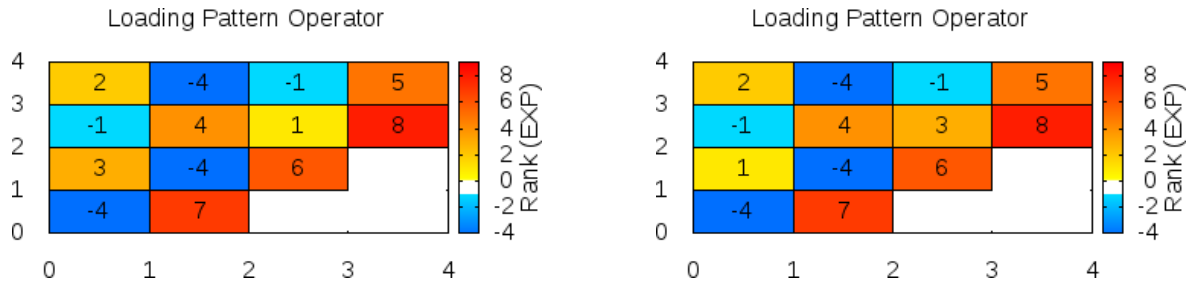

Figure 3.3 – Example of solution change type 1. (1,2) exchanged with (3,3).

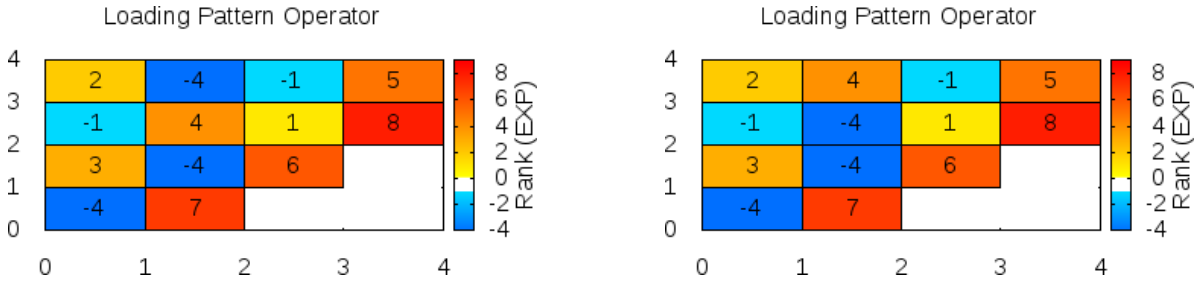

Figure 3.4 – Example of solution change type 2. (2,3) exchanged with (2,4).

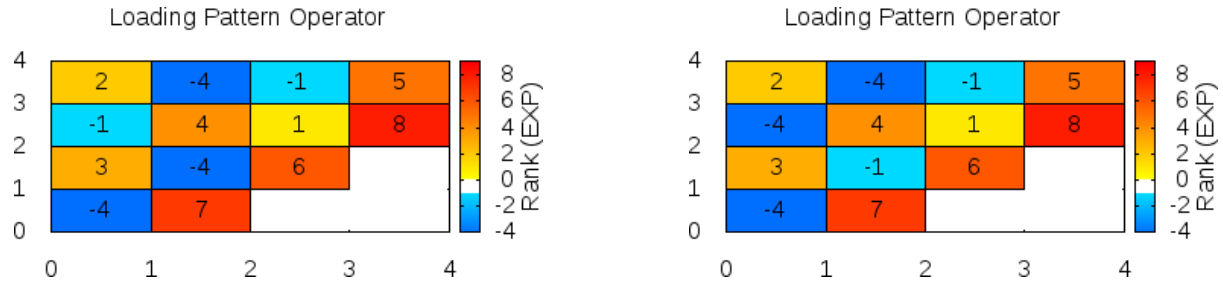

Figure 3.5 – Example of solution change type 3. (1,3) exchanged with (2,2).

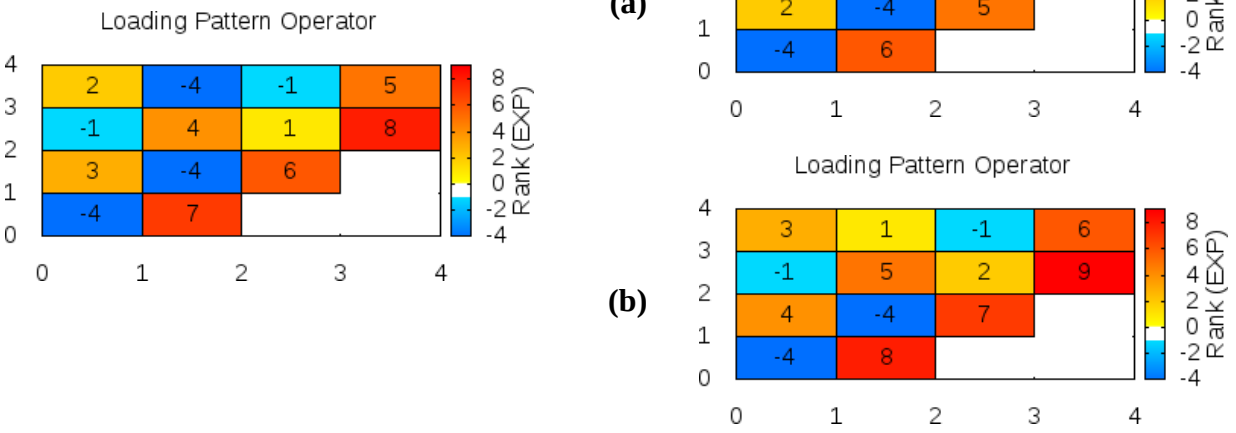

Figure 3.6 – Example of solution change type 4. (a) new fuel increased (b) new fuel decreases.

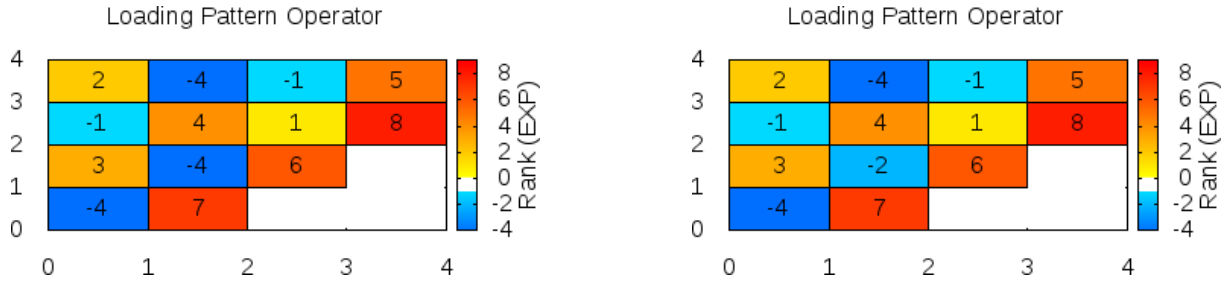

Figure 3.7 – Example of solution change type 6. New type of location (2,2) changed.

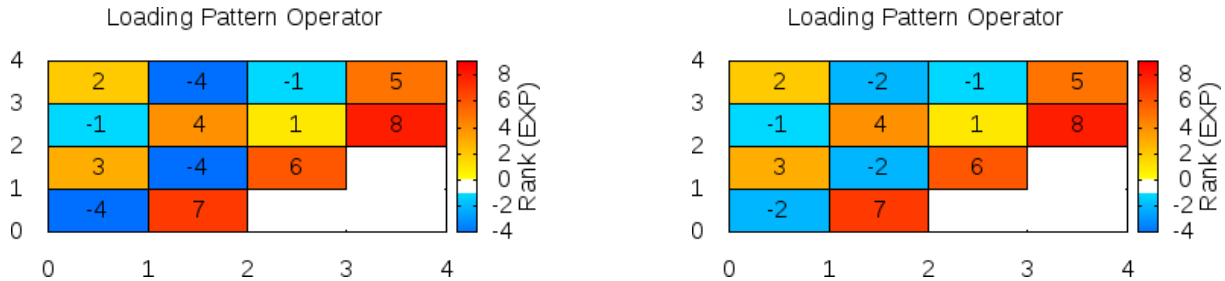

Figure 3.8 – Example of solution change type 8. The type 4 new fuel was replaced with type 2.

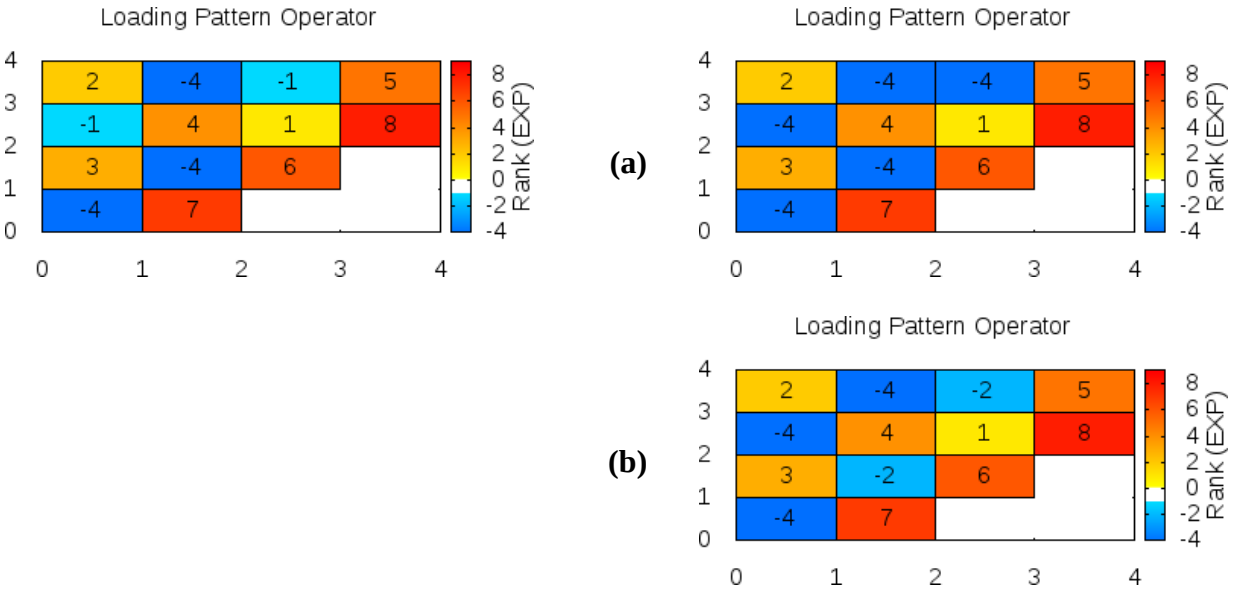

Figure 3.9 – Example of solution change type 10. (a) batches in original solution are combined (b) combined batch is split.

3.1.6 New Fuel Type Array

The new fuel types the code samples from are input into a new fuel type array of user-defined dimensionality (up to 4D). If the user selects only change types with random type sampling the structure of the array is irrelevant. However, if the user selects change types that use the new fuel type array the array should be set up so that each dimension represents a different variable in the fuel design. For instance, a 2D array with variable average enrichment from one column to another and variable Burnable Poison (BP) loading from one row to another as shown in Table 3.2. Each fuel design in the array is given a fuel type number which is used for random sampling. The ordered sampling is performed by first sampling a dimension to change and then sampling whether to increment or decrement the index of that dimension. The new type array works best if there are no empty locations but if an empty location is encountered during the sampling the code continues to change the index until a filled location is found. The

new fuel type array is intended to be used with fuel types that are ordered with respect to the design variable for each dimension, however, if ordering the fuel types for a dimension is not possible that dimension can be set to random sampling. If, for instance, the 2D array in Table 3.2 was changed to be a 3D array with the third dimension being assembly design, which is not readily ranked; this new dimension could be randomly sampled.

Table 3.2 – Example 2D new fuel type array with fuel type numbers for each assembly present.

BP Loading	Average Enrichment (percent U^{235} by weight)				
	2	2.5	3	3.5	4
0	1	4	6	9	12
2	2	-	7	10	13
4	3	5	8	11	14

3.1.7 Sampling Probabilities

The user can set the initial probability of sampling each change type or use the default of equal sampling probabilities. Also the user can select to have constant or variable sampling probabilities for the change types. Two types of variable sampling probabilities are currently available in BWROPT. The first is individual change type convergence, for which, after a change type goes a set number of cooling steps without a solution being accepted the sampling probability for that change type is linearly decreased to zero over a set number of cooling steps and the other sampling probabilities are increased to compensate. This leads to the phasing out of large changes late in the optimization because they are less likely to be accepted and increases the frequency with which small changes are sampled at the same time. The second method, which is still being developed, is called fully variable. In this method the sampling probabilities vary throughout the optimization based on a function of the fraction of accepted solutions for

each change type and the average magnitude of the OF change for each change type. This method has the same goal as the first but starts earlier and is more gradual. This method could also be used to skew the sampling toward larger changes early in the optimization to better explore the solution space early and then refine the good solutions once the large change types are phased out.

3.1.8 Temperature Adjustment and Solution Acceptance

After the initial temperature is calculated the optimization begins by creating a random starting solution for each process. Each process then starts a Markov chain in which the process of generating and evaluating new solutions (described in the initialization) is carried until an end criterion is met. The major difference being that the new solutions are not automatically accepted, instead their OF is used in Equation 3.4 to calculate an acceptance probability. If the new solution OF is greater than the old solution OF a random number from a uniform [0, 1] distribution is used to determine if the new solution is accepted. As can be seen from the equation solutions of equal or greater quality (lower OF) are always accepted but there is also some chance of accepting worse solutions. This helps avoid getting stuck in a local minimum. If the new solution is accepted the new solution becomes the old solution and is changed in the next iteration, otherwise the current old solution is changed again in the next iteration. The Markov chain end criterion is either a user defined number of solution evaluations per process or a total number of solution evaluations over all processes. The set of Markov chains on all the processes is referred to as a Cooling Step (CS).

$$P\ \ accept\ solution\ \ = \begin{matrix} \exp\ -\ C - C^*\ /T & C > C^* \\ 1 & otherwise \end{matrix} \quad 3.4$$

Where,

C = the OF of the new solution
C^* = the OF of the old solution (last accepted solution)

At the end of each cooling step statistics about all the solutions evaluated on each process are gathered on the master process. The gathered data is used to generate statistics that are printed to the screen to inform the user of the code's progress and is also used to calculate the standard deviation of the OFs of the accepted solutions and the solution acceptance ratio. This data is then used in the Lam adaptive cooling schedule (Equations 3.5 and 3.6) [27, 28], which is specified in the PSA by mixing of states algorithm, to update the algorithm's temperature. Two methods of adjusting the standard deviation were implemented to help the code deal with calculations that do not have enough solution evaluations per CS to consistently produce good statistics. The first is limiting the fractional decrease allowed for each CS and the second is using a weighted moving average.

$$T_{k+1} = \frac{1}{s_{k+1}} \quad 3.5$$

$$s_{k+1} = s_k + \lambda\ \ \frac{1}{\sigma_k}\ \ \ \frac{1}{s_k^2 \sigma_k^2}\ \ \ \frac{4\rho_k\ \ 1 - \rho_k\ ^2}{2 - \rho_k\ ^2} \quad 3.6$$

Where,

σ_k = standard deviation of the accepted solutions for cooling step k
ρ_k = acceptance ratio for cooling step k
λ = quality factor (> 0, smaller values → more thorough optimization)

3.1.9 Mixing of States

A new cooling step is started by using the new temperature in the mixing of states calculation which determines which solutions will be used in the next cooling step. There are four methods for determining the solutions to be sampled from. The default is to sample from the current solution on each process. The other methods are soft restarts because they select solutions from the archive of each process or the combined archive. The most basic of these is to sample from the best solution on each process at user specified CS intervals. The third method is to select all solutions from the combined archive with OF within a user specified percentage of the minimum OF solution (up to two times the number of Markov Chains). The final method samples solutions from the best new fuel loadings in the combined archive. In this method the best solution with each new fuel loading and a user specified number of randomly selected solutions are chosen for each new fuel loading (up to the number of Markov chains). The last two selection methods can be set to always on, on after the acceptance ratio falls below a user defined threshold, or on after the OF increase ratio falls below a user defined threshold.

The formula for the sampling probability of each solution is given in Equation 3.7. This equation preferentially samples the best solutions but all solutions have nonzero sampling probabilities. This leads to a more global search which results in more diverse and, on average, better near-optimum solutions. Once the new solutions have been chosen they are sent to the selected processes and the next set of Markov chains is started.

$$P_{s,k} = \frac{exp\ -C^*_{s,k-1}/T_k}{\sum_{s=1}^{N} exp\ -C^*_{s,k-1}/T_k} \quad 3.7$$

Where,

$P_{s,k}$ = probability of sampling the solution on process s for the beginning of cooling step k

$C^*_{s,k-1}$ = objective function of the current solution on process s at the end of cooling step k-1

3.1.10 Algorithm Convergence

The five user specifiable convergence criteria in BWROPT are summarized in Table 3.3. The main convergence criterion is a user specified number of cooling steps completed with a solution acceptance ratio below a user-defined threshold. Typically the acceptance ratio threshold is set to 0 so the algorithm converges when no solutions have been accepted for the desired number of cooling steps. The second convergence criterion is a user defined number of cooling steps completed since the last decrease in the OF of the best solution. This convergence criterion is helpful if the optimization space has very large flat areas, which can happen if all of the constraints can be met for many solutions with the same new fuel loading. The third convergence criterion ends the calculation after a specified number of CSs in which only fuel shuffles (change types 1-3) are accepted. This convergence criterion can be used if the user is only interested in the new fuel inventory and plans on performing his/her own LP optimization. There is also a variation of this convergence criterion for optimizations using variable sampling probabilities which terminates the calculation if all change types except shuffles have zero sampling probability. The final convergence criterion is simply a user defined maximum number of CS, which is mostly useful for debugging but can also be used as an upper bound for calculation runtime.

Table 3.3 – Summary of convergence criteria in BWROPT

Convergence Criterion	Description
1	Number of CS with acceptance ratio below threshold
2	Number of CS without new best solution
3a	Number of CS without a non-shuffle change type (1, 2, or 3) acceptance
3b	Only shuffle change types being considered (variable sampling probability cases only)
4	Maximum number of CS

3.2 Depletion Methods and Control Rod Pattern Search

There are three depletion methods available in BWROPT for evaluating LPs. The first depletion method uses the depletion steps and CRP specified in the initial guess NESTLE input deck, the second method uses the Haling depletion [12] (described in detail in the next section), and the last method generates a customized long term CRP at user specified depletion intervals for each new LP. A depletion method must be specified for each cycle being optimized.

3.2.1 Haling Depletion

A typical BWR depletion is divided into many depletion steps with each potentially having a different CRP, core power distribution, and/or flow. The depletion begins by calculating the RPF at BOC and thereafter using Equation 3.8 to determine the RPF used for depletion. The Haling depletion option relies on the Haling principle which, as stated previously, assumes that the minimum power peaking achievable for any given EOC state is attainable only by having a constant power profile throughout the cycle. Thus, the Haling depletion option uses a single depletion step with a constant power profile (the Haling Power

Distribution (HPD)) to deplete the fuel for each cycle [12]. The Haling power distribution is calculated using Equation 3.9 with an initial guess of the previous depletion point RPF or the NESTLE default (for a single step calculation) [29]. The ability to perform a Haling depletion was added to NESTLE as part of this work. The EOC state used for the Haling depletion in BWROPT is All Rods Out (ARO) because this produces the highest EOC reactivity and is generally the desired EOC state.

$$RPF_{Ave} = \frac{RPF_{BOC} + RPF_{EOC}}{2} \tag{3.8}$$

$$RPF_{Haling}^{n} = \alpha RPF_{Haling}^{n-1} + \ 1 - \alpha \ RPF_{EOC} \tag{3.9}$$

Where,

α = weight used to optimize convergence (0.5 is used in BWROPT).

The Haling depletion has many advantages which have led to its use in a number of fuel cycle optimization codes. [13, 30, 31] The biggest advantage is that it is much faster than performing a standard depletion. Another advantage is that the Haling depletion is CRP independent when the EOC condition is ARO. CRP independence allows for LPs to be evaluated without using a fixed CRP, which is very restrictive, or having to generate customized CRPs for each LP which, as described in the next section, is very computationally intensive. There are also several drawbacks to using the Haling depletion. The biggest drawback is that the constraint values calculated using the Haling depletion are not generally achievable with BWRs because of the limitation imposed by using the CRs to shape the core power distribution. Another drawback is that BWRs typically use the spectral shift operation strategy which is more

efficient than the Haling depletion (yields more power from the same LP) [11]. Spectral shift operation maintains a bottom skewed power profile relative to the HPD throughout most of the cycle, which increases the production of Pu-239 (from U-238) in the upper region of the core due to a harder neutron energy spectrum caused by the higher voiding in that region of a BWR, and at the end of the cycle the power distribution switches to being top skewed and takes advantage of the extra fissile plutonium created. In BWROPT the Haling depletion is intended mainly for use testing the code's functionality and features, and for analyzing cycles beyond the first for which an approximate solution can be acceptable since only the first cycle is actually used.

3.2.2 Control Rod Pattern Search Algorithm

Because of the coupled nature of the in-core fuel cycle parameters, the only way to truly optimize the LP (including the new fuel inventory) is to perform a CRP search for each LP. The methodology used in BWROPT for CRP determination is similar to that used in FORMOSA-B. In both a long-term CRP is generated for the current solution at regular intervals but in FORMOSA-B the interval is user defined whereas in BWROPT a customized CRP is generated for every solution [6]. This is done because holding the CRP (or any other major parameter) constant even for a few iterations limits the variation in the LP which in turn limits the variation in the optimum CRP, effectively making the optimization less global.

The major problem FORMOSA-B found with performing CRP updates frequently, which is also a problem in BWROPT, is that a CRP update takes much longer than simply running a cycle with a set CRP. However, the better the initial guess the less time CRP optimization takes. [6] Updating the CRP for every solution provides excellent initial guesses because the initial guess CRP (from the previous solution) was generated for an LP separated from the current LP

by only one LP change. Since updating the CRP for every new LP provides the best initial guess it should result in the lowest per update runtime.

There are two long-term CRP search algorithms in BWROPT both of which use the same ROI as FORMOSA-B. The first algorithm is simple and relatively fast and, consequently, has minimal position refinement and conflict resolution. The basic premise of this algorithm is to insert the CR with the largest weighted constraint violation if k_{eff} is greater than the upper limit or withdraw the CR with the largest weighted constraint margin if k_{eff} is less than the lower limit. The second CRP search algorithm is more thorough that the first method. In this algorithm the sum of the distance weighted constraint violation/margin is used, instead of only using the largest violation/margin, to decide which CR to move. Also, in the second method all moves are checked and refined to produce a more optimal CRP. However, refining a CR position takes several iterations and was determined to be unfeasible for use in a full multi-cycle optimization; thus, the first method is currently used for CRP searches in BWROPT. However, even using the simple CRP search the runtime for a single cycle is on average more than an order of magnitude greater than the runtime for the Haling depletion. To try to minimize the effect of this increase in runtime two new features were added to BWROPT: variable length Markov chains and the ability to restart calculations that fail due to cluster issues. These features are described in the following subsections.

3.2.4 PSA Restart

Even though the computational resources available for this research are excellent and currently include a Beowulf cluster with up to 397 modern CPUs, the long runtime of the CRP search means that optimizations utilizing the CRP search can take weeks or months instead of

days for equivalent optimizations using the Haling depletion. This poses problems on a cluster without backup power or which occasionally has software/hardware issues (this describes the University of Tennessee Knoxville Nuclear Engineering Department's Beowulf Cluster which BWROPT was tested on). Both the likelihood of a calculation being affected by these problems and the amount of computational effort lost if the calculation fails increase with the duration of the calculation. To limit the loss if a calculation fails an option was added to write restart files at the end of CSs at user specified intervals. Along with the restart file a new BWROPT input file is written which is the same as the original input file but has a line added to specify it is a restart case and give the location of the restart file. This input file can be used to restart the calculation from the last completed CS. In a restart run the BWROPT and NESTLE input files are parsed just like a standard case, but instead of running the PSA initialization the restart file is read to determine the state of the PSA calculation. The calculation then proceeds as normal and the archive will be identical to what it would have been without a restart.

3.2.3 Variable Length Markov Chains

The long runtime of the CRP search led to the decision to use it only for the first cycle being optimized and to use Haling depletions for the remaining cycles. For a three cycle optimization this reduces the average runtime of evaluating a solution by about 66%, but it also introduces a large amount of variability in the runtime of each Markov chain, because the cycle changed is randomly selected and the runtime is almost exclusively controlled by the number of times the first cycle (CRP search) is selected. This variation in runtime causes much of the processing power allocated to the run to be wasted waiting on the longest Markov chain to complete. To limit the variability in the runtime of the Markov chains it was decided to allow

the number of solutions evaluated in each Markov chain to vary within user specified limits. This idea had been previously suggested by Kropaczek [32] as an improvement in the PSA algorithm but was not used because the results of a variable length Markov chain calculation are not repeatable, which adds additional uncertainty when comparing calculation options/methods. Also, there is very little benefit if the variability in the runtime of the Markov chains is small. One exception to this would be running a PSA calculation that normally has small runtime variation Markov chains on a nonhomogeneous cluster. The variable length Markov chain implementation required effectively removing one process from the calculation (one solution is evaluated on it each CS) to be used as very low latency data storage.

3.2.5 Output Plotting

The automatic generation of several plot types using gnuplot [33] has been programed into the code to allow the user to visualize important distributions and aid further development. These include the LP operator plot shown above as well as 2D plots of the following: RPF, k_{inf}, assembly exposure, CRP, and any other general distributions available in the code. Sample plots of all of these distributions are included below in Figure 3.10- Figure 3.13. Also, multiplots, pictures with more than one plot in them, can be generated with 2 to 6 plots. A sample multiplot used to aid the development of the CRP development is included in Figure 3.14.

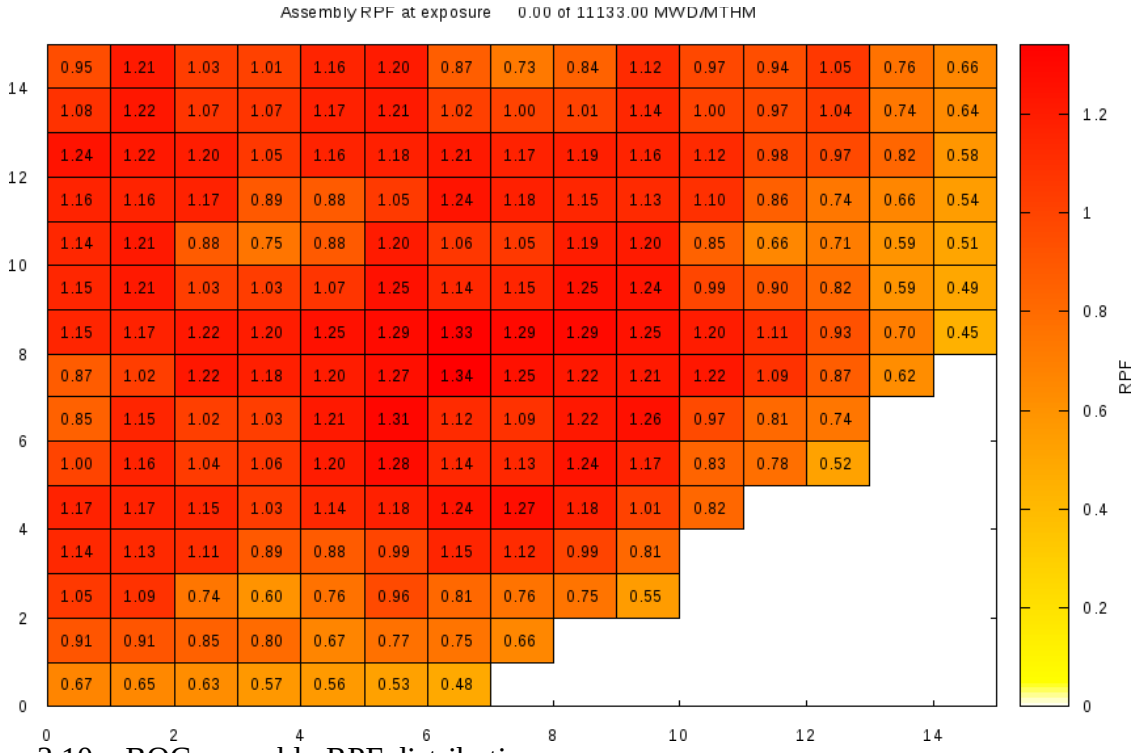

Figure 3.10 – BOC assembly RPF distribution.

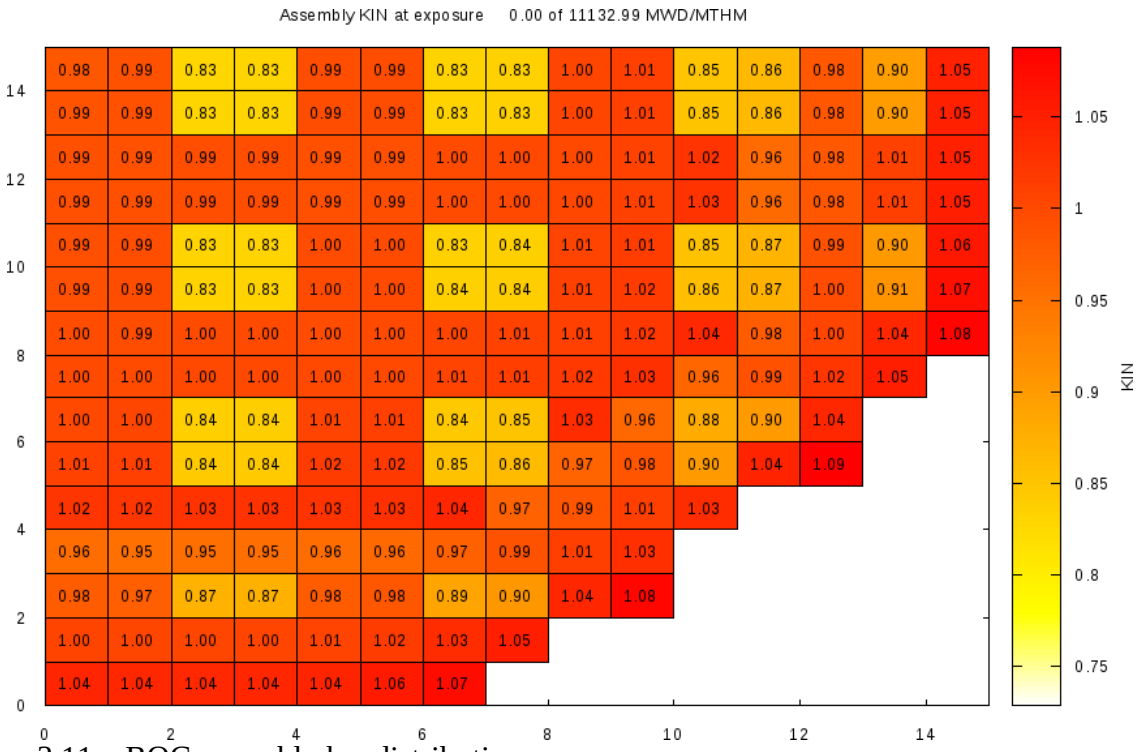

Figure 3.11 – BOC assembly k_{inf} distribution.

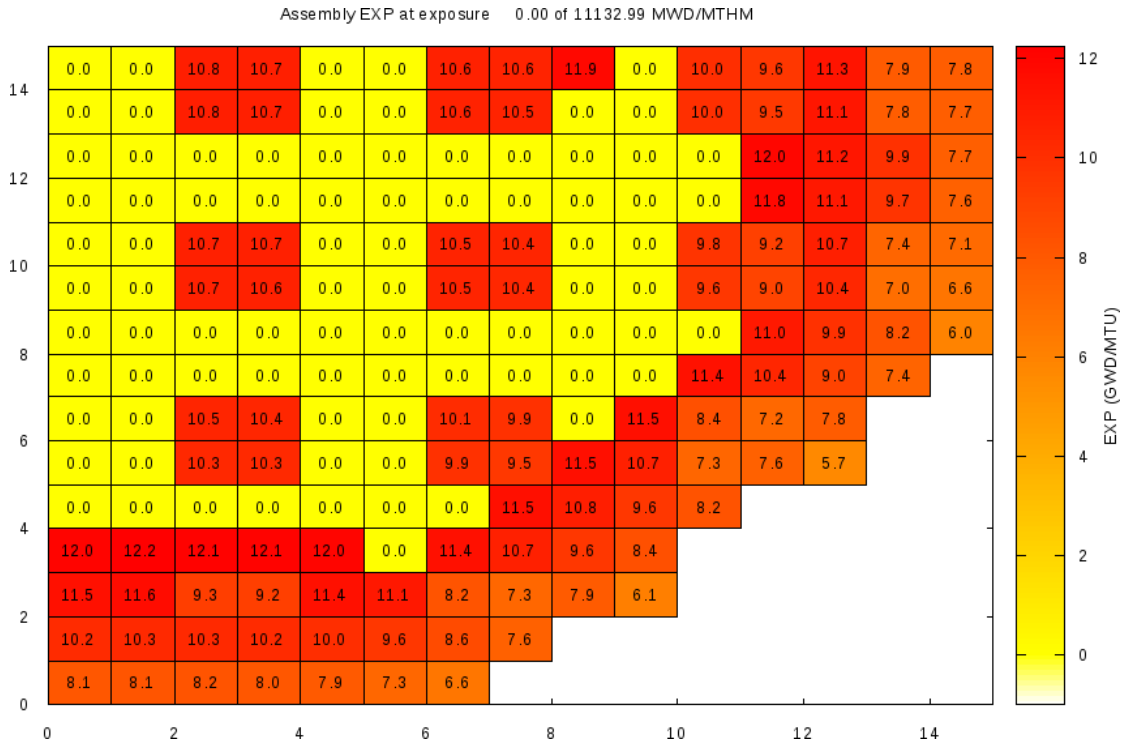

Figure 3.12 – BOC assembly exposure distribution (in GWD/MTHM).

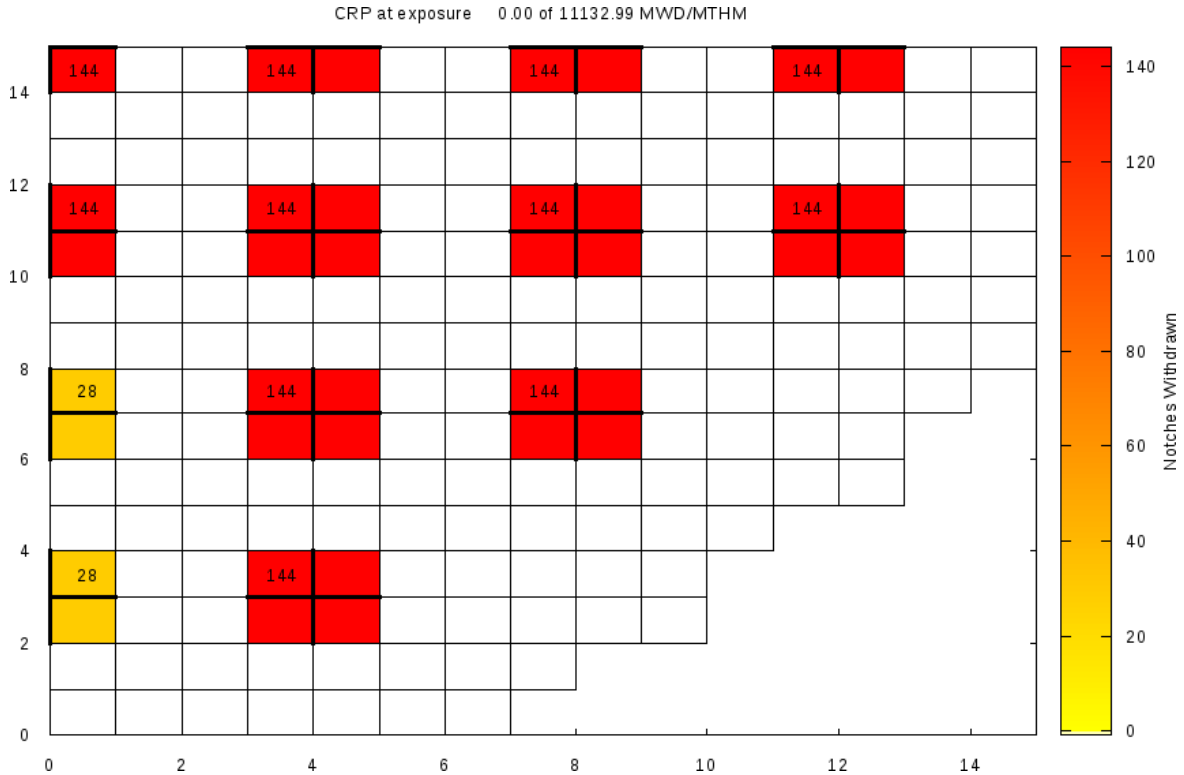

Figure 3.13 – Plot of CR positions for a CVC CR group (one notch = 1 inch).

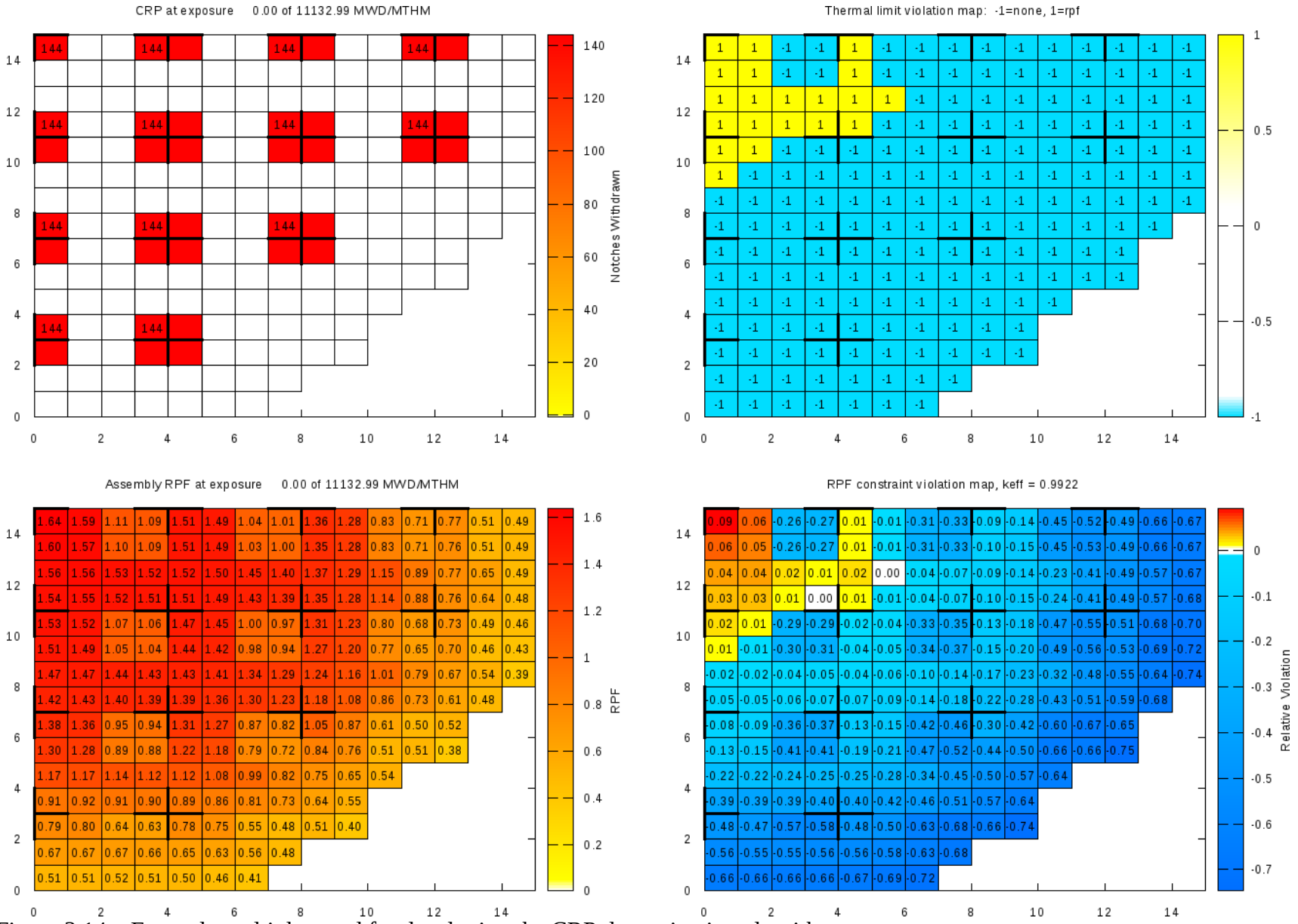

Figure 3.14 – Example multiplot used for developing the CRP determination algorithm.

Chapter 4 NESTLE

As stated previously the NESTLE core simulator [25] , which was originally developed at NCSU, is used for analyzing solutions generated by BWROPT. As far as BWROPT is concerned NESTLE is a black box that evaluates the constraints in the OF so only a brief description of the code will be given. Nuclear reactor core simulators, including NESTLE, solve the coupled neutronic and thermal hydraulic problems to determine the steady state conditions in the reactor core. The version of NESTLE used with BWROPT has undergone significant modifications from version 5.2.1 [34] which is available from RSICC. The modifications to create the new version of NESTLE have been performed in collaboration between ORNL and several students from UTK. The major improvements during this collaboration were: the conversion of the input from a fixed format style to a keyword style input using the SCALE input processing routines, adding a two-phase thermal hydraulics solver so BWRs can be accurately modeled, and implementing generalized isotope tracking/depletion. [35, 36, 37] Improvements to NESTLE are ongoing at UTK and several of the improvements implemented in conjunction with this work are described later in this chapter. In the next section a description of the basic equations NESTLE solves and the methods used to solve them is given.

4.1 NESTLE Algorithm

4.1.1 Neutronics

NESTLE, like most nuclear reactor core simulators, solves the multi-group neutron diffusion equation, which models the production, loss, and flow of neutrons. The general form of this equation with the spatial dependence suppressed (all quantities are node dependent) is

given in Equation 4.1. This equation is solved for each node and energy group in the reactor with the gradient/diffusion term modeling the flow between nodes. The left hand side of the equation represents losses of neutrons (except for within group scattering) and the right hand side of the equation represents gains. The simple matrix expression for used for solving the diffusion equation is given in Equation 4.2. NESTLE uses the Nodal Expansion Method (NEM) to solve the diffusion equation. [34]

$$-\nabla \cdot D_g \nabla \phi_g + \Sigma_{tg}\phi_g = \sum_{g'=1}^{G} \Sigma_{sg'g}\phi_{g'} + \frac{\chi_g}{k} \sum_{g'=1}^{G} \nu_{g'}\Sigma_{fg'}\phi_{g'} \quad 4.1$$

$$\mathrm{A}\,\phi = \frac{1}{k}\mathrm{F}\,\phi \quad 4.2$$

Where,

D_g= diffusion coefficient of group g
ϕ_g= neutron flux in group g
Σ_{tg}= total macroscopic cross section
$\Sigma_{sg'g}$= macroscopic scattering cross section from group g' to g
χ_g= fraction of fission neutrons with initial energy in group g
k= multiplication factor (eigenvalue)
ν_g= average number of neutrons produced from a fission in group g
Σ_{fg}= macroscopic fission cross section for group g

A typical full core BWR calculation has ~20000 nodes including the reflector and 2 energy groups are usually considered. This results in a very large A matrix which is time consuming to invert and, consequently, NESTLE uses iterative methods to solve Equation 4.2. To further complicate the problem the cross sections and other parameters in Equation 4.1 typically depend on the solution. This creates a nonlinear feedback and actually requires multi-level nested outer iterations around the solution to the matrix problem in which the parameters the cross sections depend on (node thermal hydraulics parameters and burnup), the cross sections themselves, the nodal expansion method coefficients, and k are updated.

To facilitate updating the cross sections for each set of conditions encountered in the NESTLE calculation the cross sections are precalculated by a lattice physics code for a number of values covering the expected range of each parameter. Lattice physics codes model detailed assembly lattices, such as the BWR lattice shown in Figure 4.1, using transport theory. The detailed nature of the transport solution and the necessity of evaluating many state points cause the runtime for a lattice evaluation to be much greater than the NESTLE calculation runtime, which is the primary reason for precalculating cross sections. The detailed solution generated using transport theory is then used by the lattice physics code to generate homogenized cross sections representative of the lattice for use in diffusion theory calculations. TRITON is typically used to calculate the lattice cross sections and a post processor T2N (TRITON to NESTLE) is used to convert the Triton output to a format useable by NESTLE [35, 38]. Typical cross section parameters for BWRs include: burnup, control rod in/out, fuel temperature, and void fraction (moderator density). [34]

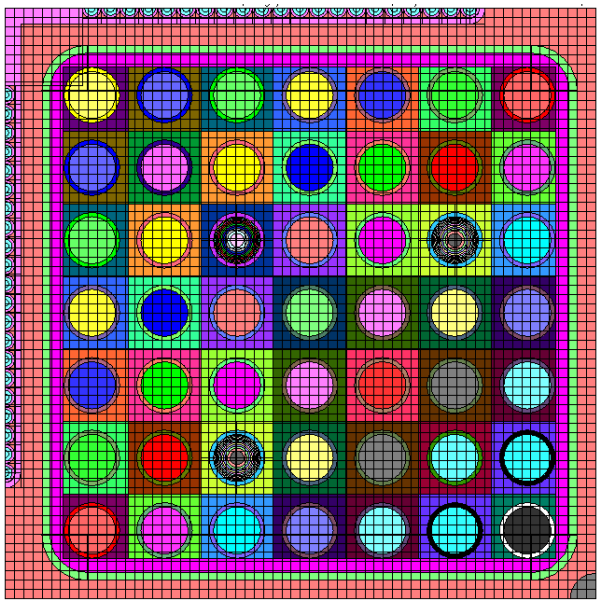

Figure 4.1 – Example BWR lattice generated by TRITON.

4.1.2 Thermal Hydraulics

The primary purpose of thermal hydraulic models in reactor core simulators for steady state calculations is to determine the fuel temperature and moderator density to update the cross sections. There are three thermal hydraulic options in NESTLE: no thermal feedback, the Homogeneous Equilibrium Mixture (HEM) Model, and the drift flux model. The first option is not capable of modeling power reactors because it uses the same conditions everywhere. The HEM model can model single phase flow well and works well for PWRs but is not capable of accurately modeling the two phase flow which occurs in BWRs. This led to the recent addition of the drift flux model to NESTLE by Jack Galloway, a former student of the University of Tennessee, Knoxville. Both the HEM and drift flux models solve the three conservation equations: mass, momentum, and energy; but the HEM model assumes that the steam and water move at the same velocity and the drift flux model accounts for slip. [34, 37]

4.2 NESTLE Improvements

Three major improvements were made to NESTLE as part of this work as well as numerous smaller improvements such as the Haling depletion option and several bug fixes.

4.2.1 Assembly Input

The first improvement was modifying the lattice input map read routine to handle assemblies (see example input below). The original input required the user to specify a radial lattice map for each unique axial plane (17x17 matrix in the example). For reactors that have a large number of unique lattice arrays this input was tedious to write and highly error prone. For instance the test case used for this research has seven unique axial arrays, but with the assembly

input only a single array has to be specified along with the three assemblies and reflector and the code will expand the assemblies to create the lattice maps.

```
assem_ara=0 fill  6  1  2  3  4  5  7 end fill
assem=1     fill  1  1  1  1  1  1  1 end fill
assem=2     fill  1  5  7  8  8  7  2 end fill
assem=3     fill  1  4  4  4  4  4  2 end fill
assem=4     fill  1  3  6  6  3  3  2 end fill

ara=0 nux=17 nuy=17 fill
  2 2 3 3 2 2 3 3 2 2 3 3 4 3 4 1 1
  2 2 3 4 2 2 4 3 2 2 3 3 4 3 4 1 1
  2 2 2 2 2 2 2 2 2 2 2 2 4 4 4 4 1 1
  2 2 2 2 2 2 2 2 2 2 3 4 4 4 4 1 1
  2 2 3 3 2 2 3 3 2 2 3 3 3 3 4 1 1
  2 2 3 4 2 2 3 3 2 2 3 3 4 3 4 1 1
  2 2 2 2 2 2 2 2 2 2 2 3 4 4 4 1 1
  2 2 2 2 2 2 2 2 2 2 4 4 4 4 1 1 0
  2 2 3 3 2 2 3 3 2 4 3 3 4 1 1 0 0
  2 2 3 3 2 2 3 3 4 3 3 4 4 1 1 0 0
  2 2 2 2 2 2 2 4 4 4 4 1 1 1 0 0 0
  4 2 2 2 4 2 4 3 4 4 1 1 0 0 0 0 0
  4 4 3 3 4 4 3 3 4 4 1 1 0 0 0 0 0
  4 4 4 4 4 4 4 4 1 1 1 0 0 0 0 0 0
  4 4 4 4 4 4 4 1 1 0 0 0 0 0 0 0 0
  1 1 1 1 1 1 1 1 0 0 0 0 0 0 0 0 0
  1 1 1 1 1 1 1 0 0 0 0 0 0 0 0 0 0 end fill
```

4.2.2 New Output Format and Summary Distributions

The second major improvement was updating the output format used for writing distributions to the output file and adding the ability to specify summary distributions to output. NESTLE allows the user to select from a number of distributions to be written to an output file for each depletion step. The old style NESTLE output only allowed full 3D distributions and wrote the distributions six columns of data at a time in order to keep the output file less than 80 characters wide. Appendix A illustrates a comparison between the old and new output styles,

where it is noted that the old approach allowed the output to fit on a single page without being wrapped, but it also made the distributions take up 2-5 times as many lines, which makes it harder to visualize. The new output prints these distributions a half-core at a time, which means for full-core geometry the distributions are split in two and for half-core and quarter-core they are not split at all. In addition to this change, the ability to request 2D, 1D, and 0D summary distributions of the min, max, and average of the 3D distributions was also added. Often times these distributions contain the information desired by user in a much more condensed format which is helpful when viewing the output directly because the full 3D distributions typically contain thousands of values.

4.2.3 Distribution Plotting

The ability to generate 2D plots of the axial planes of a 3D distribution or of one of the 2D summary distributions was also added to NESTLE. Constraint violation plots can also generated by specifying a target value selecting one of four difference operators: positive difference (dist - target), negative difference (target - dist), positive relative difference (dist - target) / target, or negative relative difference (target - dist) / target. The plotting routine is based on the plotting routine developed for BWROPT but without multiplot capability. As in BWROPT the code writes and executes gnuplot scripts to generate the plots. The plots can be customized in a number of ways including specification of the color scheme and whether or not numbers are printed for each node. Two sample plots are included of the assembly maximum PREL (3D RPF). The first (Figure 4.2) is at BOC and shows the actual distribution. The second (Figure 4.3) is early in the cycle and shows a constraint violation plot with a target value of 1.6.

Another feature that was added is the ability to write an input file for 3D visualization software such as VISIT. The files are written in vtu format which is an XML version of the VTK format for use with unstructured grids. These files can also be opened with other 3D visualization software such as Paraview. The grid can be specified as having no gaps between the nodes or gaps can be specified for any of the x, y, and, z directions. Three sample plots of the 3D RPF of a BWR are included below to demonstrate the different plots that can be generated. The first plot (Figure 4.2) shows a visualization with no gaps, which is not particularly insightful though operations can be performed on this within the visualization software to extract more information. Figure 4.5 shows a visualization with gaps in the x and y directions which simulates assemblies and by rotating this plot the RPF distribution along the xz and yz planes can be seen. In Figure 4.6 a visualization of a different reactor model with gaps in z direction almost the full width of the node shows the distribution along the xy plane for several z values at once.

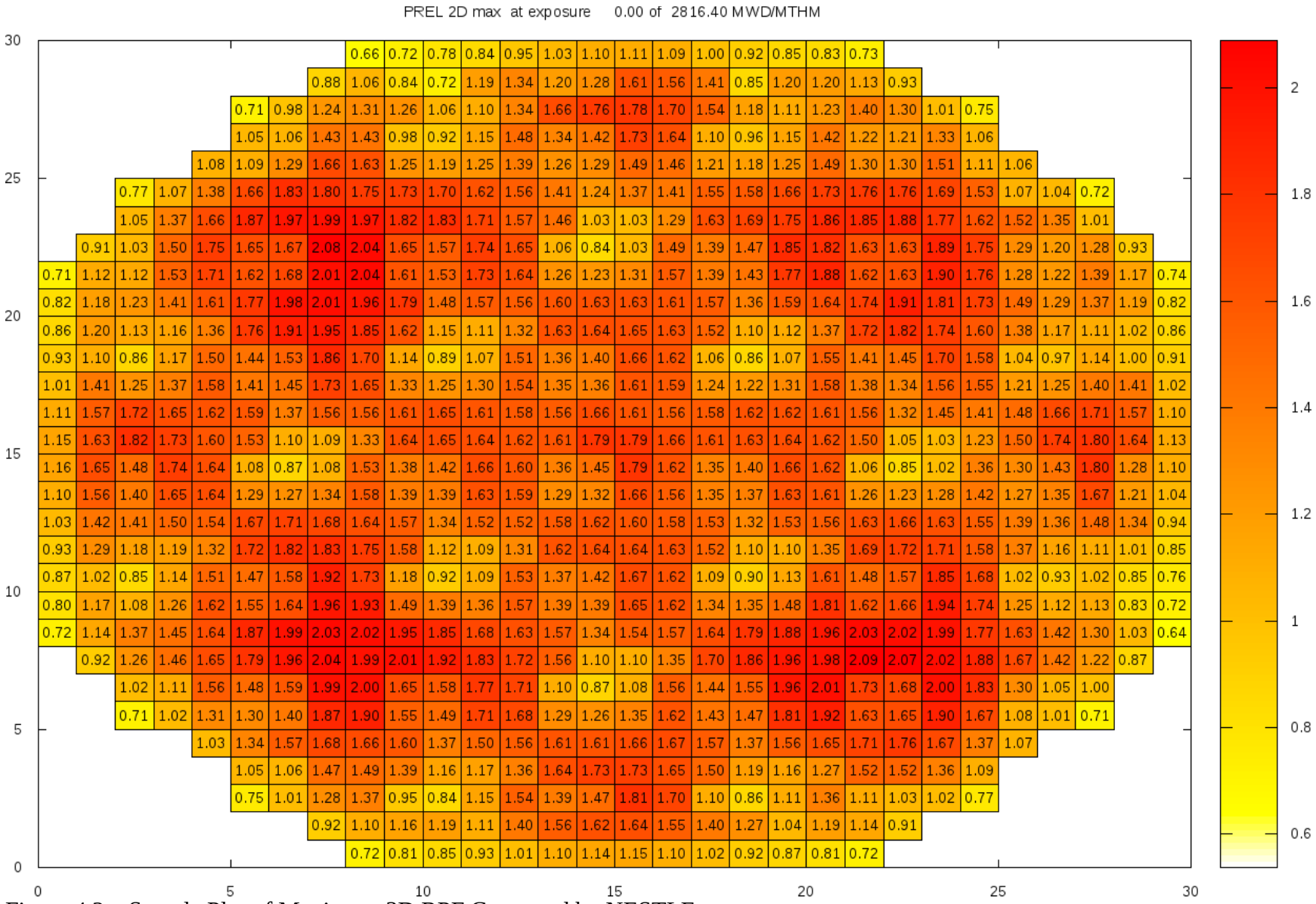

Figure 4.2 – Sample Plot of Maximum 3D RPF Generated by NESTLE.

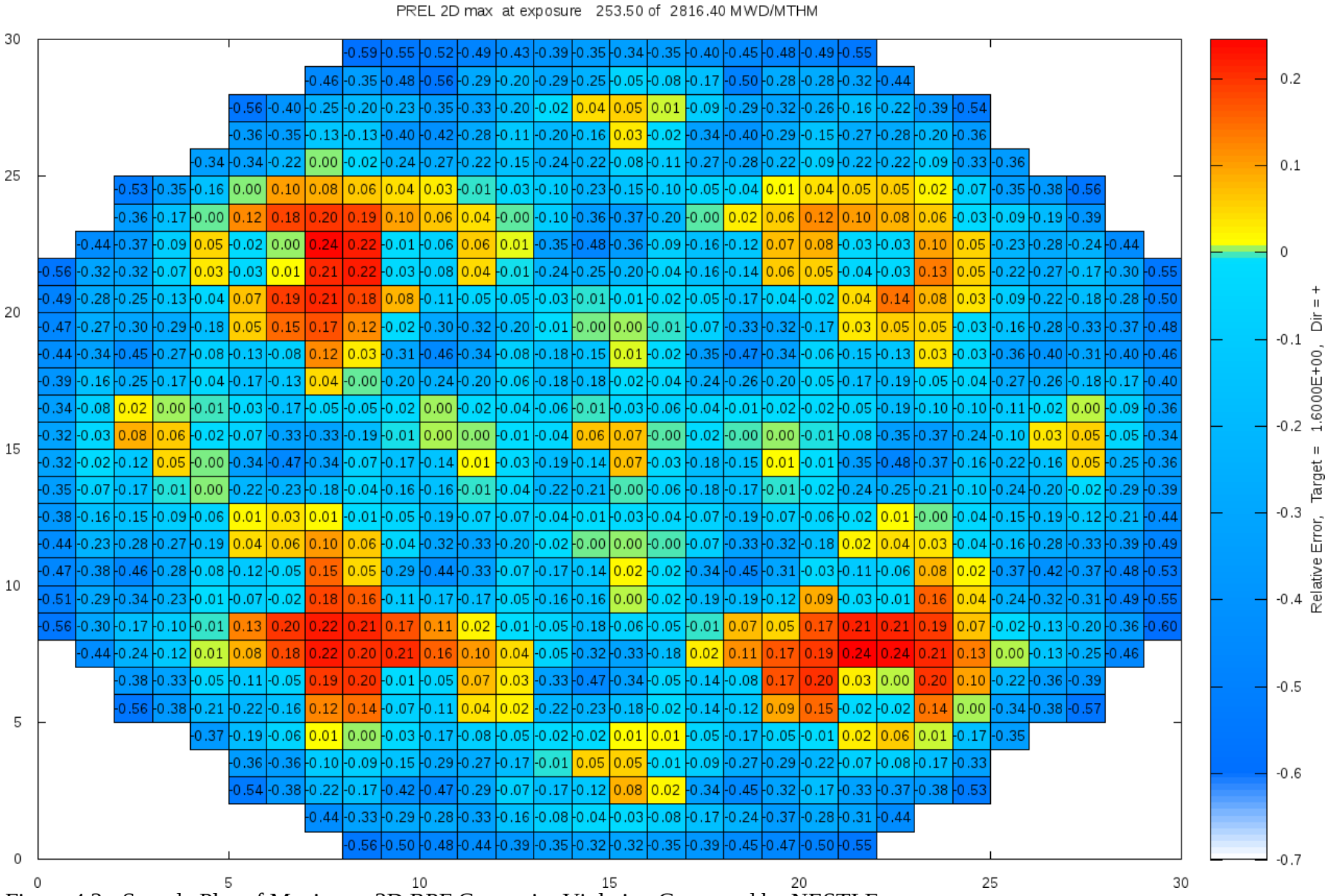

Figure 4.3 - Sample Plot of Maximum 3D RPF Constraint Violation Generated by NESTLE.

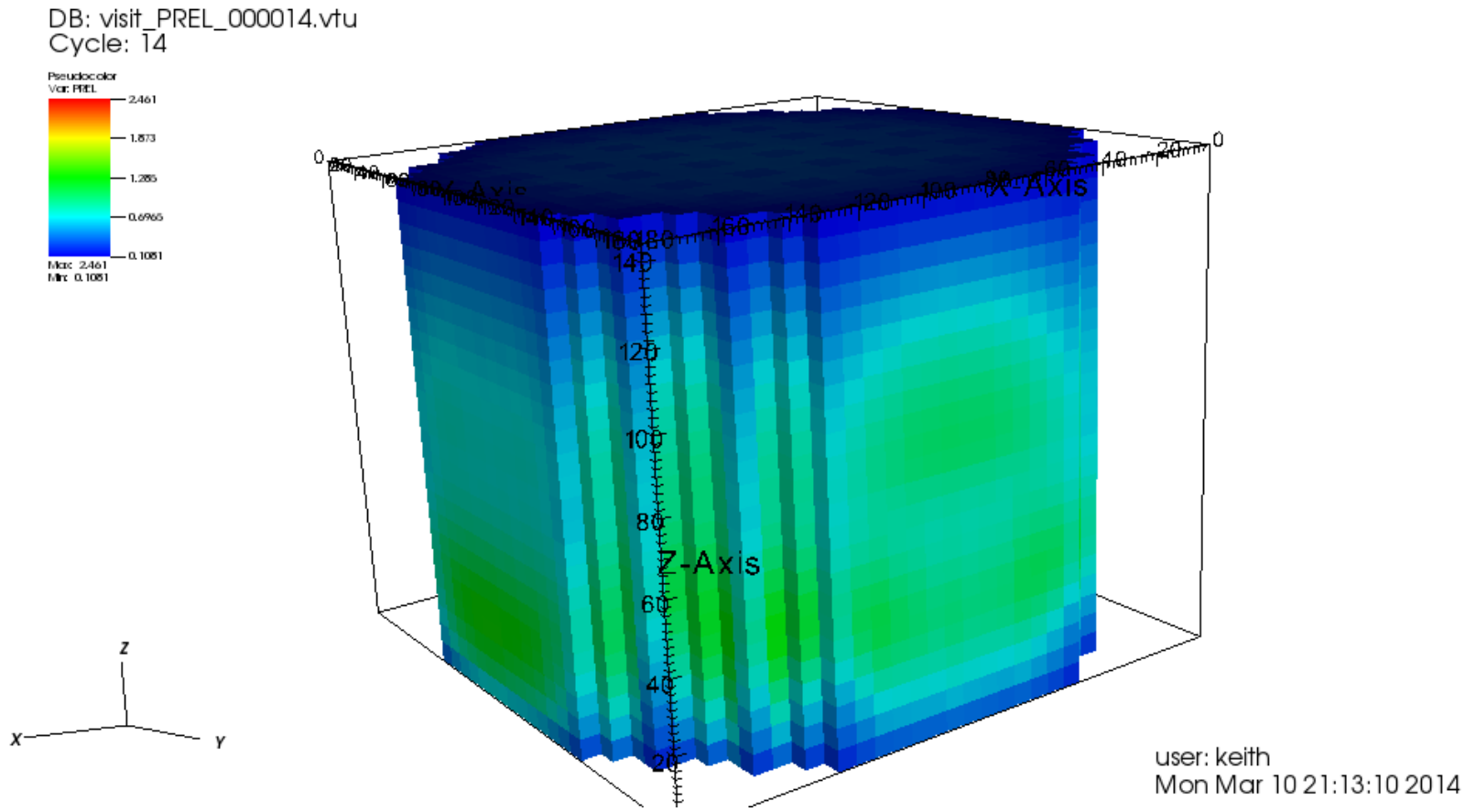

Figure 4.4 – Sample VISIT visualization of 3D RPF with no gaps.

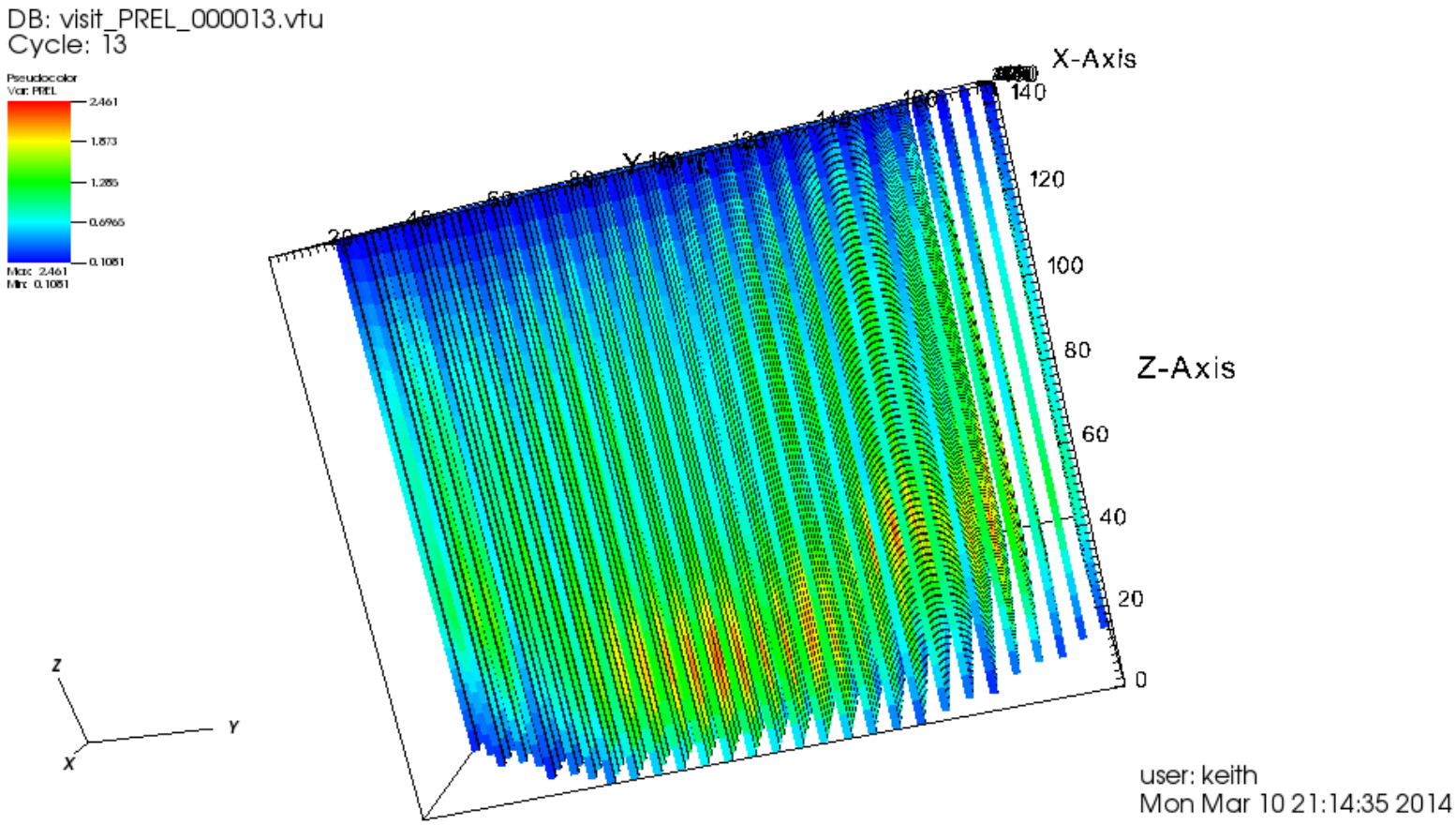

Figure 4.5 – Sample VISIT visualization of 3D RPF with gaps in the x and y directions to simulate assemblies.

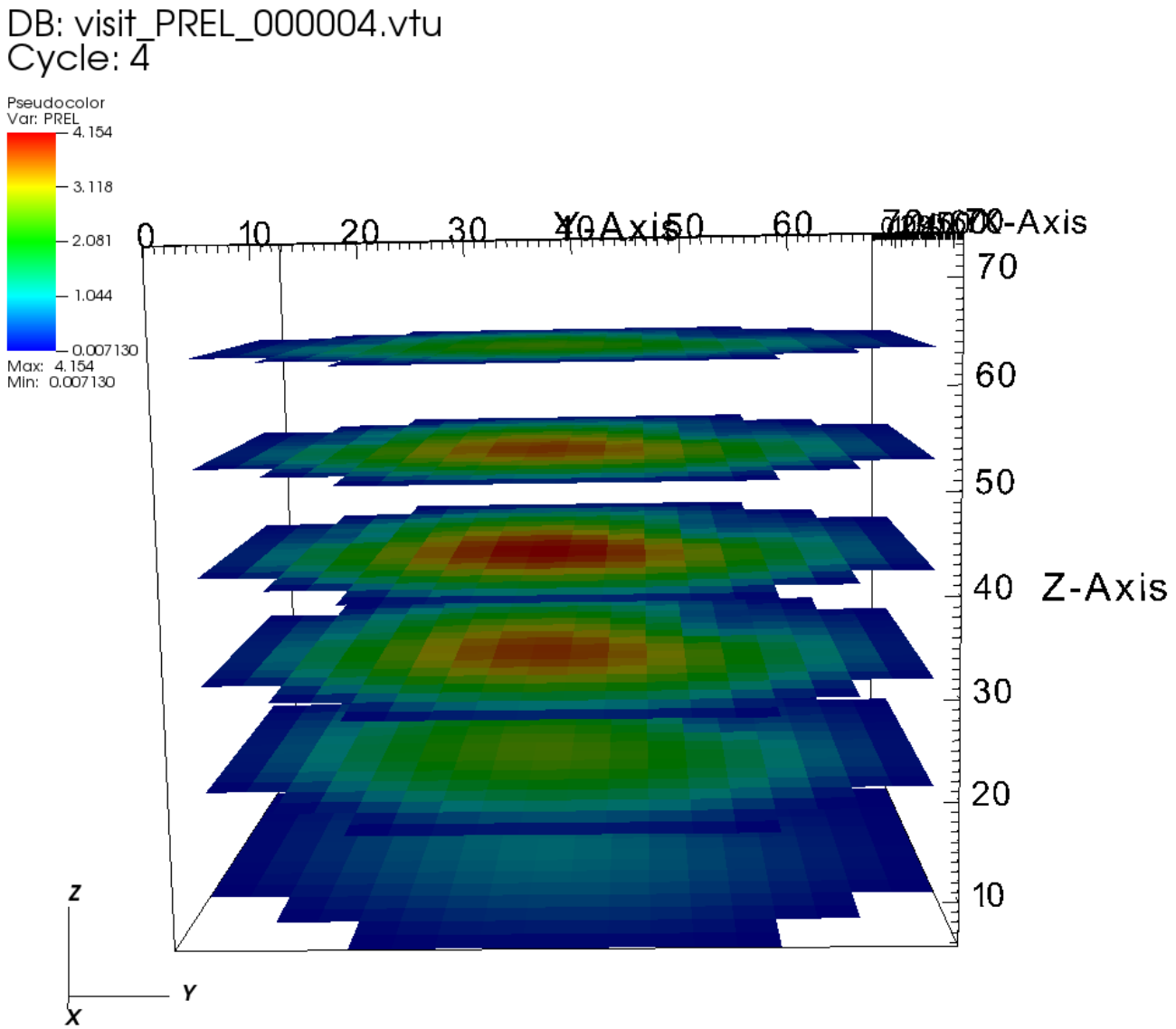

Figure 4.6 – Sample VISIT visualization of 3D RPF with gaps in the z direction so the radial power profile can be seen.

Chapter 5 Application of the Optimization Algorithm to Several Test Cases

The functionality and effectiveness of BWROPT were evaluated using several test cases. These test cases were based on the initial cycle of the Peach Bottom 2 (PB2) BWR. The PB2 reactor and the modifications made to the original cycle for the test cases are described in the next section. The first test was to ensure the code is capable of minimizing the OF, all of the sampling types work, and to determine appropriate values for the constraint weights. Once the basic function of the code was verified several additional test cases were ran with the same parameters. Three sets of test cases were evaluated to test the effectiveness of using variable sampling probabilities and the new fuel type array. Finally, the CRP search functionality was tested. The cases used for these tests are described in detail after the description of the PB2 reactor.

5.1 Description of the Peach Bottom 2 BWR

5.1.1 Original Cycle 1

The PB2 reactor is located in Southeast Pennsylvania and began operating in 1974. The first two cycles of the reactor were thoroughly documented in an EPRI report [39] to provide data for benchmarking reactor analysis tools. Jack Galloway used this data to benchmark the two-phase flow model he implemented in NESTLE [37]. His work, in particular the input file used for the benchmark, was used as the starting point for developing the test cases for testing BWROPT with a model of a real (though vintage) BWR. Due to the highly competitive and

proprietary nature of nuclear reactor core and fuel assembly design, multiple attempts to obtain core design and operational data for a more modern or contemporary BWR unfortunately failed.

The original NESTLE BWR benchmark used a full core model of the PB2 reactor with the operating parameters specified in Table 5.1. The LP for the original benchmark model is shown in Figure 5.1. As can be seen from the figure three assembly types are used in the model and unlike modern LPs the LP used in this cycle is not symmetric. Assembly type 1 has an average enrichment of 1.1% while assembly types 2 and 3 have an average enrichment of 2.5%. Also, assembly types 2 and 3 have Gd_2O_3, a Burnable Poison (BP), loaded into some of the fuel rods (4 for type 2 and 5 for type 3) [37]. These low enrichments are characteristic of initial cores, whereby the low reactivity fuel is used to mimic spent assemblies to help shape a flatter power distribution than otherwise.

Table 5.1 – Peach Bottom 2 Cycle 1 Operating Parameters for the Original Full Core Model [39].

Parameter	**Value**
Thermal Power	3293 MW
Core Flow	102.5 Mlbm/hr
Energy	1772 GWD
Burnup	11133 MWD/MTU
Fuel Assemblies	764
Control Rods	185

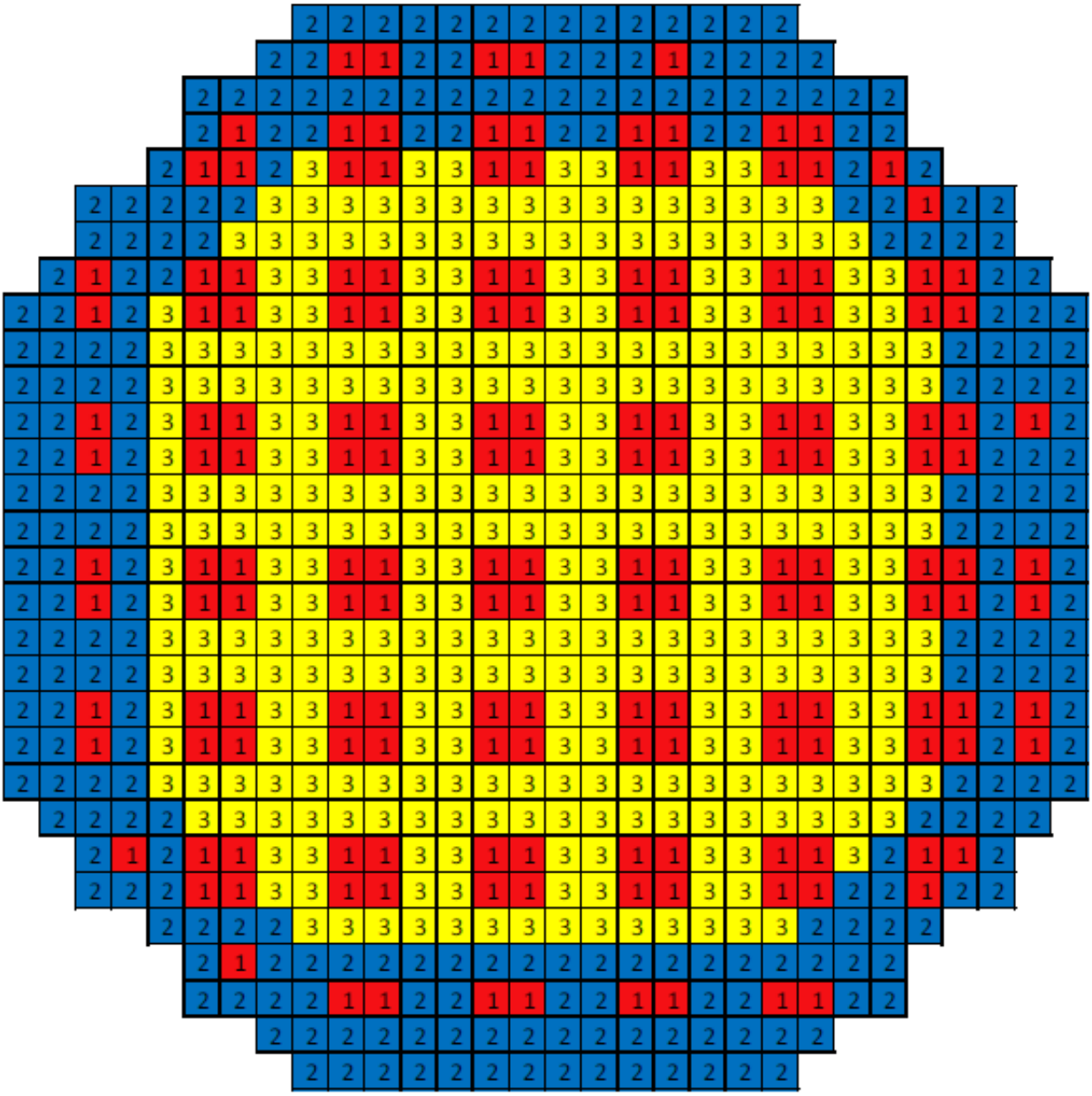

Figure 5.1 - Peach Bottom 2 Cycle 1 Loading Pattern for the Original Full Core Model [37].

5.1.2 Modified Cycle 1

Many changes were made to the benchmark case to fully test BWROPT and also to reduce the runtime of the NESTLE calculations. The most significant change to the model was switching to a quarter core symmetric core. This change significantly reduces the runtime of the

model but also requires changes to most of the model parameters. The new model parameters, given in Table 5.2, as might be expected are generally about a quarter of the parameters for the full core model. The burnup is listed as variable because it is calculated based on the mass of fuel in the core and the energy production requirement for each cycle. The mass of fuel in the core is determined by summing the original (undepleted) fuel mass for each assembly and is usually expressed with unit of Metric Tons of Uranium (MTU) or Metric Tons of Heavy Metal (MTHM) if non-uranium isotopes are used as fuel. The cycle energy requirement is a user input and for the test cases was 402.0 GWD (roughly one quarter of the original PB2 cycle 1).

Table 5.2 – Peach Bottom 2 Operating Parameters for the Quarter Core Model.

Parameter	**Value**
Thermal Power	823.75 MW
Core Flow	25.625 Mlbm/hr
Burnup	variable
Fuel Assemblies	191
Control Rods	54

The fuel assemblies used in the new model were created by linearly modifying the pin enrichments in assembly types 1 and 2 from the original PB2 cycle 1 core. Nine new assemblies were generated with enrichments ranging from 1.1 to 5 percent and 0 or 4 BP rods. Table 5.3 shows these assemblies sorted into the 2D new fuel type array used in the BWROPT test cases. The 2 dimensions are average enrichment which has 5 roughly evenly spaced values and number of BP containing fuel rods (really whether or not there are fuel rods that contain BPs since there are only 2 values). The new NESTLE input file used for the base case in all of the optimization runs is included in Appendix A.

Table 5.3 – New fuel assemblies used for test cases sorted into a new fuel type array.

Number of Burnable Poison Containing Rods	Average Enrichment				
	1.1	2.0	3.0	4.0	5.0
0	1	2	4	6	8
4	-	3	5	7	9

5.2 Algorithm Evaluations

5.2.1 Parallel Simulated Annealing Algorithm Evaluation

To evaluate the PSA implementation and functionality of the code three cycles (2-4) of the PB2 reactor were optimized using the Haling depletion option. All 10 sampling types were used to generate optimal LPs. The input file for this case, which includes a description of all of the inputs, is given in Appendix B. Many iterations of this input file were tested to determine FCC and constraint limits/weights that ensure all components of the OF impact the optimization as much as possible while also trying to maintain realistic constraint values. The constraint limits and weights selected for use in the test cases are given in Table 5.4 (the same values were used for all 3 cycles).

Table 5.4 – Constraint limits and weights used for test cases.

Constraint	Units	Limit	Weight
FCC	($/kwh)	-	10.
Min k_{eff}	-	1.000	100.
Max k_{eff}	-	1.005	100.
Max Assembly RPF	-	1.5	1.
Max Node RPF	-	2.0	1.
Max Assembly EXP	(GWD/MTHM)	35.0	10.
Max Node EXP	(GWD/MTHM)	45.0	10.

In addition to the selection of the constraint limits and weights the initial test case was used to determine appropriate values for the PSA parameters. It was decided to run the calculations with 40 Markov chains, because the most common node type on the Beowulf cluster can run 8 processes per node and the queue time for a 40 process calculation is generally short. Chu et al. found the optimum number of solutions evaluations per Markov chain to be 50% to 60% of the number of processes [3]. Thus, a value of 20 was selected for the Markov chain length. The temperature initialization parameter, α, was set to 2.0 which is the largest typical value according to Kropaczek [2]. The quality factor, λ, was set to .25 to produce a reasonably thorough optimization. The convergence criteria used for this calculation are given in Table 5.5.

Table 5.5 – Convergence criteria used for test cases.

Convergence Criterion	**Value**
1	2 CSs without any solution acceptances
2	200 CSs without a best solution change
3a	10 CS without a change type other than a shuffle (1-3) being accepted
3b	Not used
4	Not used

Once the function of the PSA algorithm was verified three additional test cases were run with different random numbers used for sampling and a different initial guess. The initial guess for the additional cases was generated by modifying the previous cases initial guess by adding additional new fuel assemblies and randomly changing the LP using sampling types 1-3. The 2nd, 3rd and 4th initial solutions had 5, 10, and 15 additional new fuel assemblies, respectively; and after the new fuel assemblies were added they were shuffled 10000, 20000, and 30000 times, respectively.

5.2.2 New Fuel Type Array and Variable Sampling Probability Evaluations

After the functionality of BWROPT was verified and the PSA and SA comparison was complete the new fuel type array and variable sampling probabilities were evaluated. The same PSA parameters and constraint limits/weights that were used in the PSA evaluation were used for these tests. The same three cycles (2-4) were optimized and the Haling depletion was also used for these cases. To evaluate the new fuel type array three different sampling type sets were used in optimizations with four different starting solutions and random number vectors (the same two used in the PSA/SA comparison). The three sampling type sets were: random new fuel sampling (all sampling types except 7 and 9), ordered new fuel sampling (all sampling types except 6 and 8), and all sampling types. The cases using all sampling types were the same as the four cases used to evaluate the PSA implementation. All of the cases for the new fuel type array evaluation were evaluated using equal and constant sampling probabilities. To evaluate the variable sampling probability function a second set of the all sampling type cases was run using individual change type convergence with 5 CSs required for convergence and a phase out period of 5 CSs. Convergence criteria 3b was enabled for the variable sampling probability test cases.

5.2.3 Control Rod Pattern Search Evaluation

Several additional test cases were run using the CRP search for depletion to test both the function of the CRP search and the optimization capability of the code when using the CRP search. The main focus of these tests was to analyze the ability of the CRP search algorithm to eliminate constraint violations and also a comparison of the CRP search case results with the Haling depletion case results. It was also desired to know the benefit of using the CRP found for the previous solution as the initial guess in the CRP search. To test this two cases were run with

the same parameters except one used ARO as the initial guess and the other used the CRP from the previous solution as the initial guess. Both of these test cases used a constant Markov chain length of 10. Two test cases using the variable Markov chain length option with average values of 10 and 20 iterations per Markov chain were run to evaluate the effectiveness of the variable Markov chain option. Because of the long runtime of the CRP search compared to the Haling depletion it was decide to run all of the CRP search test cases with a temperature initialization parameter, α, of 1.0. The quality factor, λ, was set to .1 for the constant calculations with a Markov chain length of 10 and .5 for the calculation with an average Markov chain length of 20. The depletion step size (CRP evaluation interval) was set to 2000 MWD/MTU for all of these cases. The CRP test cases were run with all of the sampling types enabled and all of the other calculation parameters were the same as for the other test cases. Individual change type convergence was used for the case with an average Markov chain length of 20 with 5 CS to converge and 5 CS phase out. Also because of the long runtime of these cases the calculation restart option was enabled and used as necessary.

5.2.4 Fuel Cost Data Used for Test Cases

For the test cases the actual cost of the fuel is not very important. However, it is important that the relative assembly costs be reasonable so the code can differentiate between the assemblies. The data used to calculate the cost of the assemblies used in the test cases is included in Table 5.6. The uranium ore and conversion prices were obtained from the Ux Consulting Company website [40]. This website also has SWU cost but the SWU cost used is believed to be the result of a typographical error based on the data from the website because 10 $/SWU is much too low. The assembly cost was set to an even 100000 $ per assembly and the burnable poison

cost was set to 10000 $ per kg to make the assemblies with burnable poisons somewhat more expensive than those without burnable poisons. Losses during the fabrication and conversion steps were set to half a percent each and an interest rate of 15 % was used.

Table 5.6 – Fuel cost parameters used for test cases.

Component	Time (months)	Cost
Uranium Ore	15	42.25 $/lb U_3O_8 [40]
Ore Conversion	12	10.5 $/kg UF_6 [40]
Enrichment	9	10.0 $/SWU
Fabrication	3	100000 $/assembly
Burnable Poison	3	10000 $/kg

Chapter 6 Results and Discussion

6.1 Starting Solutions for Test Cases

The OFs for each of the starting solutions used in the test cases are given in Table 6.1. The constraint values and FCC for the first cycle as well as the new fuel inventory for all cycles are also included. From the table it can be seen that the OF for initial solution 1 is about 7 while the OFs for initial solutions 2-4 are all approximately 2.5 (roughly one third). This is due to the LP operator used in initial solution 1 which can be seen in Figure 6.1. This LP is used in all of the cycles and as can be seen the new fuel is much too clumped together for a practical implementation. Oddly enough, this does not impact the first cycle much due to the reactivity distribution of the old fuel but causes high power peaking in the latter cycles being considered. Loading pattern operator plots for initial solutions 2-4 are also included in Figure 6.2 through Figure 6.4, respectively. From the plots it can be seen that the new fuel is distributed much more evenly in these solutions, which is due to the large number of random changes (10k, 20k, and 30k, respectively) used to create them.

Table 6.1 – Starting parameters for each test case.

Constraint	Limit	Initial 1	Initial 2	Initial 3	Initial 4	Average
New Fuel Inventory		4 – Type 1 20 – Type 2 40 – Type 6 Total = 64	9 – Type 1 20 – Type 2 40 – Type 6 Total = 69	14 – Type 1 20 – Type 2 40 – Type 6 Total = 74	19 – Type 1 20 – Type 2 40 – Type 6 Total = 79	
OF	-	6.96	2.66	2.35	2.70	3.67
Fuel Cost ($/kWh)	-	$4.23*10^{-3}$	$4.47*10^{-3}$	$4.71*10^{-3}$	$4.96*10^{-3}$	$4.59*10^{-3}$
EOC k_{eff}	1.0	.953	.957	.953	.954	.954
Max 2D RPF	1.5	1.55	1.56	1.42	1.44	1.49
Max 3D RPF	2.0	1.92	1.91	1.75	1.76	1.84
Max 2D EXP (GWD/MTU)	35.0	26.8	25.5	25.7	25.1	25.8
Max 3D EXP (GWD/MTU)	45.0	32.7	31.2	31.4	30.6	31.5

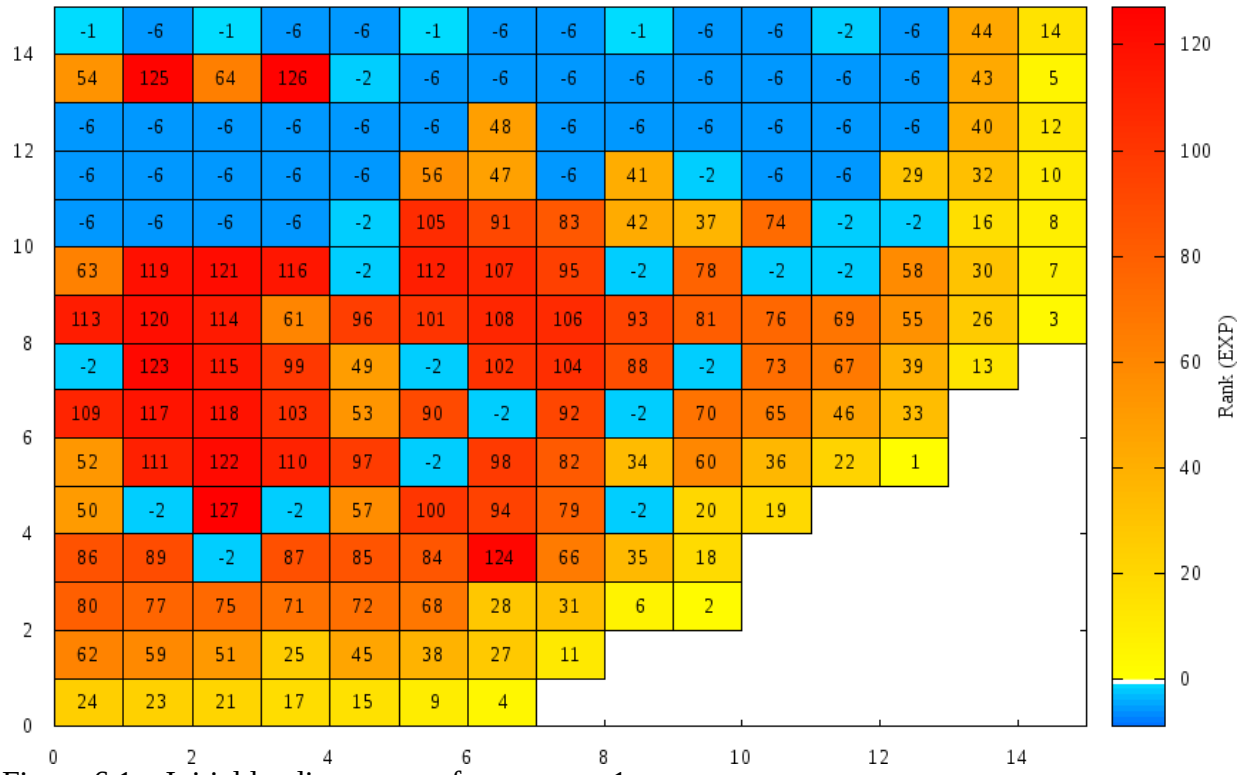

Figure 6.1 – Initial loading pattern for test case 1.

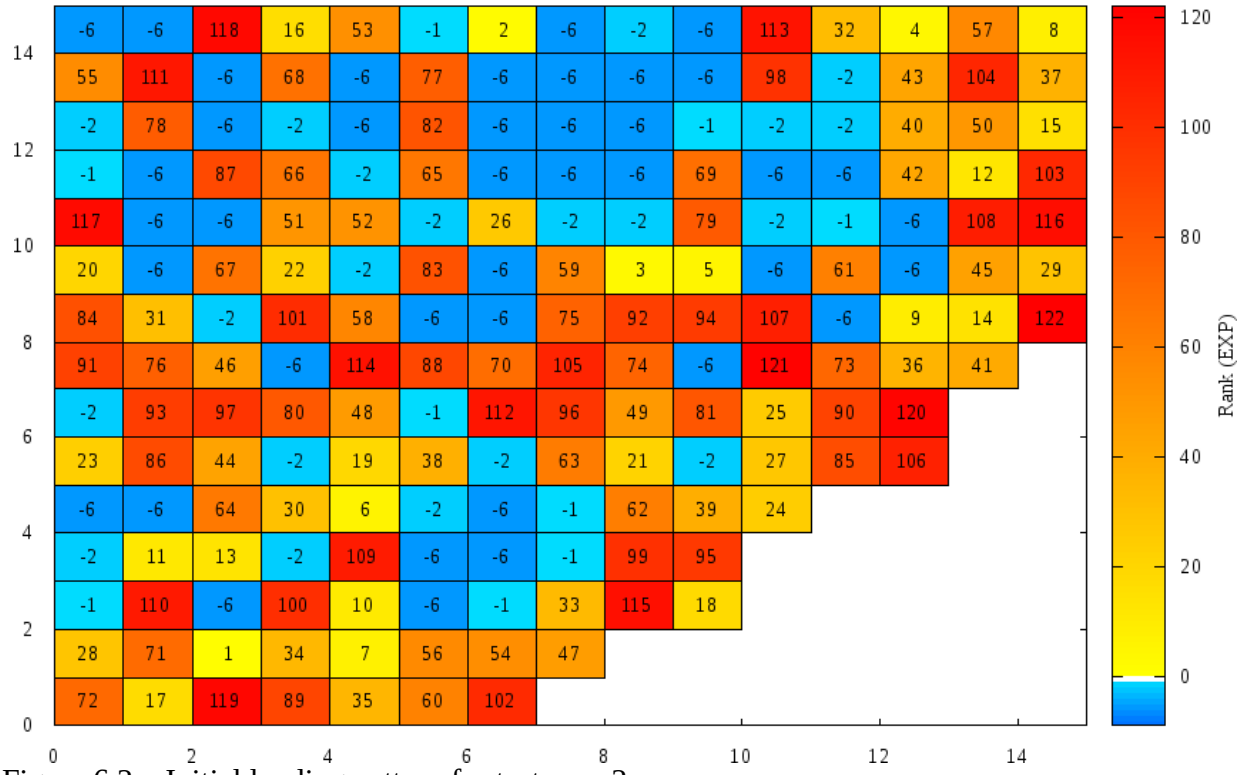

Figure 6.2 – Initial loading pattern for test case 2.

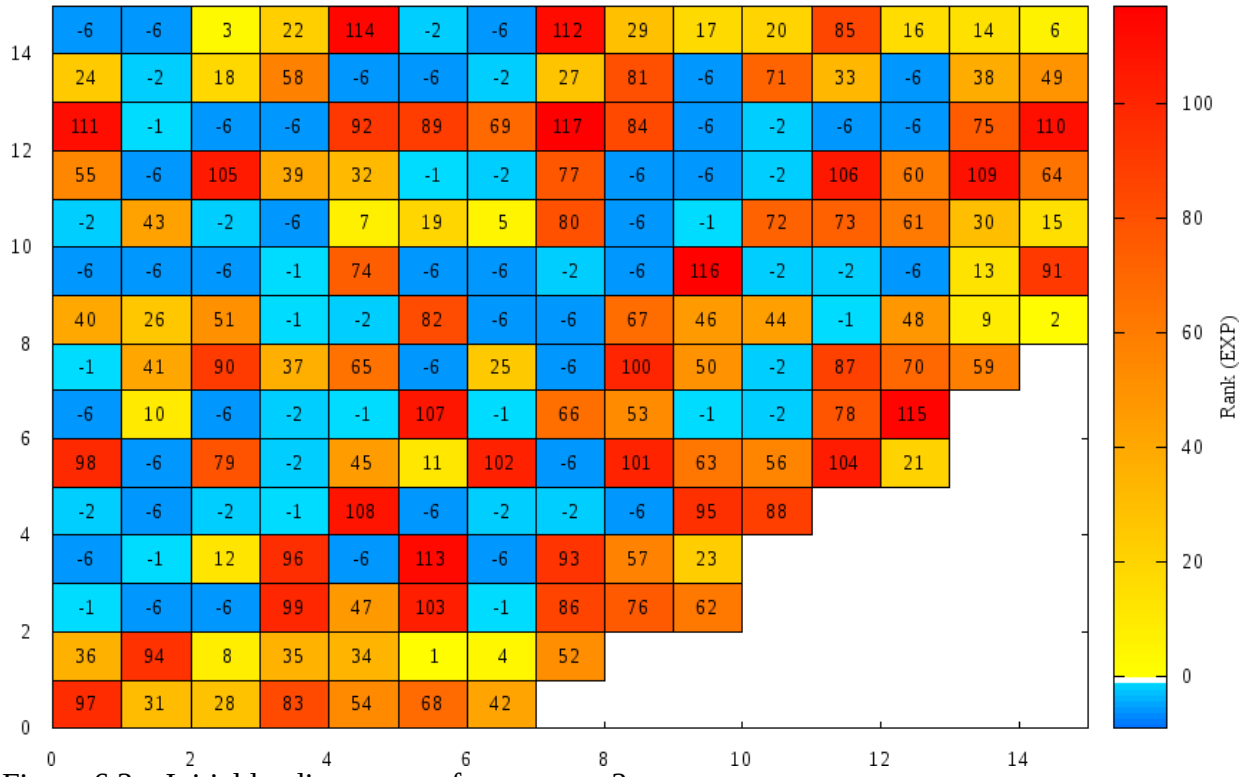

Figure 6.3 – Initial loading pattern for test case 3.

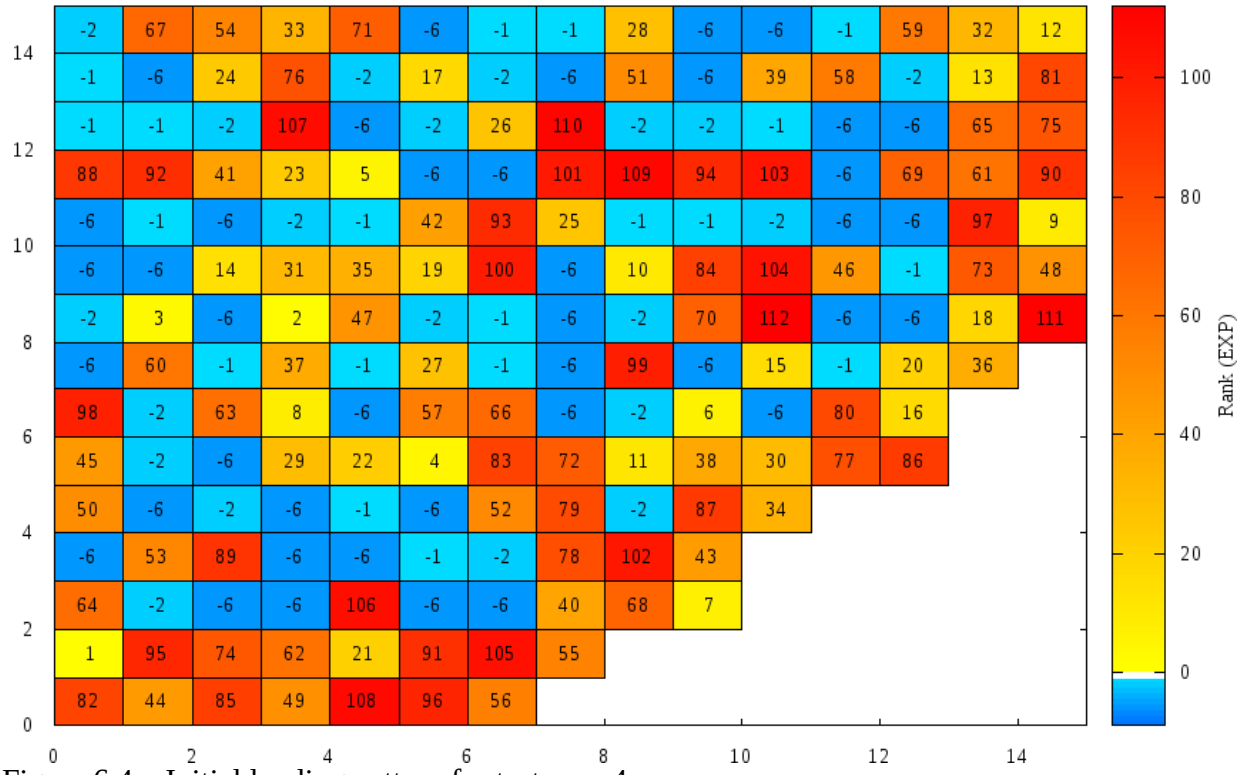

Figure 6.4 – Initial loading pattern for test case 4.

6.2 PSA Implementation Evaluation Results

The results of the PSA implementation evaluation are presented in Table 6.2, which includes: the number of cooling steps, convergence criteria met, new fuel inventory for the first cycle of the best solution, OF of the best solution, and the constraint values for the first cycle of the best solution (data for all cycles is available in Appendix D). The number of CSs is used as a substitute for runtime because of the heterogeneity of the Beowulf cluster. The Haling depletion optimizations generally took between 2 and 3 days to complete. Calling the solutions presented the best is a bit of a misnomer because there were often multiple solutions with the minimum OF and the same new fuel inventory in the first cycle. If there were multiple solutions with the minimum OF the first solution in the archive is presented as the best. Comparing the OF values for the test cases given in this table to the initial values given in Table 6.1 shows a substantial improvement in the OF for all of the test cases with a reduction of approximately 98 percent for the first test case and 94 percent for test cases 2, 3, and 4. The constraint values shown in the table show the optimization was also able to remove all of the constraint violations for these test cases.

The new fuel inventory for the first cycle of the best solution is very different for all of the test cases. The total number of new assemblies varies from 79 for test case 1 to 93 for test case 2 with test cases 3 and 4 having 82 and 90 new assemblies, respectively. The variation in the number of new fuel assemblies is somewhat offset by the average enrichment of the new fuel assemblies being lower for the cases with more new fuel but the FCC still increases with the number of new fuel assemblies. All of the new fuel types except 4, 5, and 9 were used in the solutions. Fuel type 7 which has an enrichment of 3% and contains burnable poison rods makes up a large portion of the new fuel in every test case. The remainder of the new fuel is mostly

types 6 and 2 (2% enrichment with and without burnable poisons, respectively) with a moderate number of type 1 in test case 1.

Table 6.2 - Summary of results for the all sampling type test cases (All Values except Cooling Steps and OF are for the First Cycle).

Constraint	Limit	All 1	All 2	All 3	All 4	Average
Cooling Steps	-	275	274	231	246	256.5
Convergence Criteria Met	-	3a	3a	3a	3a	
New Fuel Inventory	-	10 – Type 1 1 – Type 2 2 – Type 3 1 – Type 6 64 – Type 7 1 – Type 8 Total = 79	4 – Type 2 2 – Type 3 44 – Type 6 42 – Type 7 1 – Type 8 Total = 93	23 – Type 2 3 – Type 3 56 – Type 7 Total = 82	43 – Type 2 2 – Type3 2 – Type 6 43 – Type7 Total = 90	86
OF	-	.1461	.1547	.1493	.1587	.1522
Fuel Cost ($/kWh)	-	$6.48*10^{-3}$	$7.16*10^{-3}$	$6.69*10^{-3}$	$6.95*10^{-3}$	$6.82*10^{-3}$
EOC k_{eff}	1.0	1.001	1.001	1.004	1.005	1.003
Max 2D RPF	1.5	1.48	1.50	1.50	1.50	1.50
Max 3D RPF	2.0	1.87	1.89	1.88	1.88	1.88
Max 2D EXP (GWD/MTU)	35.0	24.8	23.5	24.4	24.0	24.2
Max 3D EXP (GWD/MTU)	45.0	30.6	29.2	30.1	29.8	29.9

Plots of the LP for the first cycle of the best solution found in test cases 1 through 4 using all of the sampling types are included in Figure 6.5 through Figure 6.8, respectively (LP plots for cycles 2 and 3 are included in Appendix E). The new fuel in these plots is somewhat more grouped than would be expected especially for test cases 2 and 4. Test case 2 looks much more grouped that test case 4 because the new fuel in test case 2 is mostly types 6 and 7 (dark blue) whereas there is a large fraction of type 2 (light blue) in test case 4. The increased fuel grouping is mostly the result of the large number of new fuel assemblies used in these LPs (roughly half new fuel for test case 2 and 4). Generally, around a third of the core is replaced with new fuel during reloading for equilibrium cycles, which for the test cases would be 64 assemblies.

However, this is only the second cycle of operation for the reactor modeled in the test cases so the fuel cycle has not reached equilibrium. The number of new fuel assemblies decreases for all of the test cases in the following two cycles.

Having the new fuel as grouped as it is in these LPs would generally cause the power to be highly peaked especially at BOC, which would violate the constraints. The LPs determined by the optimization are only possible because a significant portion of the new fuel used contains burnable poisons which significantly reduce the reactivity of the assemblies at low burnup. Also, as mentioned previously the peaking calculated with the Haling depletion is supposed to be best case and is not necessarily achievable.

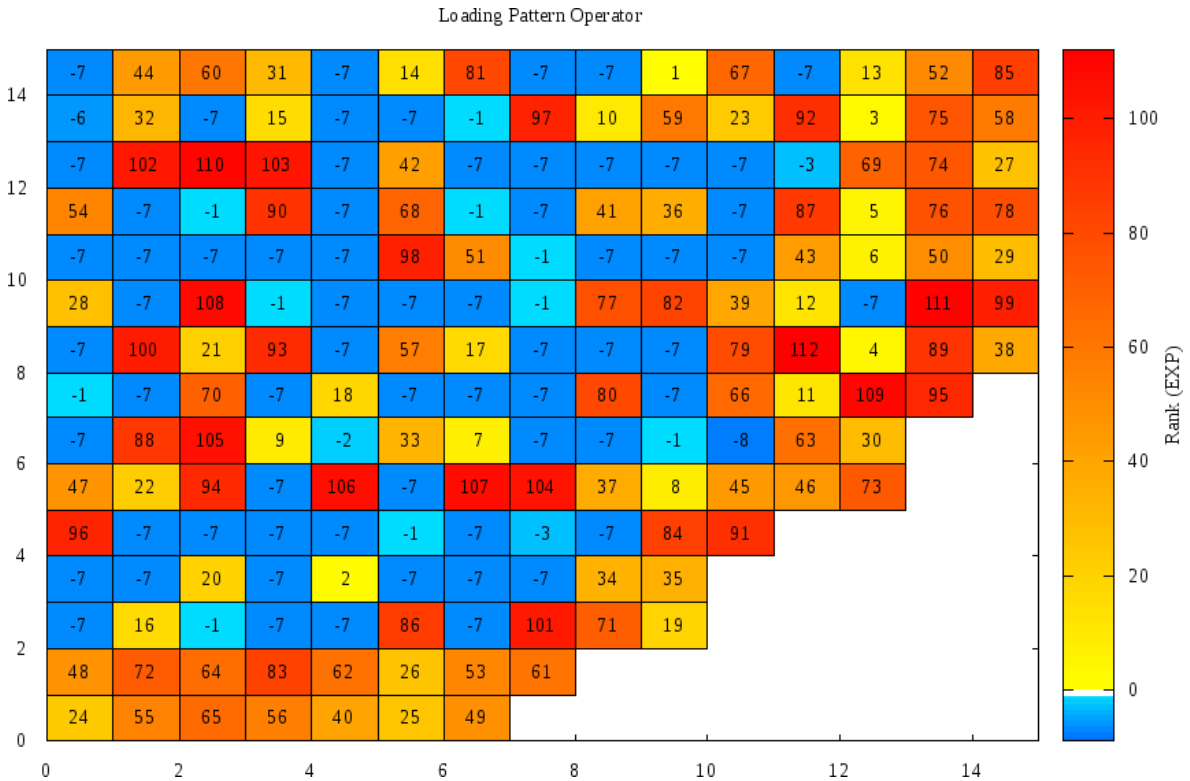

Figure 6.5 – Initial cycle LP for the best solution for test case 1 using all sampling types.

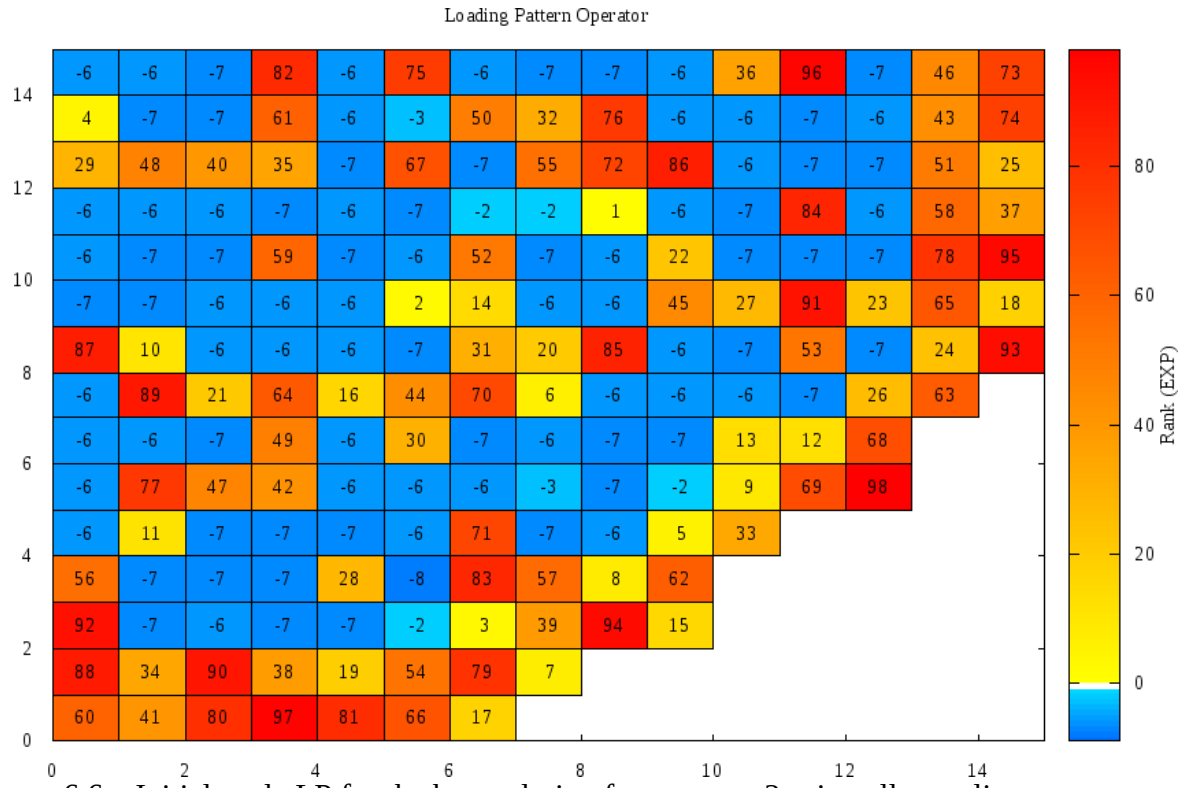

Figure 6.6 – Initial cycle LP for the best solution for test case 2 using all sampling types.

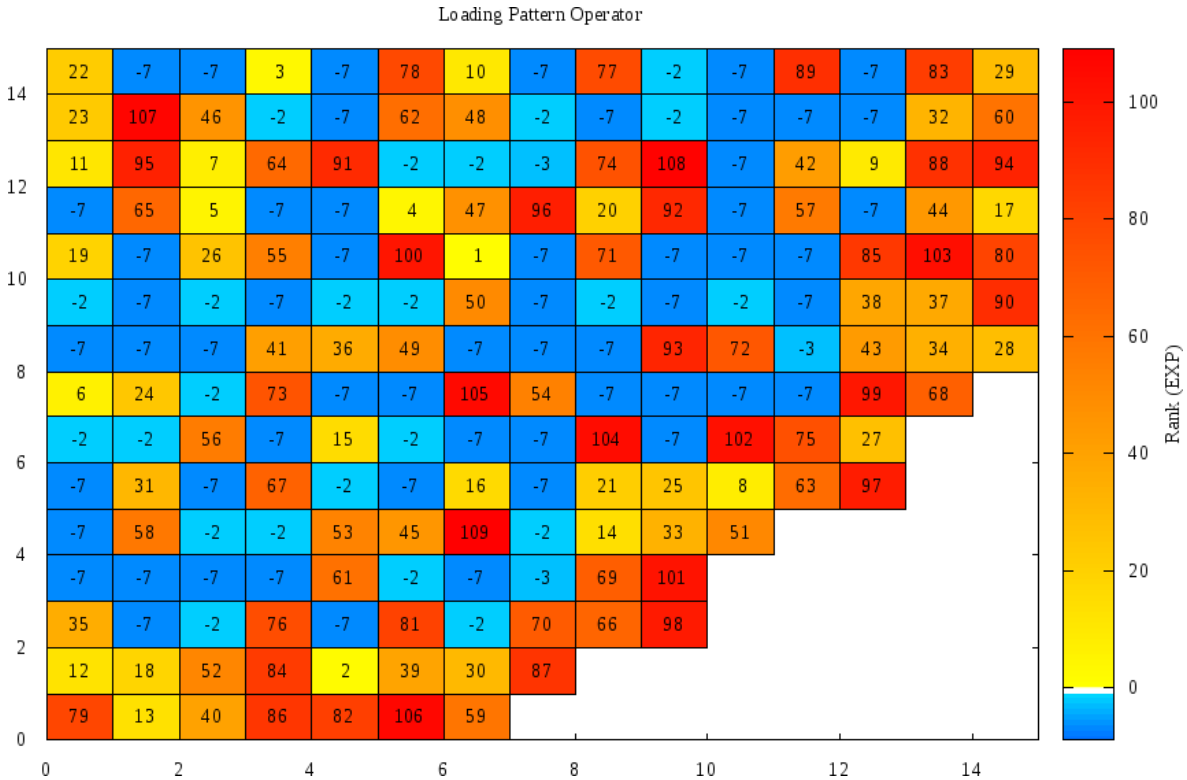

Figure 6.7 - Initial cycle LP for the best solution for test case 3 using all sampling types.

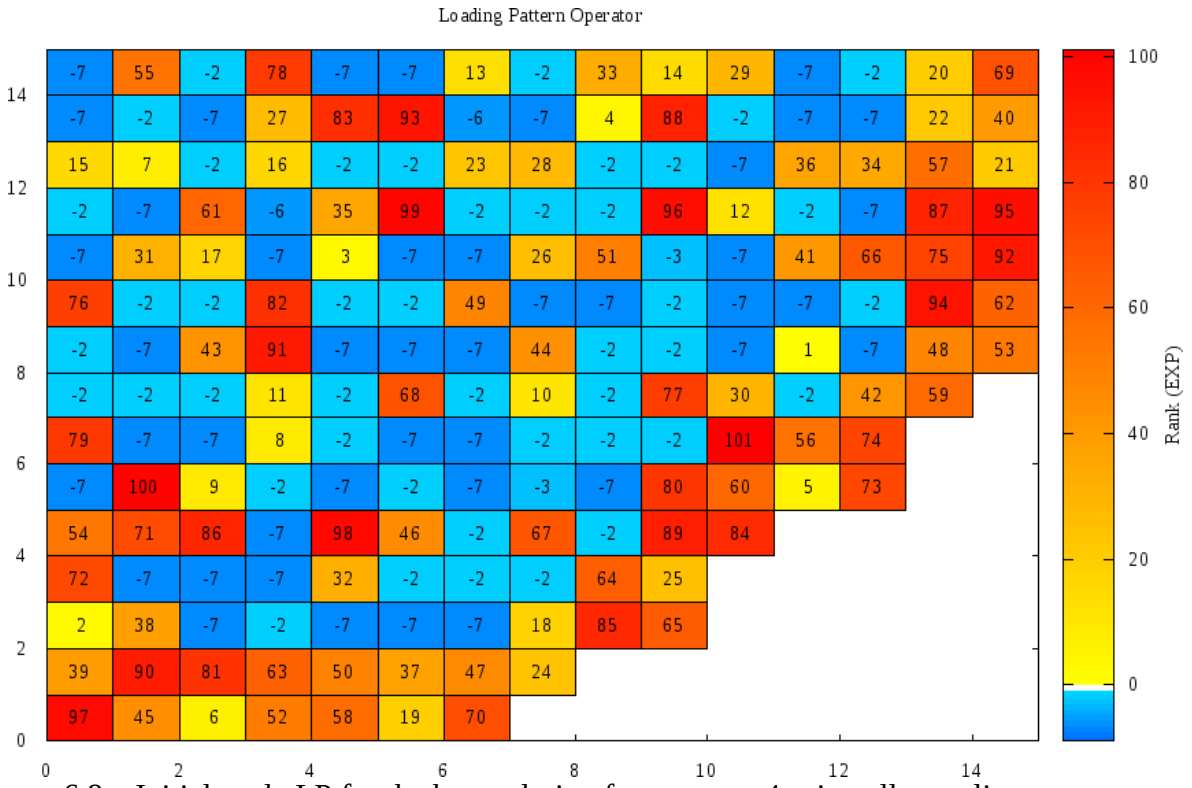

Figure 6.8 – Initial cycle LP for the best solution for test case 4 using all sampling types.

The convergence behavior of test case 1 using all sampling types is shown in Figure 6.9 and Figure 6.10. Figure 6.9 shows the general trend of the OF throughout the optimization is a negative exponential but there are several bumps were the OF increases somewhat potentially avoiding a local minima. In Figure 6.10 the acceptance ratio of each change type at each CS is shown. This plot shows that the larger change types 6, 8 (single assembly and batch random new fuel type sampling, respectively), and 10 (batch split and combine) generally have the lowest acceptance ratio early in the optimization. Latter in the optimization change types 8 and 10 are still among the lowest acceptance ratio change type 6 has a relatively high acceptance ratio and types 4 and 5 (random and ordered number of new fuel assemblies, respectively) have low acceptance ratios. Change type 9 (ordered batch type change) also drops below change type 6 at the end of the optimization. Change types 6 and 7 (ordered assembly type change) are the last to

be regularly accepted except for change types 1-3 which shuffle the fuel in the LP. Of the shuffle change types 1 (exchanging 2 old assemblies) is the most likely to be accepted with types 2 (exchanging an old and new assembly) and 3 (exchanging 2 new assemblies) tied. This convergence order mirrors the magnitude of the changes and was the inspiration for implementing variable sampling probabilities.

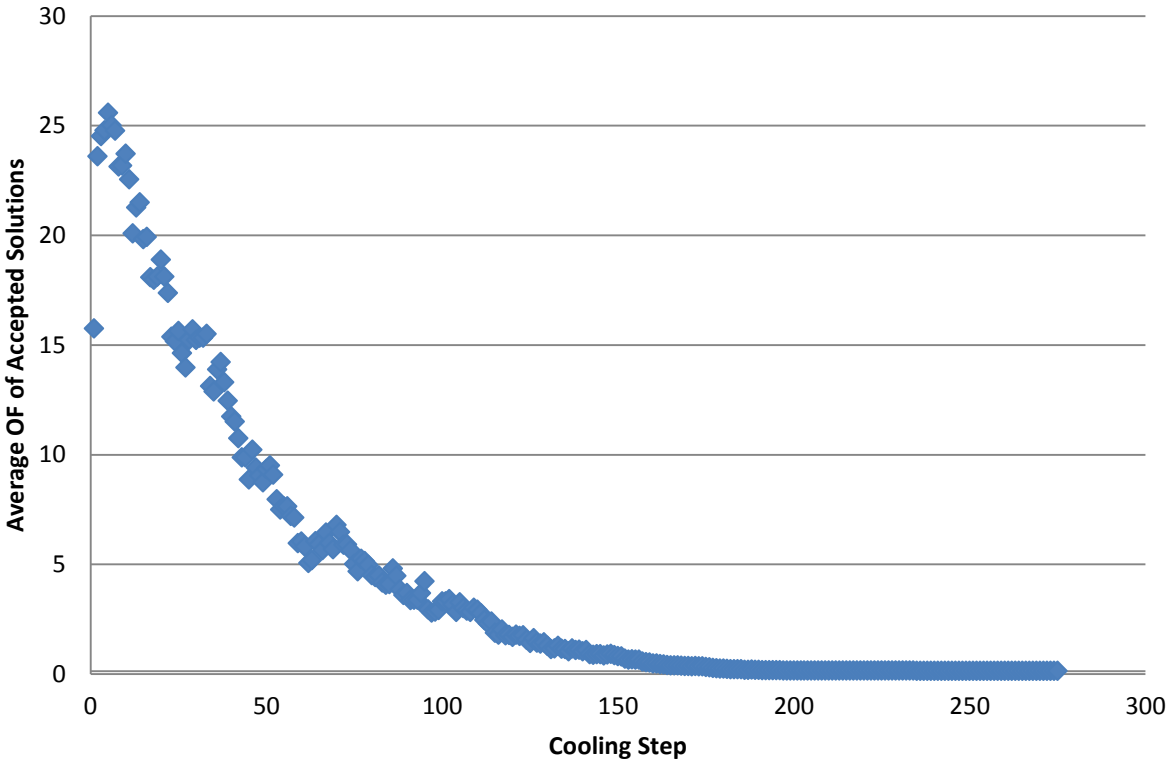

Figure 6.9 – Average OF vs. cooling step for test case 1 using all sampling types.

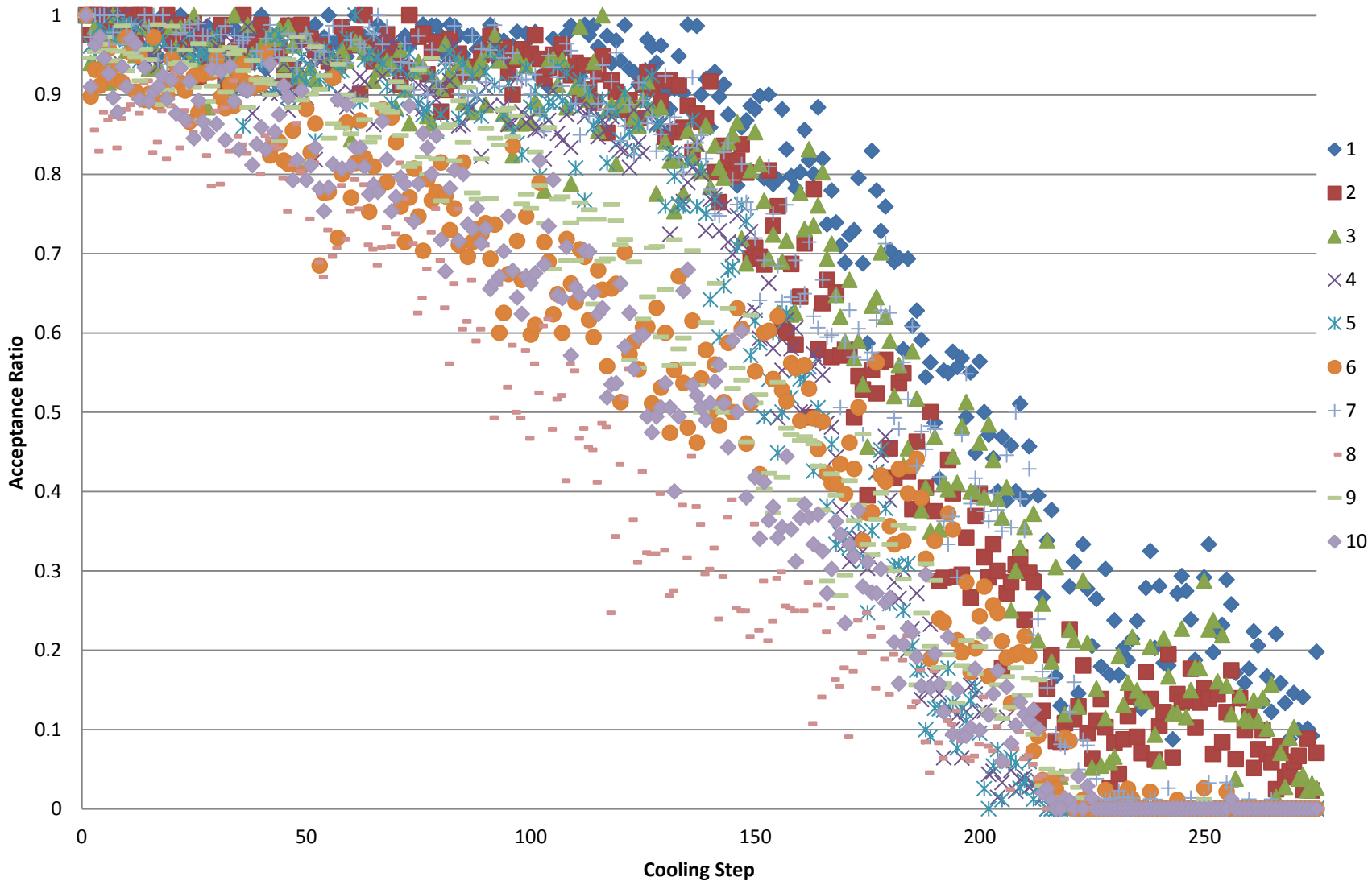

Figure 6.10 – Change type acceptance ratio versus cooling step for test case 1 using all sampling types.

When selecting the constraint values and weights the fraction of the OF made up by each component of the OF was used to find appropriate values. To illustrate this, the average fraction of the OF made up by each component for the solutions in each CS is plotted in Figure 6.11. The plot shows that all of the constraints except for the assembly and node exposure contribute significantly to the OF. The burnup limits were set to mimic real world reactor operations where fuel assemblies can typically stay in the core for 3 cycles without violating the burnup limits. Coupled with the decision to use cycles 2 through 4 for the test cases this made the impact of the burnup limits minimal. In Figure 6.12 the same fractional OF data is plotted for accepted solutions only. This plot show that at the end of the optimization all accepted solutions have no constraint violations and, consequently, their OF is entirely dependent on their FCC. In Figure 6.14 the fractional OF data for accepted solutions is converted to OF data to show that the FCC is fairly constant throughout the optimization but the constraints start large and then decrease.

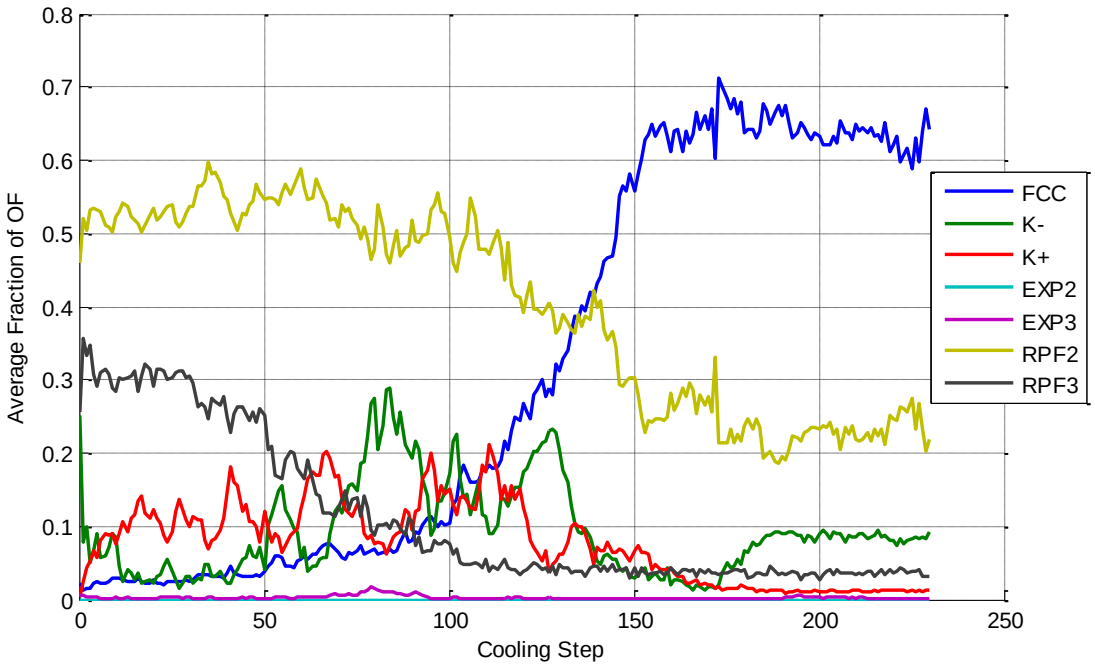

Figure 6.11 – Average fraction of the OF contributed by each component for all solutions as a function of the cooling step.

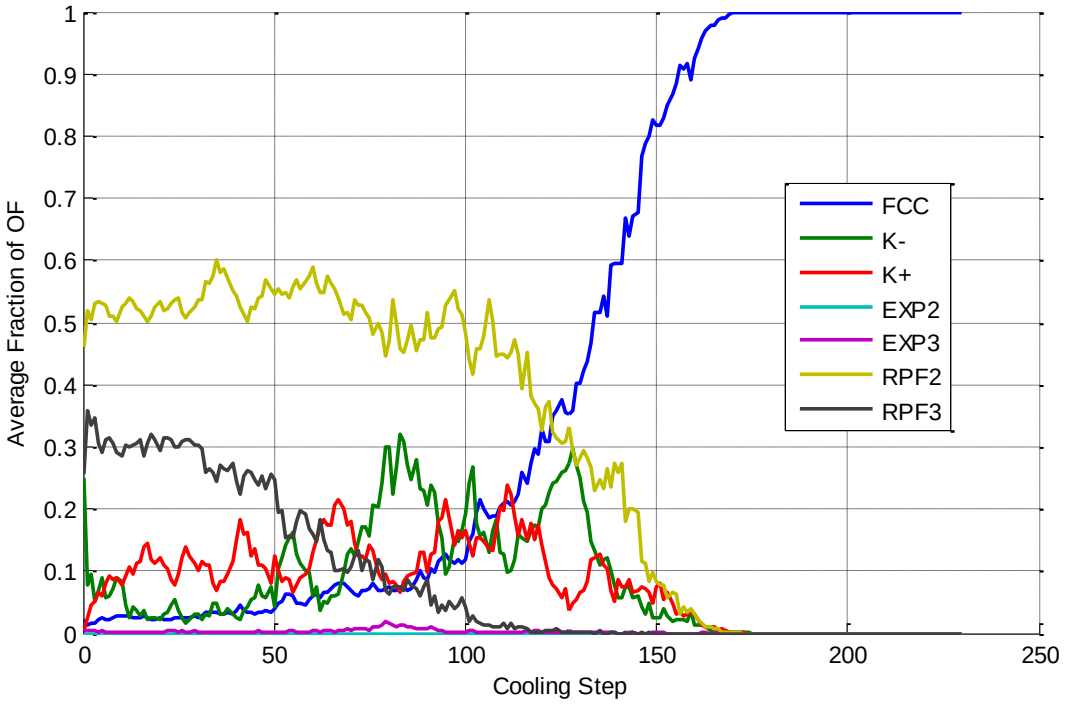

Figure 6.12 – Average fraction of the OF contributed by each component for accepted solutions as a function of the cooling step.

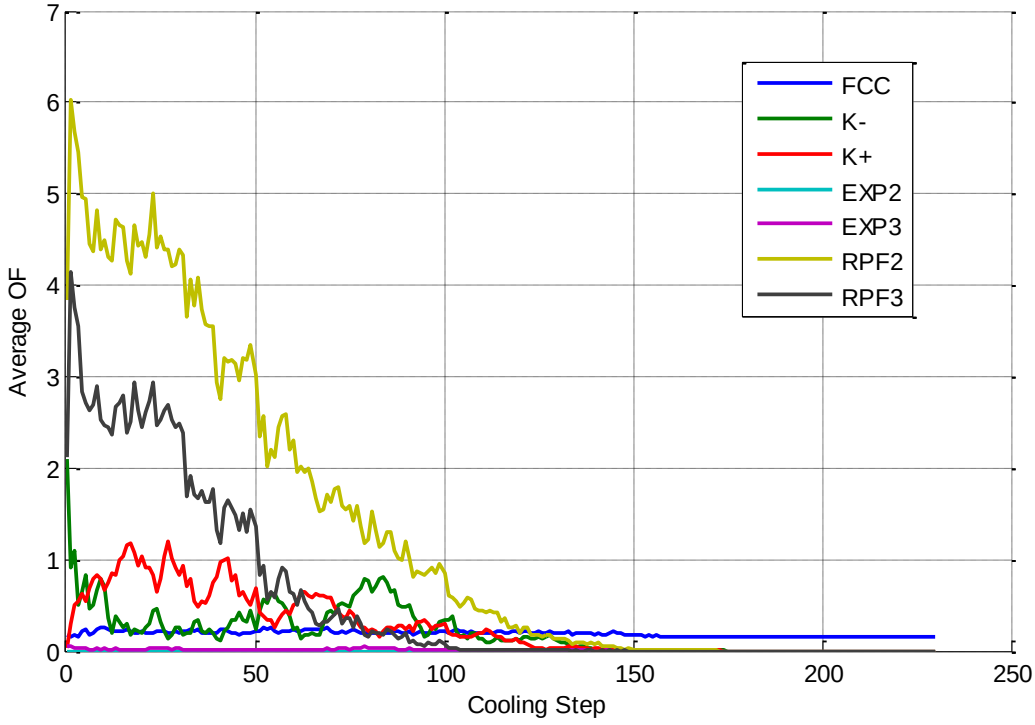

Figure 6.13 – Average OF of the individual OF components for accepted solutions as a function of the cooling step.

6.4 New Fuel Type Array Evaluation Results

The new fuel type array evaluation consists of comparing the results of the ordered only and random only new fuel type sampling test cases with each other and the all sampling type cases used to test the PSA implementation. The results of the ordered and random test cases are presented in Table 6.3 and Table 6.4, respectively, with more data and LP plots included in Appendices D and E, respectively. Random sampling produced lower OF solutions than ordered sampling in every test case except the 3rd and required more CSs to converge for all of the test cases. This is the result of ordered sampling only being able to change the fuel types incrementally, which makes significant change slower and causes the optimization to be more likely to get stuck in a local minimum. This limitation is evidenced by the ordered cases best new fuel inventory being much closer to the initial new fuel inventory of the test cases (large number of type 2 assemblies) than the best new fuel inventory in the random cases. Because of this limitation random only sampling will generally produce better results than ordered only, with the possible exception of using the code to try to improve on a very good initial guess.

Comparing the cases that used both random and ordered sampling (all sampling types) to the random sampling only cases is a little less clear cut. The OF found using all sampling types was better for 3 of the test cases, but the number of CSs required for convergence was also higher using all of the sampling types for 3 test cases. On average the optimizations using all sampling types produced slightly better results but required 5.6 % more cooling steps. Since the calculations only took a few days to complete and nuclear reactors are only refueled every 1-2 years the runtime increase is not very significant. Therefore, the lower average OF obtained using all sampling types makes this the better option.

Table 6.3 - Summary of results for the ordered sampling test cases (All Values except Cooling Steps and OF are for the First Cycle).

Constraint	Limit	Ordered 1	Ordered 2	Ordered 3	Ordered 4	Average
Cooling Steps	-	279	308	240	259	272
Convergence Criteria Met	-	3a	3a	3a	3a	
New Fuel Inventory	-	32 – Type 2 1 – Type 3 1 – Type 6 48 – Type 7 Total = 82	38 – Type 2 6 – Type 3 3 – Types 6 38 – Type 7 Total = 85	18 – Type 2 1 – Type 6 60 – Type 7 1 – Type 8 Total = 80	1 – Type 1 81 – Type 2 16 – Type 3 4 – Type 6 Total = 102	87
OF	-	.1520	.1524	.1538	.1650	.1558
Fuel Cost ($/kWh)	-	$6.49*10^{-3}$	$6.60*10^{-3}$	$6.61*10^{-3}$	$7.18*10^{-3}$	$6.72*10^{-3}$
EOC k_{eff}	1.0	1.000	1.000	1.003	1.001	1.001
Max 2D RPF	1.5	1.50	1.49	1.48	1.49	1.49
Max 3D RPF	2.0	1.87	1.87	1.86	1.85	1.86
Max 2D EXP (GWD/MTU)	35.0	24.6	24.2	24.0	23.2	24.0
Max 3D EXP (GWD/MTU)	45.0	30.4	30.1	30.0	28.8	29.8

Table 6.4 - Summary of results for the random sampling test cases (All Values except Cooling Steps and OF are for the First Cycle).

Constraint	Limit	Random 1	Random 2	Random 3	Random 4	Average
Cooling Steps	-	266	235	239	232	243
Convergence Criteria Met	-	3a	3a	3a	3a	
New Fuel Inventory		6 – Type 2 16 – Type 6 59 – Type 7 Total = 81	4 – Type 1 2 – Type 2 1 – Type 6 69 – Type 7 Total = 76	1 – Type 1 16 – Type 2 5 – Type3 2 – Type 6 54 – Type 7 Total = 78	1 – Type 1 34 – Type 2 1 – Type 3 1 – Type 6 46 – Type 7 Total = 83	80
OF	-	.1494	.1472	.1554	.1594	.1529
Fuel Cost ($/kWh)	-	$6.61*10^{-3}$	$6.40*10^{-3}$	$6.40*10^{-3}$	$6.50*10^{-3}$	$6.48*10^{-3}$
EOC k_{eff}	1.0	1.000	1.002	1.002	1.000	1.001
Max 2D RPF	1.5	1.49	1.49	1.49	1.49	1.49
Max 3D RPF	2.0	1.93	1.90	1.87	1.88	1.90
Max 2D EXP (GWD/MTU)	35.0	24.9	24.7	24.2	24.4	24.6
Max 3D EXP (GWD/MTU)	45.0	31.0	30.5	30.3	30.3	30.5

6.5 Variable Sampling Probability Evaluation Results

The results of the variable sampling probability test cases are presented in Table 6.5 while constraint values for additional cycles and LP plots are included in Appendices D and E, respectively. The new fuel inventory in the first cycle is the same as the non-variable sampling probability calculations for test cases 1 and 2 with only slightly different LPs. The new fuel inventory for the variable and non-variable cases in the 2nd and 3rd cycles optimized is slightly different, but overall the results are very similar. The major difference in the variable and non-variable sampling probability optimizations is the run time; the variable cases took ~8 % fewer CSs to converge. The OF of the best solution found for each of the test cases was also marginally better for the variable sampling probability optimizations than the non-variable optimizations. This shows that using variable sampling probabilities is clearly better than using constant sampling probabilities.

Table 6.5 - Summary of results for the random and ordered sampling with variable sampling probability test cases (All Values except Cooling Steps and OF are for the First Cycle).

Constraint	Limit	Variable 1	Variable 2	Variable 3	Variable 4	Average
Cooling Steps	-	253	249	240	222	241
Convergence Criteria Met	-	3b	3b	3b	3b	
New Fuel Inventory		10 – Type 1 1 – Type 2 2 – Type 3 1 – Type 6 64 – Type 7 1 – Type 8 Total = 79	4 – Type 2 2 – Type 3 44 – Type 6 42 – Type 7 1 – Type 8 Total = 93	23 – Type 2 3 – Type 3 56 – Type 7 Total = 82	43 – Type 2 2 – Type 3 2 – Type 6 43 – Type 7 Total = 90	86
OF	-	.1456	.1539	.1494	.1586	.1519
Fuel Cost ($/kWh)	-	$6.48*10^{-3}$	$7.16*10^{-3}$	$6.69*10^{-3}$	$6.95*10^{-3}$	$6.82*10^{-3}$
EOC k_{eff}	1.0	1.001	1.001	1.004	1.005	1.003
Max 2D RPF	1.5	1.48	1.50	1.50	1.50	1.50
Max 3D RPF	2.0	1.87	1.90	1.88	1.88	1.88
Max 2D EXP (GWD/MTU)	35.0	24.8	23.5	24.4	24.0	24.2
Max 3D EXP (GWD/MTU)	45.0	30.6	29.2	30.1	29.9	30.0

6.6 Control Rod Pattern Search Evaluation Results

There was an error in the depletion of the CRP test cases with a Markov chain length of 10 (fixed and variable) so these calculations cannot be compared to the Haling depletion test cases. However, these cases can be used to compare variable length Markov chains with fixed length Markov chains and using the previous solutions CRP as the initial guess with starting the CRP search at ARO. The comparison with the Haling depletion optimizations was done using the variable length Markov chain case with an average length of 20.

6.6.1 Variable Length Markov Chain Evaluation Results

The node utilization for the fixed and variable length Markov chain calculations are shown in Ganglia plots in Figure 6.14 and Figure 6.15, respectively. These plots both represent one day of calculations for nodes with similar specifications. The red on these plots (denoted as system on the legend) represents a process being idle while waiting at a synchronization point and the user (blue) represents a process performing calculations. From looking at the plots it is clear that the variable length Markov chain calculation has much higher process utilization. The average user values given on the figures, 62.9% for fixed and 83.8% for variable, show that the variable length case had 33% higher utilization than the fixed length case. This higher utilization allowed the variable length case to complete an additional CS (the end of a CS is denoted by the large inverted red peaks) over the course of the day even though there are slightly more solutions evaluated in each CS for the variable length case.

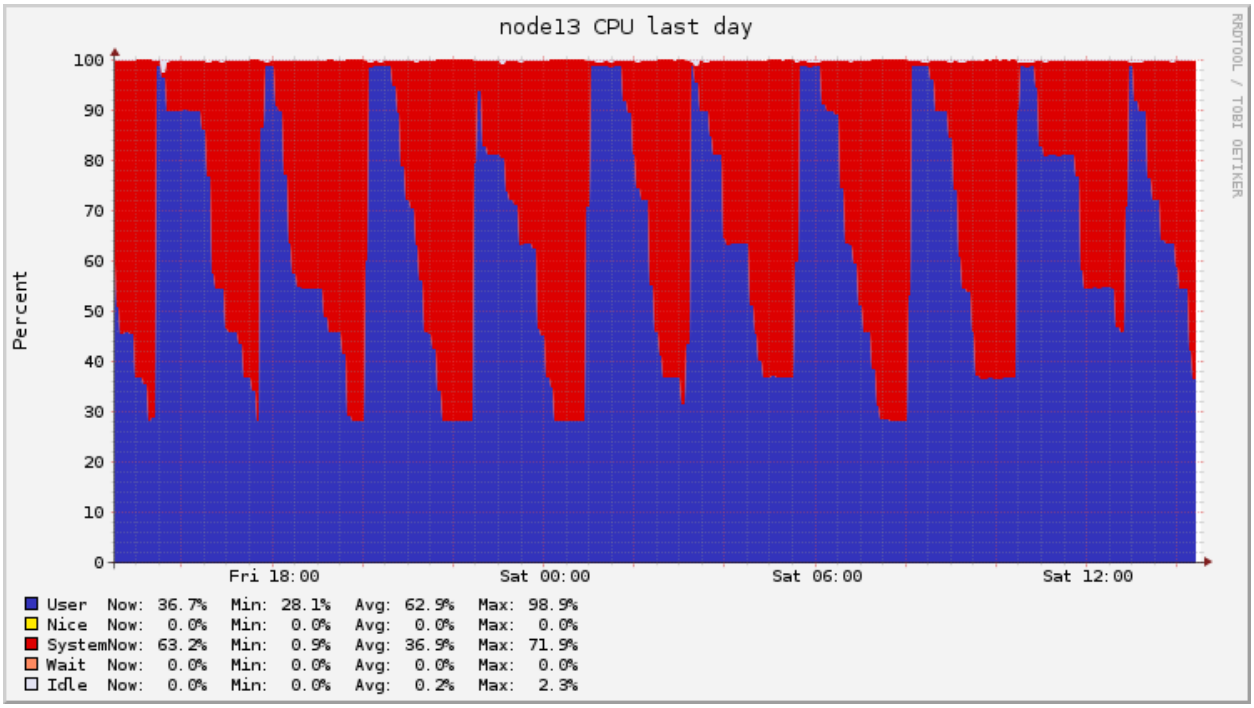

Figure 6.14 - Fixed length Markov chain node utilization produced by Ganglia.

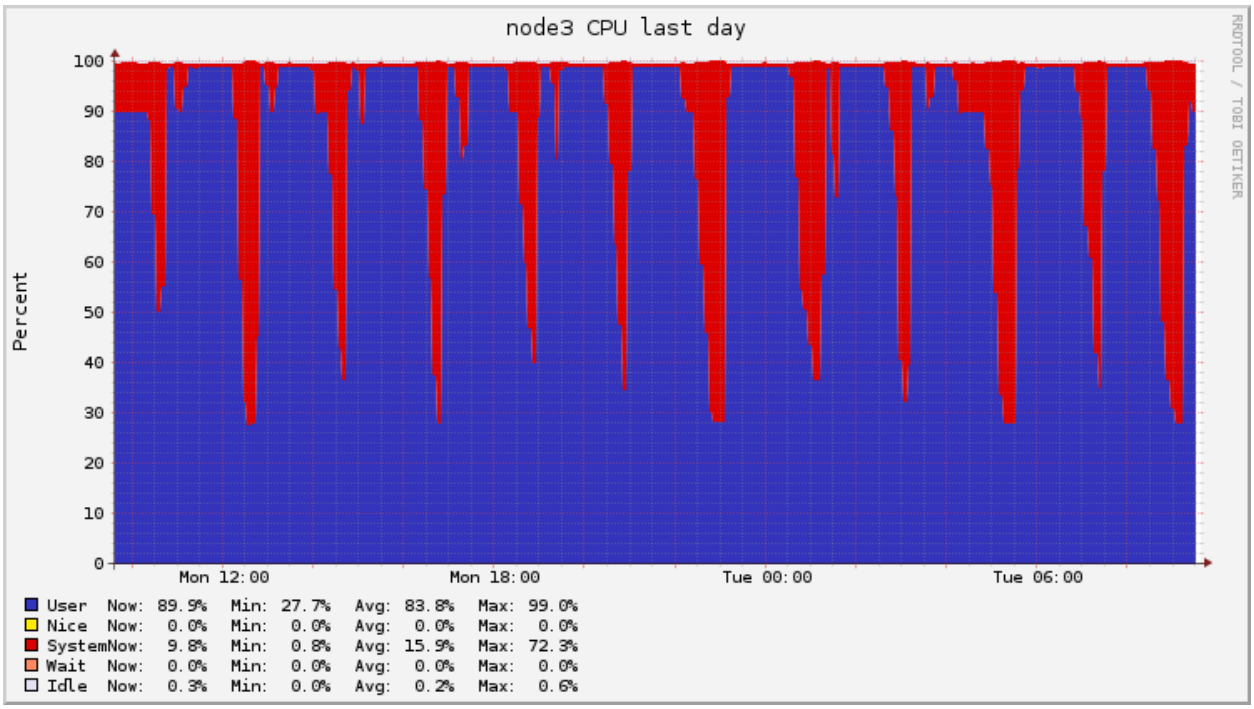

Figure 6.15 - Variable length markov chain node utilization plot produced by Ganglia.

6.6.2 Starting CRP ARO vs Previous Solution Evaluation Results

The average number of iterations necessary for the CRP search at each depletion step for both of the test cases is shown in Figure 6.16. Based on this figure starting the CRP search with the previous solution will on average require fewer iterations than starting ARO. The constraint elimination ratio for both cases is shown in Figure 6.17, which also shows clear benefits for starting with the previous solution. It should be noted that neither the ARO nor the previous solution CRP search optimizations converged so the data used for this comparison is cumulative up to CS 607 (the last CS both completed, ~97000 CRP searches). This may not be the best way to compare the methods because the CRP search success rate should increase as the optimization nears convergence and the solution acceptance fraction for CS 607 was 13.3% for the previous solution case and 7.0% for the ARO case. However, since this favors starting the CRP search with the previous solution and the data presented in Figure 6.16 and Figure 6.17 also favors starting the CRP search with the previous solution the comparison should be accurate.

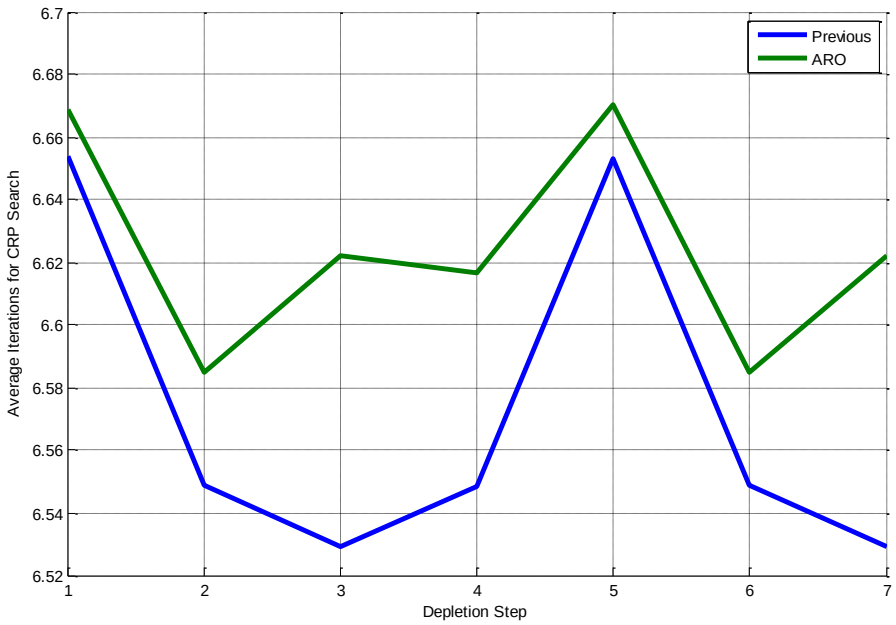

Figure 6.16 – Average number of iterations used to find CRP for ARO and previous start.

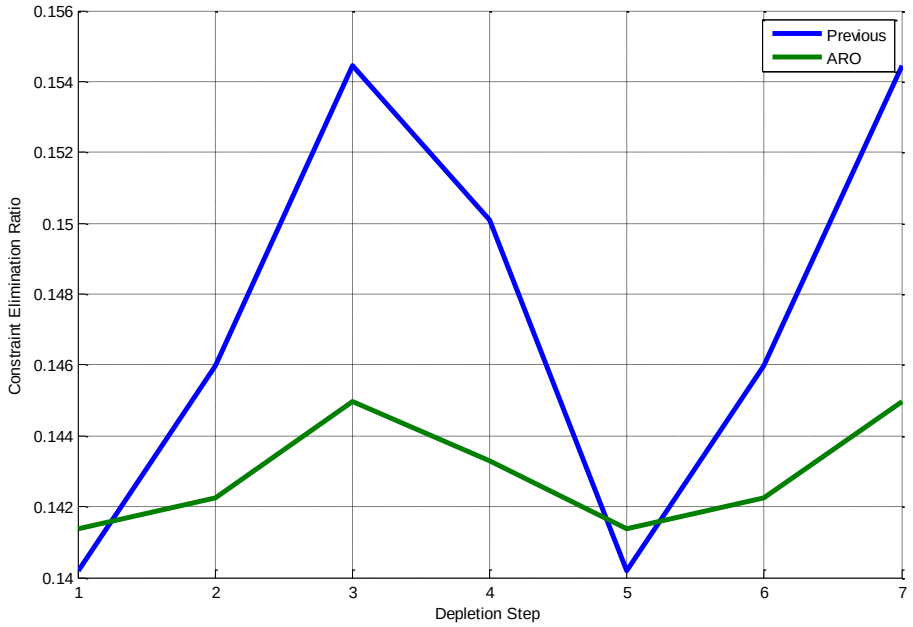

Figure 6.17 – CRP search success ratio for the ARO and previous start cases.

6.6.3 CRP Search Comparison with Haling Depletion

The CRP search test case intended to be compared to the Haling depletion test case 1 using all sampling types and variable sampling probabilities did not complete. The current best solution from the calculation after 30 days of running is presented in Table 6.6 with data for additional cycles available in Appendix D and LP operator plots in Appendix E. The OF for this case is much higher than the minimum OF found in the Haling depletion test case. There are also constraint violations for the 2D and 3D RPF. The poor performance of this test case is at least partially due to the larger quality factor which was used to try to reduce the calculations runtime but also reduces the thoroughness of the optimization.

Table 6.6 - Summary of results for the CRP search test case (All Values except Cooling Steps and OF are for the First Cycle).

Constraint	Limit	Case 1
Cooling Steps	-	212
Convergence Criteria Met	-	none
New Fuel Inventory		1 – Type 6 83 – Type 7 Total = 84
OF	-	4.460
Fuel Cost ($/kWh)	-	$7.29*10^{-3}$
EOC k_{eff}	1.0	1.001
Max 2D RPF	1.5	1.57
Max 3D RPF	2.0	2.06
Max 2D EXP (GWD/MTU)	35.0	24.5
Max 3D EXP (GWD/MTU)	45.0	29.4

Chapter 7 Conclusions and Future Work

BWROPT a BWR fuel cycle optimization code using the PSA algorithm was developed and shown to be capable of performing multi-cycle BWR fuel cycle optimization. The code eliminated all of the constraints and significantly reduced the OF in 16 test cases that used the Haling depletion option. Several of the improvements on past work in BWR fuel cycle optimization that were developed and implemented in BWROPT were successful. The use of variable sampling probabilities decreased the runtime and improved average solution quality compared to the standard approach of using constant sampling probabilities. Using random and ordered new fuel sampling improved the average solution quality but also increased the average runtime compared to using random sampling only. This presents a bit of a tradeoff but since fuel cycle optimization only has to be done every 18-24 months and the runtime increase was only a few hours using random and ordered sampling is probably the better option. Variable length Markov chains were shown to improve process utilization and reduce CS runtime for cases using the CRP search for only the first cycle. This result should be applicable to other cases which have a large variation in runtime for solution evaluations or cases with consistent runtimes evaluated on nonhomogeneous cluster nodes. Also starting the CRP search with the previous solution's CRP was shown to be modestly better than starting ARO. The CRP search test case that was to be compared with an equivalent Haling depletion test case did not converge in 30 days of running, but the acceptance ratio was less than 5% indicating the case is nearly converged. The results of the CRP search test case compared poorly with the results of the Haling depletion test case. The CRP search was also very slow compared to the Haling depletion test cases even though the quality factor, λ, used for the CRP search case was twice the value used in the Haling depletion cases. The greater quality factor used for the CRP search case

which was used to try to reduce the runtime may have contributed to the poorer results by causing the optimization to be more like simulated quenching than simulated annealing.

The most significant future work related to this research would be improving NESTLE by decreasing runtime and/or adding thermal limit calculations so more appropriate constraints can be considered in BWROPT. One method of improving the runtime would be to add an octant symmetry option to NESTLE which would roughly half the complexity of the test cases used in this research. Alternatively, BWROPT could be modified to work with a more advanced core simulator that already has these features. If the solution evaluation time was reduced through one of these improvements then performing optimizations with the CRP search would be much more feasible and the CRP search could maybe even be made more thorough without having excessive runtimes.

References

[1] R. Hays, Boiling Water Reactor In-Core Fuel Management through Parallel Simulated Annealing in FORMOSA-B, Raleigh: MS thesis, North Carolina State Univerity, 2009.

[2] D. Kropaczek, "COPERNICUS: A MultiCycle Nuclear Fuel Optimization Code Based on Coupled In-core Constraints," in *Advances in Nuclear Fuel Management IV,* Hilton Head Island, 2009.

[3] K.-W. Chu, Y. Deng and J. Reinitz, "Parallel Simulated Annealing by Mixing of States," *Journal of Computational Physics,* vol. 148, pp. 646-662, 1999.

[4] S. Kirkpatrick, C. D. Gelatt and M. P. Vecchi, "Optimization by Simulated Annealing," *Science,* vol. 220, pp. 671-680, 1983.

[5] B. Moore, P. Turinsky and A. Karve, "FORMOSA-B: A Boiling Water Reactor In-Core Fuel Managment Optimization Package," *Nuclear Technology,* vol. 126, pp. 153-169, 1999.

[6] A. Karve and P. Turinsky, "FORMOSA-B: a Boiling Water Reactor In-Core Fuel Managment Optimization Package II," *Nuclear Technology,* vol. 131, pp. 48-68, 2000.

[7] Hays, R. and Turinsky, P., "BWR in-core fuel management optimization using parallel simulated in FORMOSA-B," *Progress in Nuclear Energy,* vol. 53, pp. 600-606, 2011.

[8] F. Glover, E. Taillard and D. de Werra, "A User's Guide to Tabu Serach," *Annals of Operations Research,* vol. 41, no. 1, pp. 3-28, 1993.

[9] D. Kropaczek and W. Russel, "Method for Optimization of BWR Fuel Managment and Plant Operations," in *Advances in Nuclear Fuel Managment III,* Hilton Head Island, 2003.

[10] C. Oyarzun and et al, "The GNF Optimization System for BWR Fuel Managment," in *Advances in Nuclear Fuel Managment III*, Hilton Head Island, 2003.

[11] J. Ortiz and et al, "A New System to Fuel Loading and Control Rod Pattern Optimization in Boiling Water Reactors," *Nuclear Science and Engineering,* vol. 157, pp. 236-244, 2007.

[12] R. K. Haling, "Operating Strategy for Maintaining an Optimum Power Distribution Throughout Life," TID-7672, US Atomic Energy Commission, 1964.

[13] J. J. Ortiz and I. Requena, "Using a multi-state recurrent neural network to optimize loading patterns in BWRs," *Annals of Nuclear Energy,* vol. 31, pp. 789-803, 2004.

[14] J. J. Oritz and I. Requena, "Azcatl-CRP: An ant colony-based system for searching full

power control rod patterns in BWRs," *Annals of Nuclear Energy,* vol. 33, pp. 30-36, 2006.

[15] M. Dorigo and L. M. Gambardella, "Ant colony system: a cooperative learning approach to the traveling salesman problem," in *IEEE Transactions on Evolutionary Computation*, 1997.

[16] J. J. Oritz and I. Requena, "An Order Coding Genetic Algorithm to Optimize Fuel Reloads in a Nuclear Boiling Water Reactor," *Nuclear Science and Engineering,* vol. 146, pp. 88-98, 2004.

[17] A. Yamamoto and et al, "Simultaneous Loading Patterns Optimization for Two Successive Cycles of Pressurized Water Reactors," *Nuclear Science and Technology,* vol. 41, no. 11, pp. 1065-1074, 2004.

[18] S. Du, Implementation of Genetic Algorithms and Parallel Simulated Annealing in OCEON-P, Raleigh: MS Thesis, North Carolina State University, 2008.

[19] K. A. Anderson, P. J. Turinsky and P. M. Keller, "Improvement of OCEON-P Optimization Capabilities," in *Trans. Am. Nucl. Soc. 96*, 2007.

[20] K. A. Anderson and et al, "OCEON-P Linkage with SIMULATE3," in *Trans. Am. Nucl. Soc. 96*, 2007.

[21] L. S. Lin and C. Lin, "A Rule-Based Expert System for Automatic Control Rod Pattern Generation for Boiling Water Reactors," *Nuclear Technology,* vol. 95, pp. 1-8, 1991.

[22] M. S. Taner, S. H. Levine and M. Hsiao, "A Two-Step Method for Developing a Control Rod Program for Boiling Water Reactors," *Nuclear Technology,* vol. 97, pp. 27-38, 1992.

[23] N. Metropolis, A. Rosenbluth, M. Rosenbluth, A. Teller and E. Teller, "Equation of State Calculations by Fast Computing Machines," *Journal of Chemical Physics,* vol. 21, no. 6, pp. 1087-1092, 1953.

[24] D. J. Kropaczek, "COPERNICUS: A Multi-Cycle Optimization Code for Nuclear Fuel Based on Parallel Simulated Annealing with Mixing of States," *Progress in Nulcear Energy,* vol. 53, pp. 554-561, 2011.

[25] P. J. Turinsky, R. M. Al-Chalabi, P. Engrand, H. N. Sarsour, F. X. Faure and W. Guo, "Code Abstract - NESTLE: A Few-Group Neutron Diffusion Equation Solver Utilizing the Nodal Expansion Method for Eigenvalue, Adjoint, Fixed-Source Steady-State and Transient Problems,"," *Nucl. Sci. & Engr.,* vol. 120, p. 72, 1995.

[26] Galloway, J., Hernandez, H., Maldonado, G. I., Jessee, M., Popov, E., Clarno, K., "BWR Modeling Capability and SCALE/TRITON Lattice-to-Core Integration of the NESTLE Nodal Simulator," in *CD-ROM, PHYSOR 2010*, Pittsburgh, PA, May 9-14, 2010.

[27] J. Lam and J.-M. Delosme, "An Efficient Simulated Annealing Schedule: Derivation," Technical Report 8816, Electrical Engineering Department, Yale, New Haven, CT, 1988.

[28] J. Lam and J.-M. Delosme, "An Efficient Simulated Annealing Schedule: Implementation and Evaluation," Technical Report 8817, Electrical Engineering Department, Yale, New Haven, CT, 1988.

[29] T. J. Downar and J. K. Young, "A Reverse Depletion Method for Pressurized Water Reactor Core Reload Design," *Nuclear Technology,* vol. 73, pp. 42-54, 1986.

[30] J. S. Suh and S. H. Levine, "Optimized Automatic Reload Program for Pressurized Water Reactors Using Simple Direct Optimization Techniques," *Nuclear Science and Technology,* vol. 105, no. 4, pp. 371-382, 1990.

[31] Y. Kobayashi and E. Aiyoshi, "Optimization of Boiling Water Reactor Loading Pattern Using Two-Stage Genetic Algorithm," *Nuclear Science and Engineering,* vol. 142, pp. 119-139, 2002.

[32] D. Kropaczek, *personal communication,* 2010.

[33] T. Williams and C. Kelley, "gnuplot 4.6," 2012.

[34] Electric Power Research Center at North Carolina State University, "NESTLE Version 5.2.1: Few-Group Neutron Diffusion Equation Solver Utilizing The Nodal Expansion Method for Eigenvalue, Adjoint, Fixed-Source Steady-State and Transient Problems," July 2003.

[35] M. D. DeHart and S. M. Bowman, "Reactor Physics Methods and Analysis Capabilities in SCALE," *Nuclear Technology,* vol. 174, no. 2, pp. 196-213, 2011.

[36] G. I. Maldonado, J. Galloway, H. Hernandez, K. T. Clarno, E. L. Popov, M. A. Jessee, "Integration of the NESTLE Core Simulator with SCALE," *Transactions of the ANS,* vol. 100, p. 619, 2009.

[37] J. Galloway, Boiling Water Reactor Core Simulation with Generalized Isotopic Inventory Tracking for Actinide Management, Knoxvile: PhD Dissertation, University of Tennessee

Knoxvile, 2010.

[38] H. Hernandez, Pin-Wise Loading Optimizationand Lattice-to-Core Coupling for Isotopic Management in Light Water Reactors, Knoxville: PhD Dissertation, University of Tennessee Knoxvile, 2010.

[39] N. H. Larson, "Core Design and Operating Data for Cycles 1 and 2 of Peach Bottom 2," Electric Power Research Institute (EPRI), 1978.

[40] The Ux Consulting Company, "Fuel Cost Calculator," 2014. [Online]. Available: http://www.uxc.com/tools/FuelCalculator.aspx. [Accessed May 2013].

Appendix

Appendix A – Comparison of Old and New NESTLE Output Formats

A.1 - Old Output Format

```
        (( POINTWISE KINF  EDIT ))

                            PLANE #  4


 AVERAGE BURNUP :      0.00 MWD/MTM

 Y/X       3           4           5           6           7           8

   3
   4
   5                                                                 0.11322E+01
   6                                                                 0.11316E+01
   7                                                     0.11316E+01 0.10332E+01
   8                           0.11321E+01 0.11314E+01 0.11309E+01 0.11307E+01
   9                           0.11315E+01 0.11309E+01 0.11305E+01 0.11304E+01
  10               0.11319E+01 0.10332E+01 0.11305E+01 0.11302E+01 0.10328E+01
  11  0.11323E+01 0.11317E+01 0.10331E+01 0.11304E+01 0.11378E+01 0.10324E+01
  12  0.11322E+01 0.11317E+01 0.11313E+01 0.11306E+01 0.11379E+01 0.11379E+01
  13  0.11322E+01 0.11318E+01 0.87583E+00 0.87670E+00 0.11385E+01 0.11381E+01
  14  0.11322E+01 0.11320E+01 0.77617E+00 0.87645E+00 0.11384E+01 0.10330E+01
  15  0.11322E+01 0.11318E+01 0.10334E+01 0.11312E+01 0.11383E+01 0.10326E+01
  16  0.11322E+01 0.11317E+01 0.11316E+01 0.11309E+01 0.11383E+01 0.11381E+01
  17  0.11322E+01 0.11318E+01 0.87563E+00 0.87634E+00 0.11387E+01 0.11383E+01
  18  0.11322E+01 0.11320E+01 0.77619E+00 0.87630E+00 0.11385E+01 0.10330E+01
  19  0.11322E+01 0.11318E+01 0.10334E+01 0.11312E+01 0.11384E+01 0.10327E+01
  20  0.11322E+01 0.11318E+01 0.11316E+01 0.11309E+01 0.11383E+01 0.11381E+01
  21  0.11322E+01 0.11318E+01 0.87568E+00 0.87643E+00 0.11387E+01 0.11382E+01
  22  0.11322E+01 0.11320E+01 0.77614E+00 0.87657E+00 0.11383E+01 0.10329E+01
  23  0.11322E+01 0.11317E+01 0.10332E+01 0.11309E+01 0.11381E+01 0.10325E+01
  24  0.11323E+01 0.11316E+01 0.11310E+01 0.11304E+01 0.11378E+01 0.11378E+01
  25               0.11319E+01 0.11312E+01 0.11305E+01 0.11302E+01 0.11380E+01
  26                           0.11316E+01 0.10330E+01 0.11306E+01 0.10330E+01
  27                           0.11322E+01 0.11316E+01 0.11312E+01 0.10330E+01
  28                                                     0.11316E+01 0.11311E+01
  29                                                                 0.11315E+01
  30                                                                 0.11321E+01
  31
  32


        (( POINTWISE KINF  EDIT ))

                            PLANE #  4


 AVERAGE BURNUP :      0.00 MWD/MTM

 Y/X       9          10          11          12          13          14
```

3			0.11324E+01	0.11324E+01	0.11324E+01	0.11324E+01
4		0.11320E+01	0.11318E+01	0.10338E+01	0.10340E+01	0.11321E+01
5	0.11317E+01	0.11313E+01	0.11312E+01	0.11314E+01	0.87543E+00	0.87515E+00
6	0.10332E+01	0.11307E+01	0.11306E+01	0.10333E+01	0.77600E+00	0.87593E+00
7	0.10328E+01	0.11303E+01	0.11380E+01	0.10327E+01	0.10329E+01	0.11388E+01
8	0.11308E+01	0.11380E+01	0.11379E+01	0.11380E+01	0.11386E+01	0.11383E+01
9	0.88992E+00	0.88983E+00	0.11383E+01	0.11380E+01	0.88990E+00	0.88995E+00
10	0.77558E+00	0.88982E+00	0.11378E+01	0.10328E+01	0.77558E+00	0.88991E+00
11	0.10324E+01	0.11382E+01	0.11377E+01	0.10323E+01	0.10324E+01	0.11383E+01
12	0.11383E+01	0.11377E+01	0.11376E+01	0.11377E+01	0.11382E+01	0.11378E+01
13	0.88983E+00	0.88975E+00	0.11382E+01	0.11378E+01	0.88976E+00	0.88976E+00
14	0.77563E+00	0.88983E+00	0.11378E+01	0.10328E+01	0.77555E+00	0.88982E+00
15	0.10326E+01	0.11383E+01	0.11378E+01	0.10324E+01	0.10324E+01	0.11382E+01
16	0.11385E+01	0.11379E+01	0.11377E+01	0.11377E+01	0.11383E+01	0.11378E+01
17	0.88994E+00	0.88984E+00	0.11382E+01	0.11379E+01	0.88978E+00	0.88976E+00
18	0.77567E+00	0.88989E+00	0.11379E+01	0.10328E+01	0.77555E+00	0.88981E+00
19	0.10326E+01	0.11383E+01	0.11378E+01	0.10324E+01	0.10324E+01	0.11382E+01
20	0.11385E+01	0.11379E+01	0.11377E+01	0.11377E+01	0.11383E+01	0.11378E+01
21	0.88989E+00	0.88979E+00	0.11382E+01	0.11378E+01	0.88976E+00	0.88975E+00
22	0.77560E+00	0.88981E+00	0.11378E+01	0.10327E+01	0.77553E+00	0.88980E+00
23	0.10325E+01	0.11382E+01	0.11377E+01	0.10323E+01	0.10324E+01	0.11382E+01
24	0.11383E+01	0.11377E+01	0.11376E+01	0.11377E+01	0.11382E+01	0.11378E+01
25	0.88984E+00	0.88976E+00	0.11382E+01	0.11378E+01	0.88977E+00	0.88978E+00
26	0.77567E+00	0.88986E+00	0.11379E+01	0.10328E+01	0.77560E+00	0.88991E+00
27	0.10327E+01	0.11384E+01	0.11379E+01	0.10325E+01	0.10326E+01	0.11385E+01
28	0.11306E+01	0.11302E+01	0.11378E+01	0.11380E+01	0.11386E+01	0.11383E+01
29	0.10331E+01	0.11305E+01	0.11304E+01	0.11306E+01	0.87672E+00	0.87656E+00
30	0.11315E+01	0.11311E+01	0.11309E+01	0.10334E+01	0.77613E+00	0.87564E+00
31		0.11318E+01	0.11317E+01	0.11317E+01	0.11318E+01	0.11320E+01
32			0.11323E+01	0.11322E+01	0.11322E+01	0.11322E+01

((POINTWISE KINF EDIT))

PLANE # 4

AVERAGE BURNUP : 0.00 MWD/MTM

Y/X	15	16	17	18	19	20
3	0.11324E+01	0.11324E+01	0.11324E+01	0.11324E+01	0.11323E+01	0.11323E+01
4	0.11320E+01	0.10339E+01	0.10340E+01	0.11321E+01	0.11320E+01	0.11320E+01
5	0.11319E+01	0.11317E+01	0.87518E+00	0.87512E+00	0.11318E+01	0.11317E+01
6	0.11313E+01	0.10335E+01	0.77610E+00	0.87582E+00	0.11313E+01	0.10335E+01
7	0.11385E+01	0.10330E+01	0.10331E+01	0.11389E+01	0.11386E+01	0.10330E+01
8	0.11382E+01	0.11383E+01	0.11388E+01	0.11384E+01	0.11383E+01	0.11383E+01
9	0.11385E+01	0.11382E+01	0.89004E+00	0.89003E+00	0.11386E+01	0.11382E+01
10	0.11380E+01	0.10329E+01	0.77566E+00	0.88998E+00	0.11381E+01	0.10329E+01
11	0.11379E+01	0.10325E+01	0.10325E+01	0.11384E+01	0.11379E+01	0.10325E+01
12	0.11377E+01	0.11378E+01	0.11384E+01	0.11379E+01	0.11378E+01	0.11378E+01
13	0.11382E+01	0.11379E+01	0.88982E+00	0.88980E+00	0.11383E+01	0.11379E+01
14	0.11379E+01	0.10328E+01	0.77557E+00	0.88984E+00	0.11379E+01	0.10328E+01
15	0.11378E+01	0.10324E+01	0.10325E+01	0.11383E+01	0.11378E+01	0.10324E+01
16	0.11377E+01	0.11378E+01	0.11383E+01	0.11378E+01	0.11377E+01	0.11378E+01
17	0.11382E+01	0.11379E+01	0.88979E+00	0.88978E+00	0.11382E+01	0.11379E+01

18	0.11378E+01	0.10328E+01	0.77556E+00	0.88983E+00	0.11379E+01	0.10328E+01
19	0.11378E+01	0.10324E+01	0.10324E+01	0.11382E+01	0.11378E+01	0.10324E+01
20	0.11377E+01	0.11377E+01	0.11383E+01	0.11378E+01	0.11377E+01	0.11377E+01
21	0.11382E+01	0.11378E+01	0.88977E+00	0.88976E+00	0.11382E+01	0.11378E+01
22	0.11378E+01	0.10328E+01	0.77555E+00	0.88981E+00	0.11378E+01	0.10328E+01
23	0.11377E+01	0.10324E+01	0.10324E+01	0.11382E+01	0.11378E+01	0.10324E+01
24	0.11377E+01	0.11378E+01	0.11383E+01	0.11378E+01	0.11377E+01	0.11377E+01
25	0.11383E+01	0.11379E+01	0.88985E+00	0.88982E+00	0.11383E+01	0.11379E+01
26	0.11380E+01	0.10329E+01	0.77567E+00	0.88996E+00	0.11381E+01	0.10329E+01
27	0.11381E+01	0.10327E+01	0.10327E+01	0.11386E+01	0.11381E+01	0.10326E+01
28	0.11383E+01	0.11383E+01	0.11388E+01	0.11384E+01	0.11383E+01	0.11383E+01
29	0.11312E+01	0.11310E+01	0.87640E+00	0.87645E+00	0.11312E+01	0.11309E+01
30	0.11314E+01	0.10336E+01	0.77618E+00	0.87560E+00	0.11314E+01	0.10336E+01
31	0.11318E+01	0.11318E+01	0.11318E+01	0.11320E+01	0.11317E+01	0.11317E+01
32	0.11322E+01	0.11322E+01	0.11322E+01	0.11322E+01	0.11322E+01	0.11322E+01

((POINTWISE KINF EDIT))

PLANE # 4

AVERAGE BURNUP : 0.00 MWD/MTM

Y/X	21	22	23	24	25	26
3	0.11323E+01	0.11324E+01	0.11323E+01	0.11324E+01		
4	0.10340E+01	0.11320E+01	0.11319E+01	0.11319E+01	0.11320E+01	
5	0.87532E+00	0.87531E+00	0.11316E+01	0.11313E+01	0.11315E+01	0.11318E+01
6	0.77606E+00	0.87609E+00	0.11310E+01	0.10330E+01	0.10331E+01	0.11313E+01
7	0.10330E+01	0.11388E+01	0.11383E+01	0.10327E+01	0.10328E+01	0.11309E+01
8	0.11387E+01	0.11382E+01	0.11381E+01	0.11381E+01	0.11387E+01	0.11308E+01
9	0.89000E+00	0.88996E+00	0.11384E+01	0.11381E+01	0.89000E+00	0.89011E+00
10	0.77565E+00	0.88992E+00	0.11380E+01	0.10329E+01	0.77567E+00	0.89005E+00
11	0.10325E+01	0.11383E+01	0.11379E+01	0.10325E+01	0.10326E+01	0.11385E+01
12	0.11383E+01	0.11379E+01	0.11378E+01	0.11378E+01	0.11384E+01	0.11381E+01
13	0.88982E+00	0.88980E+00	0.11383E+01	0.11380E+01	0.88989E+00	0.88995E+00
14	0.77558E+00	0.88986E+00	0.11379E+01	0.10328E+01	0.77566E+00	0.89004E+00
15	0.10325E+01	0.11383E+01	0.11379E+01	0.10325E+01	0.10326E+01	0.11386E+01
16	0.11383E+01	0.11379E+01	0.11378E+01	0.11379E+01	0.11385E+01	0.11382E+01
17	0.88981E+00	0.88980E+00	0.11383E+01	0.11380E+01	0.88994E+00	0.89003E+00
18	0.77557E+00	0.88985E+00	0.11379E+01	0.10329E+01	0.77567E+00	0.89008E+00
19	0.10325E+01	0.11383E+01	0.11378E+01	0.10325E+01	0.10326E+01	0.11386E+01
20	0.11383E+01	0.11378E+01	0.11377E+01	0.11378E+01	0.11384E+01	0.11381E+01
21	0.88978E+00	0.88976E+00	0.11382E+01	0.11379E+01	0.88986E+00	0.88995E+00
22	0.77554E+00	0.88980E+00	0.11378E+01	0.10328E+01	0.77558E+00	0.88995E+00
23	0.10324E+01	0.11382E+01	0.11377E+01	0.10323E+01	0.10324E+01	0.11383E+01
24	0.11382E+01	0.11377E+01	0.11376E+01	0.11377E+01	0.11383E+01	0.11379E+01
25	0.88980E+00	0.88974E+00	0.11382E+01	0.11378E+01	0.88977E+00	0.88982E+00
26	0.77562E+00	0.88985E+00	0.11378E+01	0.10328E+01	0.77558E+00	0.88995E+00
27	0.10326E+01	0.11384E+01	0.11379E+01	0.10324E+01	0.10325E+01	0.11308E+01
28	0.11387E+01	0.11382E+01	0.11380E+01	0.11378E+01	0.11302E+01	0.11304E+01
29	0.87653E+00	0.87679E+00	0.11309E+01	0.11304E+01	0.11305E+01	0.11309E+01
30	0.77616E+00	0.87582E+00	0.11311E+01	0.10331E+01	0.10332E+01	0.11315E+01
31	0.11318E+01	0.11320E+01	0.11317E+01	0.11317E+01	0.11319E+01	
32	0.11322E+01	0.11322E+01	0.11322E+01	0.11323E+01		

((POINTWISE KINF EDIT))

PLANE # 4

AVERAGE BURNUP : 0.00 MWD/MTM

Y/X	27	28	29	30	31	32
3						
4						
5	0.11323E+01					
6	0.11317E+01					
7	0.10333E+01	0.11318E+01				
8	0.11310E+01	0.10334E+01	0.11318E+01	0.11323E+01		
9	0.11311E+01	0.11309E+01	0.11313E+01	0.11318E+01		
10	0.11383E+01	0.10328E+01	0.10331E+01	0.11315E+01	0.11321E+01	
11	0.11381E+01	0.10327E+01	0.10330E+01	0.11314E+01	0.11318E+01	0.11324E+01
12	0.11381E+01	0.11384E+01	0.11313E+01	0.11315E+01	0.11319E+01	0.11323E+01
13	0.11386E+01	0.11385E+01	0.87623E+00	0.87534E+00	0.11322E+01	0.11323E+01
14	0.11384E+01	0.10332E+01	0.77609E+00	0.87510E+00	0.10339E+01	0.11324E+01
15	0.11383E+01	0.10330E+01	0.10333E+01	0.11319E+01	0.11320E+01	0.11323E+01
16	0.11383E+01	0.11386E+01	0.11315E+01	0.11317E+01	0.11320E+01	0.11323E+01
17	0.11388E+01	0.11387E+01	0.87599E+00	0.87514E+00	0.11322E+01	0.11324E+01
18	0.11384E+01	0.10333E+01	0.77612E+00	0.87498E+00	0.10339E+01	0.11324E+01
19	0.11384E+01	0.10330E+01	0.10333E+01	0.11319E+01	0.10339E+01	0.11324E+01
20	0.11383E+01	0.11385E+01	0.11315E+01	0.11317E+01	0.11320E+01	0.11324E+01
21	0.11386E+01	0.11386E+01	0.87614E+00	0.87518E+00	0.11322E+01	0.11324E+01
22	0.11382E+01	0.10331E+01	0.77601E+00	0.87519E+00	0.10339E+01	0.11324E+01
23	0.11380E+01	0.10327E+01	0.10330E+01	0.11316E+01	0.10338E+01	0.11324E+01
24	0.11379E+01	0.11380E+01	0.11307E+01	0.11312E+01	0.11319E+01	0.11324E+01
25	0.11384E+01	0.11303E+01	0.11307E+01	0.11313E+01	0.11320E+01	
26	0.11304E+01	0.10328E+01	0.10331E+01	0.11316E+01		
27	0.11307E+01	0.10331E+01	0.11316E+01	0.11322E+01		
28	0.11310E+01	0.11315E+01				
29	0.11314E+01					
30	0.11321E+01					
31						
32						

A.2 - New Output Format

```
KINF  at Axial Node  4, Average Burnup =      0.00
Y/X   1      2      3      4      5      6      7      8      9     10     11     12     13     14     15
 1                                                          1.1324 1.1324 1.1324 1.1324 1.1324 1.1324 1.1324
 2                                                   1.1320 1.1318 1.0338 1.0340 1.1321 1.1320 1.0339 1.0340
 3                                          1.1322 1.1317 1.1313 1.1312 1.1314 0.8754 0.8751 1.1319 1.1317 0.8752
 4                                          1.1316 1.0332 1.1307 1.1306 1.0333 0.7760 0.8759 1.1313 1.0335 0.7761
 5                                   1.1316 1.0332 1.0328 1.1303 1.1380 1.0327 1.0329 1.1388 1.1385 1.0330 1.0331
 6                1.1321 1.1314 1.1309 1.1307 1.1308 1.1380 1.1379 1.1380 1.1386 1.1383 1.1382 1.1383 1.1388
 7                1.1315 1.1309 1.1305 1.1304 0.8899 0.8898 1.1383 1.1380 0.8899 0.8899 1.1385 1.1382 0.8900
 8         1.1319 1.0332 1.1305 1.1302 1.0328 0.7756 0.8898 1.1378 1.0328 0.7756 0.8899 1.1380 1.0329 0.7757
 9  1.1323 1.1317 1.0331 1.1304 1.1378 1.0324 1.0324 1.1382 1.1377 1.0323 1.0324 1.1383 1.1379 1.0325 1.0325
10  1.1322 1.1317 1.1313 1.1306 1.1379 1.1379 1.1383 1.1377 1.1376 1.1377 1.1382 1.1378 1.1377 1.1378 1.1384
11  1.1322 1.1318 0.8758 0.8767 1.1385 1.1381 0.8898 0.8898 1.1382 1.1378 0.8898 0.8898 1.1382 1.1379 0.8898
12  1.1322 1.1320 0.7762 0.8764 1.1384 1.0330 0.7756 0.8898 1.1378 1.0328 0.7755 0.8898 1.1379 1.0328 0.7756
13  1.1322 1.1318 1.0334 1.1312 1.1383 1.0326 1.0326 1.1383 1.1378 1.0324 1.0324 1.1382 1.1378 1.0324 1.0325
14  1.1322 1.1317 1.1316 1.1309 1.1383 1.1381 1.1385 1.1379 1.1377 1.1377 1.1383 1.1378 1.1377 1.1378 1.1383
15  1.1322 1.1318 0.8756 0.8763 1.1387 1.1383 0.8899 0.8898 1.1382 1.1379 0.8898 0.8898 1.1382 1.1379 0.8898
16  1.1322 1.1320 0.7762 0.8763 1.1385 1.0330 0.7757 0.8899 1.1379 1.0328 0.7756 0.8898 1.1378 1.0328 0.7756
17  1.1322 1.1318 1.0334 1.1312 1.1384 1.0327 1.0326 1.1383 1.1378 1.0324 1.0324 1.1382 1.1378 1.0324 1.0324
18  1.1322 1.1318 1.1316 1.1309 1.1383 1.1381 1.1385 1.1379 1.1377 1.1377 1.1383 1.1378 1.1377 1.1377 1.1383
19  1.1322 1.1318 0.8757 0.8764 1.1387 1.1382 0.8899 0.8898 1.1382 1.1378 0.8898 0.8897 1.1382 1.1378 0.8898
20  1.1322 1.1320 0.7761 0.8766 1.1383 1.0329 0.7756 0.8898 1.1378 1.0327 0.7755 0.8898 1.1378 1.0328 0.7756
21  1.1322 1.1317 1.0332 1.1309 1.1381 1.0325 1.0325 1.1382 1.1377 1.0323 1.0324 1.1382 1.1377 1.0324 1.0324
22  1.1323 1.1316 1.1310 1.1304 1.1378 1.1378 1.1383 1.1377 1.1376 1.1377 1.1382 1.1378 1.1377 1.1378 1.1383
23         1.1319 1.1312 1.1305 1.1302 1.1380 0.8898 0.8898 1.1382 1.1378 0.8898 0.8898 1.1383 1.1379 0.8899
24                1.1316 1.0330 1.1306 1.0330 0.7757 0.8899 1.1379 1.0328 0.7756 0.8899 1.1380 1.0329 0.7757
25                1.1322 1.1316 1.1312 1.0330 1.0327 1.1384 1.1379 1.0325 1.0326 1.1385 1.1381 1.0327 1.0327
26                                   1.1316 1.1311 1.1306 1.1302 1.1378 1.1380 1.1386 1.1383 1.1383 1.1383 1.1388
27                                          1.1315 1.0331 1.1305 1.1304 1.1306 0.8767 0.8766 1.1312 1.1310 0.8764
28                                          1.1321 1.1315 1.1311 1.1309 1.0334 0.7761 0.8756 1.1314 1.0336 0.7762
29                                                   1.1318 1.1317 1.1317 1.1318 1.1320 1.1318 1.1318 1.1318
30                                                          1.1323 1.1322 1.1322 1.1322 1.1322 1.1322 1.1322
Y/X  16     17     18     19     20     21     22     23     24     25     26     27     28     29     30
 1 1.1324 1.1323 1.1323 1.1323 1.1324 1.1323 1.1324
 2 1.1321 1.1320 1.1320 1.0340 1.1320 1.1319 1.1319 1.1320
 3 0.8751 1.1318 1.1317 0.8753 0.8753 1.1316 1.1313 1.1315 1.1318 1.1323
 4 0.8758 1.1313 1.0335 0.7761 0.8761 1.1310 1.0330 1.0331 1.1313 1.1317
```

```
 5 1.1389 1.1386 1.0330 1.0330 1.1388 1.1383 1.0327 1.0328 1.1309 1.0333 1.1318
 6 1.1384 1.1383 1.1383 1.1387 1.1382 1.1381 1.1381 1.1387 1.1308 1.1310 1.0334 1.1318 1.1323
 7 0.8900 1.1386 1.1382 0.8900 0.8900 1.1384 1.1381 0.8900 0.8901 1.1311 1.1309 1.1313 1.1318
 8 0.8900 1.1381 1.0329 0.7756 0.8899 1.1380 1.0329 0.7757 0.8900 1.1383 1.0328 1.0331 1.1315 1.1321
 9 1.1384 1.1379 1.0325 1.0325 1.1383 1.1379 1.0325 1.0326 1.1385 1.1381 1.0327 1.0330 1.1314 1.1318 1.1324
10 1.1379 1.1378 1.1378 1.1383 1.1379 1.1378 1.1378 1.1384 1.1381 1.1381 1.1384 1.1313 1.1315 1.1319 1.1323
11 0.8898 1.1383 1.1379 0.8898 0.8898 1.1383 1.1380 0.8899 0.8900 1.1386 1.1385 0.8762 0.8753 1.1322 1.1323
12 0.8898 1.1379 1.0328 0.7756 0.8899 1.1379 1.0328 0.7757 0.8900 1.1384 1.0332 0.7761 0.8751 1.0339 1.1324
13 1.1383 1.1378 1.0324 1.0325 1.1383 1.1379 1.0325 1.0326 1.1386 1.1383 1.0330 1.0333 1.1319 1.1320 1.1323
14 1.1378 1.1377 1.1378 1.1383 1.1379 1.1378 1.1379 1.1385 1.1382 1.1383 1.1386 1.1315 1.1317 1.1320 1.1323
15 0.8898 1.1382 1.1379 0.8898 0.8898 1.1383 1.1380 0.8899 0.8900 1.1388 1.1387 0.8760 0.8751 1.1322 1.1324
16 0.8898 1.1379 1.0328 0.7756 0.8899 1.1379 1.0329 0.7757 0.8901 1.1384 1.0333 0.7761 0.8750 1.0339 1.1324
17 1.1382 1.1378 1.0324 1.0325 1.1383 1.1378 1.0325 1.0326 1.1386 1.1384 1.0330 1.0333 1.1319 1.0339 1.1324
18 1.1378 1.1377 1.1377 1.1383 1.1378 1.1377 1.1378 1.1384 1.1381 1.1383 1.1385 1.1315 1.1317 1.1320 1.1324
19 0.8898 1.1382 1.1378 0.8898 0.8898 1.1382 1.1379 0.8899 0.8899 1.1386 1.1386 0.8761 0.8752 1.1322 1.1324
20 0.8898 1.1378 1.0328 0.7755 0.8898 1.1378 1.0328 0.7756 0.8899 1.1382 1.0331 0.7760 0.8752 1.0339 1.1324
21 1.1382 1.1378 1.0324 1.0324 1.1382 1.1377 1.0323 1.0324 1.1383 1.1380 1.0327 1.0330 1.1316 1.0338 1.1324
22 1.1378 1.1377 1.1377 1.1382 1.1377 1.1376 1.1377 1.1383 1.1379 1.1379 1.1380 1.1307 1.1312 1.1319 1.1324
23 0.8898 1.1383 1.1379 0.8898 0.8897 1.1382 1.1378 0.8898 0.8898 1.1384 1.1303 1.1307 1.1313 1.1320
24 0.8900 1.1381 1.0329 0.7756 0.8898 1.1378 1.0328 0.7756 0.8900 1.1304 1.0328 1.0331 1.1316
25 1.1386 1.1381 1.0326 1.0326 1.1384 1.1379 1.0324 1.0325 1.1308 1.1307 1.0331 1.1316 1.1322
26 1.1384 1.1383 1.1383 1.1387 1.1382 1.1380 1.1378 1.1302 1.1304 1.1310 1.1315
27 0.8765 1.1312 1.1309 0.8765 0.8768 1.1309 1.1304 1.1305 1.1309 1.1314
28 0.8756 1.1314 1.0336 0.7762 0.8758 1.1311 1.0331 1.0332 1.1315 1.1321
29 1.1320 1.1317 1.1317 1.1318 1.1320 1.1317 1.1317 1.1319
30 1.1322 1.1322 1.1322 1.1322 1.1322 1.1322 1.1323
```

Appendix B – NESTLE Input File Used for Initial Guess

```
Peach Bottom Cycle 1
read parameter
  xsecfile=XSEC.TOTAL.MACRO_cr
  thfeedback=yes
  thsolver=twophase
  quality=epri
  void=z-f
'  void=l-z
  powerden=50.7379
  t2n=yes
  inputedit=no
  longedit=yes
'  depl_update=3
  accel=cheby
'  chebymax=1
  diffusionmethod=nem
  outers=250
  demand_conv=yes
  specshiftcorr=no
  therms=1
  printscreen=yes
  deplete=yes
  scalefact=no
  thupdate=1
  microdeplete=no
  ratiohmfuel=0.881481
'  origen_deplete=no

  eps_pres=5E-5
  eps_void=1e-5
'  eps_void=1e-7
  pinpower=no

  sym=fourth

  haling_accel=.5

  eps_flow=.1

  output_format=new
  output_conv_data=no

' Added by Nick to avoid NANs
  coolant_molwgt= 18.0153
  solu_abund=0.197714997
  solu_atmwgt=10.811

end parameter

read edit
  kinf
  power
  bu
```

```
end edit

read heattransfer
  mcore=25.625
' total core flow rate Mlbm/hr
  bypass=1.69475
' total flow outside bundles and in water rods Mlbm/hr ?
  flow=yes
  mode=m
  rhovsat=2.3299
  tinlet=527.485
  tinletmin=500
  tinletmax=550
  tsat=548.84
  uvsat=1109.8

  rho_vs_ufit 94.1993830099764 -0.186234454371061 0.000298594316762532 -
2.16530070901634e-07 end rho_vs_ufit
  t_vs_ufit 322.415028930525 -0.645834205015149 0.00325028978652142 -
2.35946897099643e-06 end t_vs_ufit
  u_vs_Tfit -3288.145523120940 18.550809182238 -0.031790750514 0.000019485777
end u_vs_Tfit
end heattransfer

read fuelmech
  wc=1.0 wp=0 fiss_frac=0.975
  fuelden=643.994

  heff_vs_t 0.78363116E-01 -0.19203380E-04 0.73696720E-08 end heff_vs_t
  tavg_vs_lpd  530.2 99.429 0.0075 end tavg_vs_lpd
'  heff_vs_t 2.0 end heff_vs_t
  tsurf_vs_lpd  530.2 99.429 0.0075 end tsurf_vs_lpd
  cp_vs_tfit 0.8110000193E-01 end cp_vs_tfit

  fuelfrac    0.000000 0.253861 0.000000 0.242296 0.242090 0.242296 0.242090
0.253861 0.253861 end fuelfrac
  bunarea     0.250000 0.198500 0.250000 0.198500 0.198500 0.198500 0.198500
0.198500 0.198500 end bunarea
  eqdiam      0.500000 0.050830 0.500000 0.050830 0.050830 0.050830 0.050830
0.050830 0.050830 end eqdiam
  hydiam      0.063020 0.063020 0.063020 0.063020 0.063020 0.063020 0.063020
0.063020 0.063020 end hydiam
  fpinrad     0.000000 0.243500 0.000000 0.243500 0.243500 0.243500 0.243500
0.243500 0.243500 end fpinrad
  frodrad     0.000000 0.281500 0.000000 0.281500 0.281500 0.281500 0.281500
0.281500 0.281500 end frodrad
  numfrods        0       49        0       49       49       49       49
49       49    end numfrods
  wtfri       1.000000 0.573250 1.000000 0.573250 0.573250 0.573250 0.573250
0.573250 0.573250 end wtfri
  wtfro       1.000000 0.573250 1.000000 0.573250 0.573250 0.573250 0.573250
0.573250 0.573250 end wtfro
  lattice_ids     1       10        2       16       17       14       15
13       11    end lattice_ids
  losscoeffs 7r1.0 end losscoeffs
  losscoeffs_loc 2.325 4.0 5.683 7.358 9.042 10.717 12.392 end losscoeffs_loc
  orificecoeff 45.0 201.4 72.1 10. end orificecoeff
```

```
  orificecoeff_ids 1 2 3 4 end orificecoeff_ids
end fuelmech

read burndata
  pres=1050
'  burnup=0.0  sm=no xe=no crod_id=26 delbu=0.0 pctpwr=100 pctflow=100.0
bypass=13.0 tinlet=526.0 end
  burnup=0.0  sm=no xe=no crod_id=1 delbu=0.0 pctpwr=55.7 pctflow=103.3
bypass=13.37 tinlet=530.17 end
  burnup=11133 haling=yes sm=eq xe=eq crod_id=26 pctpwr=100.0  pctflow=100.0
bypass=13.0  tinlet=526.0  end
end burndata

read geom
'  inner=cyclic
  inner=refl
  outer=zero
  up=zero
  down=zero
  orifice_id=117

  bpitchx=6.0
  bpitchy=6.0

  deltax 17r6.0 end deltax
  deltay 17r6.0 end deltay
  bottomfuelnode=4 topfuelnode=27
  deltaz 3r3.0 24r6.0 3r3.0 end deltaz
  figure  3r6 2r1 6r2 4r3  2r4 6r5 4r1 3r7 end figure

  rotation=217

  crload=bottomup

  crbank 1 17
   30 144 114 144  12 144 114 144
  144 144 144 144 144 144 144 144
  114 144  12 144 114 144  24 144
  144 144 144 144 144 144 144 144
   12 144 114 144 114 144 144
  144 144 144 144 144 144
  114 144  24 144 144
  144 144 144 144
  end crbank

  crbank   26  17
  144.001 144.001 144.001 144.001 144.001 144.001 144.001 144.001
  144.001 144.001 144.001 144.001 144.001 144.001 144.001 144.001
  144.001 144.001 144.001 144.001 144.001 144.001 144.001 144.001
  144.001 144.001 144.001 144.001 144.001 144.001 144.001 144.001
  144.001 144.001 144.001 144.001 144.001 144.001 144.001
  144.001 144.001 144.001 144.001 144.001 144.001
  144.001 144.001 144.001 144.001 144.001
  144.001 144.001 144.001 144.001
  end crbank

end geom
```

```
read arrays
assem_ara=00 fill   6   1   2   3   4   5   7 end fill
assem=01     fill   1   1   1   1   1   1   1 end fill
assem=02     fill   1  10  10  10  10  10   2 end fill
assem=07     fill   1  16  17  17  16  16   2 end fill
assem=06     fill   1  14  15  15  14  14   2 end fill
assem=05     fill   1  13  13  13  13  13   2 end fill
assem=03     fill   1  11  11  11  11  11   2 end fill

ara=0 nux=17 nuy=17 fill
  6  6  6  6  6  6  6  6  6  6  6  6  6  6  2  1  1
  6  6  6  6  6  2  6  6  2  6  6  6  2  6  6  1  1
  6  6  2  6  6  6  6  6  6  6  6  6  6  6  2  1  1
  6  6  6  6  6  6  2  6  6  6  6  6  6  6  2  1  1
  6  6  6  6  2  6  6  6  6  6  6  6  2  6  2  1  1
  6  2  6  6  6  6  6  6  6  2  6  6  6  6  2  1  1
  6  6  6  2  6  6  2  6  6  6  6  6  6  6  2  1  1
  6  6  6  6  6  6  6  6  6  6  6  2  6  2  1  1  0
  6  2  6  6  6  6  6  6  6  6  6  6  6  1  1  0  0
  6  6  6  6  6  2  6  6  6  2  6  2  2  1  0  0  0
  6  6  6  6  6  6  6  6  6  6  2  1  1  1  0  0  0
  6  6  6  6  6  6  6  2  6  2  1  1  1  0  0  0  0
  6  2  6  6  2  6  6  6  6  2  1  0  0  0  0  0  0
  6  6  6  6  6  6  6  2  1  1  1  0  0  0  0  0  0
  2  6  2  2  2  2  2  1  1  1  0  0  0  0  0  0  0
  1  1  1  1  1  1  1  1  0  0  0  0  0  0  0  0  0
  1  1  1  1  1  1  1  0  0  0  0  0  0  0  0  0  0  end fill

ara=17 nux=17 nuy=17 fill
 1  2  2  3  3  4  4  5  5  6  6  7  7  8  8 0 0
 9 10 10 11 11 12 12 13 13 14 14 15 15 16 16 0 0
 9 10 10 11 11 12 12 13 13 14 14 15 15 16 16 0 0
17 18 18 19 19 20 20 21 21 22 22 23 23 24 24 0 0
17 18 18 19 19 20 20 21 21 22 22 23 23 24 24 0 0
25 26 26 27 27 28 28 29 29 30 30 31 31 32 32 0 0
25 26 26 27 27 28 28 29 29 30 30 31 31 32 32 0 0
33 34 34 35 35 36 36 37 37 38 38 39 39  0  0 0 0
33 34 34 35 35 36 36 37 37 38 38 39 39  0  0 0 0
40 41 41 42 42 43 43 44 44 45 45  0  0  0  0 0 0
40 41 41 42 42 43 43 44 44 45 45  0  0  0  0 0 0
46 47 47 48 48 49 49 50 50  0  0  0  0  0  0 0 0
46 47 47 48 48 49 49 50 50  0  0  0  0  0  0 0 0
51 52 52 53 53 54 54  0  0  0  0  0  0  0  0 0 0
51 52 52 53 53 54 54  0  0  0  0  0  0  0  0 0 0
 0  0  0  0  0  0  0  0  0  0  0  0  0  0  0 0 0
 0  0  0  0  0  0  0  0  0  0  0  0  0  0  0 0 0 end fill

ara=117 nux=17 nuy=17 fill
  1 1 3 3 1 1 3 3 1 1 3 3 1 3 2 4 4
  1 1 3 3 1 1 3 3 1 1 3 3 1 3 2 4 4
  1 1 1 1 1 1 1 1 1 1 1 1 1 1 2 4 4
  1 1 1 1 1 1 1 1 1 1 1 1 1 1 2 4 4
  1 1 3 3 1 1 3 3 1 1 3 3 1 3 2 4 4
  1 1 3 3 1 1 3 3 1 1 3 3 1 3 2 4 4
  1 1 1 1 1 1 1 1 1 1 1 1 1 1 2 4 4
  1 1 1 1 1 1 1 1 1 1 1 1 1 2 4 4 0
```

```
  1 1 3 3 1 1 3 3 1 1 3 3 2 4 4 0 0
  1 1 3 3 1 1 3 3 1 1 3 2 2 4 4 0 0
  1 1 1 1 1 1 1 1 1 1 2 4 4 4 0 0 0
  1 1 1 1 1 1 1 1 1 2 4 4 0 0 0 0 0
  1 1 3 3 1 1 3 3 2 2 4 4 0 0 0 0 0
  1 1 1 1 1 1 1 2 4 4 4 0 0 0 0 0 0
  2 2 2 2 2 2 2 4 4 0 0 0 0 0 0 0 0
  4 4 4 4 4 4 4 4 0 0 0 0 0 0 0 0 0
  4 4 4 4 4 4 4 0 0 0 0 0 0 0 0 0 0 end fill

ara=217 nux=17 nuy=17 fill
  0 1 0 1 0 1 0 1 0 1 0 1 0 1 0 0 0
  3 2 3 2 3 2 3 2 3 2 3 2 3 2 3 0 0
  0 1 0 1 0 1 0 1 0 1 0 1 0 1 0 0 0
  3 2 3 2 3 2 3 2 3 2 3 2 3 2 3 0 0
  0 1 0 1 0 1 0 1 0 1 0 1 0 1 0 0 0
  3 2 3 2 3 2 3 2 3 2 3 2 3 2 3 0 0
  0 1 0 1 0 1 0 1 0 1 0 1 0 1 0 0 0
  3 2 3 2 3 2 3 2 3 2 3 2 3 0 0 0 0
  0 1 0 1 0 1 0 1 0 1 0 1 0 0 0 0 0
  3 2 3 2 3 2 3 2 3 2 3 0 0 0 0 0 0
  0 1 0 1 0 1 0 1 0 1 0 0 0 0 0 0 0
  3 2 3 2 3 2 3 2 3 0 0 0 0 0 0 0 0
  0 1 0 1 0 1 0 1 0 0 0 0 0 0 0 0 0
  3 2 3 2 3 2 3 0 0 0 0 0 0 0 0 0 0
  0 1 0 1 0 1 0 0 0 0 0 0 0 0 0 0 0
  0 0 0 0 0 0 0 0 0 0 0 0 0 0 0 0 0
  0 0 0 0 0 0 0 0 0 0 0 0 0 0 0 0 0 end fill
end arrays
```

Appendix C – Sample BWROPT Input File with Input Descriptions

```
'DEBUG' 1 1 0 0 1 2 / debug_sample_flag, debug_archive_flag, debug_OF_flag,
      debug_cost_flag, nes_iter_flag, crp_stat_flag
'CR.OUT' 3 1 / cr_output_flag (0 = nothing, 1 = summary to screen, 2 =
      everything to screen, 3 = everything process output file), cr_plot_flag
      (1 = plot, 0 = don't plot)

'RES.OUT' 1 3 / Number of CS between writing restart data file

'REAC.TYP' 'BWR'
'CYC' 3 1 0/ Cycle Data [# of cycles to optimize (n_cyc_opt), first cycle #,
      first_cyc_opt_flag (1 = yes, 0 = no)]

'OPT' 'PSA' / Optimization Method [PSA (Parallel Simulated Annealing), SA
      (Simulated Annealing)]

'DEP.CYC' 2 / Depletion option for optimized cycles (n_cyc_opt) [0 = use
      original depletion, 1 = CR optimization, 2 = Haling depletion]
'EXP.STP' 2000. / Depletion step size for each cycle optimized if CR
      optimization used

'NES.ITER' 70 / max_nes_iter (maximum number of iterations used for NESTLE
      calculations)

'INP.EDT' 2 / Input edit flag (0 = none, 1 = just in summary file, 2 = all)
'RES' 0 / Use restart files flag  for each cycle to be optimized (0 = don't
      use, 1 = use)

'CHG'     1 2 3 4 5 6 7 8 9 10 / Change Types to Use [old shuffle, new old
      swap, # fresh change, new type (switch, change, add),CRP change]
'CHG.GRP' 1 2 3 4 5 6 7 7 8 8/ Groups used for variable sample probabilities
      (if a change type converges the probability is distributed among the
      other change types in the group if there are any)

'OF' 1 0 / OF_nan_flag, OF_mix_opt (0 = dont use initial solutions in ST_DEV
      calc, 1 = use initial solutions)

'CON' 7 0 2.0/ # of constraints, constraint weight multiplier flag, target
      T=0 constraint weight multiplier
     '$   '  0.0       10.0   / Constraints Parameters
      [constraint,limit,weight] constraints ($,A_EX,N_EX,RPF,K) CPR,TMOL,STAB
     'K-  '  1.0       10.0   /
     'K+  '  1.01      10.0   /
     'A_EX'  35.0       1.0   / (GWD/MTU)
     'N_EX'  45.0       1.0   / (GWD/MTU)
     'RPF2'  1.5       10.0   /
     'RPF3'  2.1       10.0   /

'CYC.LEN' 30  / shutdown length (days) for each cycle being optimized
'COST' .34 .15/ efficiency, carrying charge (annual interest rate)

'NEW.TYP' 9 2 0/ [max # new types, cycle 1 new type, max assembly number for
      sampling new fuel from (0 = # of new types entered)]
```

```
'ENERGY' 402000. / Energy production for cycles to be optimized (MWD) (1
      number followed by '/' -> all cycles same, otherwise specify for each
      cycle)
'POWER' 100.0 100.0 13.0 528.0 / Parameters used in cr optimization and
      haling depletion cases (pctpwr, pctflow, bypass, tinlet)

'SORT' 'EXP' / Parameter to use for sort to generate original LP_oper ['KIN'
      or 'EXP']

'ARCHIVE' 'NEW' 20 20/ Archive method ('NEW' = new inventory), archive size
      (width, depth)

'RAND' 1000 1000000 /# to add to all random seeds, number of random numbers
      to generate per process

'SOL.INI' 0 0 / Initial Solution Parameters [# of fresh to add, number of
      changes to make to LP, # to add to all random seeds]

'DIR' '/home/keith/BWR_OPT/' 'Model/' '/home/keith/BWR_OPT/Run_Files/' /
      [project dir, model dir, run cycle dir, process base run dir name]
'INP' 'PB' 'PB_q_01_haling_new2.inp' 1 1/ [reactor name,Input File for Cycle
      N-1, assembly input (1 = yes), cr_input_flag]
'NES.EXE' '/home/keith/scale_dev/build/src/nestle/' 'nestle' 1 18 / Path for
      Nestle Executable [original path, exe name, copy flag (0 = no copy, 1 =
      run path, 2 = path_proc),output_num_len]
'OUT' 2 '/home/keith/BWR_OPT/Output/' 'scr_out' / [screen print option, base
      output file location, name, ]
'SUMMARY' '/home/keith/BWR_OPT/Output/' 'Summary.out' 'Summary_full.out'
      'T_stats_out.m' 'hist_stats_out.m' 'archive.out' / [summary_path,
      summary file name]

'PLOT.INFO' 1 'gnuplot' '/home/keith/BWR_OPT/plot_dir/' 'plot_script'
      'plot_data' 'arial,11' 'arial,9.5' 2 / [plot flag, gnuplot path, script
      base name, data file base name, font, mp_font, mp_update]

'DEL.FILE' 0 / Output file delete flag (1 = delete, 0 = keep)

'PSA.STP' 10 10 0 0 / n_init_iter, n_iter, Cooling step length flag (0 = each
      process runs n trials, 1 = average of n trials run over all processes)
      [Cooling step 1, >1]
'PSA.CONV' 1 0 100 10/ PSA convergence criteria [1 (# consecutive CS, # of
      accepts per CS), 2 (# of steps without OF decrease), 3 (maximum #
      cooling steps)]
'PSA.TEMP' 2. 1.  .5   5  .3 .25 .2 .15 .1  / alpha, lambda, std_cutoff,
      n_std_avg, (std_weights if n_std_avg > 1)
'PSA.INI' 1 -1 / init flag, dist flag [-1 = keep current solution, 0 = all
      procs get best, 1 = dist n_procs best solutions (duplicate if
      necessary)]
'PSA.RES' 1000000 / n_step_res, # of iterations between restarts (sampling
      from best solutions instead of current solutions)
'PSA.MIX' 0  1.05  .25 -1.  2 1 1/ [psa_mix_flag (0= standard, 1 = limits, 2
      = always), mix_percent_lim, mix_acc_lim, mix_inc_lim, n_archive_samp
      (array of # of solutions to select from each archive level) ]

'SAMP.PR' 0 / sample prob flag [0 = use constant sample prob [sample
      probabilities for each change type (equal if not entered) will be
      weighted to sum to 1]
```

```
                        1 = decrease prob as accept prob --> 0 (# cooling
      steps with 0 accepts for convergence, # step used to decrease prob to 0
      linearly),
                        2 = fully variable based on input parameters]

'SAMP.CYC' 1. / Sample probabilty for each cycle being optimized (one number
      > all same)

'TIME' 1 / time flag (0 = runtime for each iteration given, 1 = runtime since
      start of cooling step given)

'N_ASSEM' 5 2 1 1  1 1 1 1  7/ assembly array size (#,#,#,#), sample flag for
      each direction (0=random, 1=ordered), # lattices in assembly

'ASSEM' 1 1 1 1 -1.0     1  9  9  9  9  9  2 / 1.1w/o
'ASSEM' 2 1 1 1 -1.0     1 10 10 10 10 10  2 / 2w/o
'ASSEM' 3 1 1 1 -1.0     1 11 11 11 11 11  2 / 3w/o
'ASSEM' 4 1 1 1 -1.0     1 12 12 12 12 12  2 / 4w/o
'ASSEM' 5 1 1 1 -1.0     1 13 13 13 13 13  2 / 5w/o

'ASSEM' 2 2 1 1 -1.0     1 14 15 15 14 14  2 / 2w/o
'ASSEM' 3 2 1 1 -1.0     1 16 17 17 16 16  2 / 3w/o
'ASSEM' 4 2 1 1 -1.0     1 18 19 19 18 18  2 / 4w/o
'ASSEM' 5 2 1 1 -1.0     1 20 21 21 20 20  2 / 5w/o


*'TYP.REP'     / specify types to replace and replacing type for future
      cycles (old type, new type)

'FUEL.TIME' 15. 12. 9. 3.   15./ Time before cycle starts for expense
      (months) [ore, conv, enr, fab (and gad)]; carrying charge (%)
'FUEL.COST' 42.25  10.50 10.0  100000. 10000.0/ ore cost ($/lb U3O8),
      conversion cost ($/kg UF6), SWU cost ($/SWU), fab cost ($/assembly),
      gad cost ($/kg)
'FUEL.LOSS' 0.0 .5 0.0 .5 / Fuel losses (%) (mining, conversion, enrichment,
      fabrication
'FUEL.ENR' .711 .25/ feed enrichment, tails enrichment

'PLOT' 1 3 2 type 'oper' 'skip' 'opr2' 'EXP ' 'KIN ','RPF ' step 1 1 -1 -1 1
      1

'NO.NEW'       /
 0 0 0 0 0 0 0 0 0 0 0 0 0 1 1
 0 0 0 0 0 0 0 0 0 0 0 0 0 1 1
 0 0 0 0 0 0 0 0 0 0 0 0 0 1 1
 0 0 0 0 0 0 0 0 0 0 0 0 0 1 1
 0 0 0 0 0 0 0 0 0 0 0 0 0 1 1
 0 0 0 0 0 0 0 0 0 0 0 0 0 1 1
 0 0 0 0 0 0 0 0 0 0 0 0 0 1 1
 0 0 0 0 0 0 0 0 0 0 0 0 1 1
 0 0 0 0 0 0 0 0 0 0 0 0 1 1
 0 0 0 0 0 0 0 0 0 0 0 1 1 1
 0 0 0 0 0 0 0 0 0 0 1 1
 0 0 0 0 0 0 0 0 0 1 1
 0 0 0 0 0 0 0 0 1 1 1
 1 1 1 1 1 1 1 1
 1 1 1 1 1 1 1
```

```
'LAT.DAT' 9  13   49 .253861 .1985 .05083 .06302 .2435 .2815 .57325 .57325 /
      id
      [min,max],numfrods,fuelfrac,bunarea,eqdiam,hydiam,fpinrad,frodrad,wtfri
      ,wtfro
'LAT.DAT' 14 14   49 .242296 .1985 .05083 .06302 .2435 .2815 .57325 .57325
'LAT.DAT' 15 15   49 .242090 .1985 .05083 .06302 .2435 .2815 .57325 .57325
'LAT.DAT' 16 16   49 .242296 .1985 .05083 .06302 .2435 .2815 .57325 .57325
'LAT.DAT' 17 17   49 .242090 .1985 .05083 .06302 .2435 .2815 .57325 .57325
'LAT.DAT' 18 18   49 .242296 .1985 .05083 .06302 .2435 .2815 .57325 .57325
'LAT.DAT' 19 19   49 .242090 .1985 .05083 .06302 .2435 .2815 .57325 .57325
'LAT.DAT' 20 20   49 .242296 .1985 .05083 .06302 .2435 .2815 .57325 .57325
'LAT.DAT' 21 21   49 .242090 .1985 .05083 .06302 .2435 .2815 .57325 .57325 /

* New No BP Assembly Lattices
'LAT.ENR'  9 2 18 0.71 0.0 31 1.33 0.0 / id,n_pin_type, pin_data for each pin
      type(# pins, enrichment, gad weight percent)
'LAT.ENR' 10 2 18 1.61 0.0 31 2.23 0.0 /
'LAT.ENR' 11 2 18 2.61 0.0 31 3.23 0.0 /
'LAT.ENR' 12 2 18 3.61 0.0 31 4.23 0.0 /
'LAT.ENR' 13 2 18 4.61 0.0 31 5.23 0.0 /

* New BP Assembly Lattices
'LAT.ENR' 14 5 27 2.43 0.0 12 1.44 0.0 6 1.19 0.0 1 0.83 0.0     3 2.43 3.0 /
'LAT.ENR' 15 5 26 2.43 0.0 12 1.44 0.0 6 1.19 0.0 1 0.83 0.0     4 2.43 3.0 /

'LAT.ENR' 16 5 27 3.43 0.0 12 2.44 0.0 6 2.19 0.0 1 1.83 0.0     3 3.43 3.0 /
'LAT.ENR' 17 5 26 3.43 0.0 12 2.44 0.0 6 2.19 0.0 1 1.83 0.0     4 3.43 3.0 /

'LAT.ENR' 18 5 27 4.43 0.0 12 3.44 0.0 6 3.19 0.0 1 2.83 0.0     3 4.43 3.0 /
'LAT.ENR' 19 5 26 4.43 0.0 12 3.44 0.0 6 3.19 0.0 1 2.83 0.0     4 4.43 3.0 /

'LAT.ENR' 20 5 27 5.43 0.0 12 4.44 0.0 6 4.19 0.0 1 3.83 0.0     3 5.43 3.0 /
'LAT.ENR' 21 5 26 5.43 0.0 12 4.44 0.0 6 4.19 0.0 1 3.83 0.0     4 5.43 3.0 /


'CR.ITER' 10 10 / max cr calc iter (initial, noninitial)
'CR.KEFF' 1.0000 1.0010 1.0000 1.0010

'CR.PARM' 2 3 / [cr_ini_flag (only 2), cr_manual_flag (1 = enter entire CRP
      every step, 2 = Change 1 CR at a time, 3 = check 'crd_flag' file each
      iteration for cr_manual_flag, 4 = 3 and prompt for cr_manual_flag if
      solution not found)]

'CR.PREF' 7 8 8 8 /

'CR.STEP' .02 .5 / (min, max) CR move size, fraction of range

'CR.BND' .3333 .6667 / Fractional values for boundaries between shallow,
      intermediate, deep insertions

'CR.RING' 1.0 1.0 1.0 /

'CRD.CVC' 3.01020  2.01020  3.02020  2.03020  3.05020  2.05020  3.10100
      2.12100
          4.01020  1.01020  4.02020  1.02020  4.05020  1.05100  4.09100
      1.09100
```

```
          3.03020  2.02020  3.04020  2.04020  3.07020  2.07020  3.11100
      2.13100
          4.03020  1.03020  4.04020  1.04020  4.07020  1.07100  4.11100
      1.11100
          3.06020  2.06020  3.08020  2.08020  3.09100  2.10100  3.14100     0
          4.06020  1.06100  4.08020  1.08100  4.10100  1.13100     0        0
          3.12100  2.09100  3.13100  2.11100  3.15100     0        0        0
          4.12100  1.10100  4.13100  1.12100     0        0        0        0
      /

'END'
```

Appendix D – Constraint Data for all Cycles of the Test Cases

D.1 – All Sampling Types with Constant Sampling Probabilities PSA Best Solutions

Test Case 1

								New Fuel Types						
OF	CYC	FCC	EOC KEFF	MAX(RPF2)	MAX(RPF3)	MAX(EXP2)	MAX(EXP3)	1	2	3	4	6	7	8
1.4605E-01	2	6.4753E-03	1.0014E+00	1.4823E+00	1.8725E+00	2.4789E+01	3.0587E+01 -	10	1	2		1	64	1
	3	5.5664E-03	1.0001E+00	1.4795E+00	1.8429E+00	2.9920E+01	3.7140E+01	4		11	1	3	47	
	4	5.5333E-03	1.0000E+00	1.5000E+00	1.8961E+00	3.4943E+01	4.2407E+01	2	8	1		12	46	

Test Case 2

								New Fuel Types						
OF	CYC	FCC	EOC KEFF	MAX(RPF2)	MAX(RPF3)	MAX(EXP2)	MAX(EXP3)	1	2	3	4	6	7	8
1.5468E-01	2	7.1617E-03	1.0009E+00	1.4992E+00	1.8937E+00	2.3517E+01	2.9181E+01 -		4	2		44	42	1
	3	5.9501E-03	1.0009E+00	1.4849E+00	1.8793E+00	2.9729E+01	3.6891E+01	4	2	7		11	49	
	4	5.3297E-03	1.0001E+00	1.4982E+00	1.8821E+00	3.3925E+01	4.0246E+01		20	4		10	34	

Test Case 3

								New Fuel Types						
OF	CYC	FCC	EOC KEFF	MAX(RPF2)	MAX(RPF3)	MAX(EXP2)	MAX(EXP3)	1	2	3	4	6	7	8
1.4925E-01	2	6.6870E-03	1.0042E+00	1.4974E+00	1.8774E+00	2.4439E+01	3.0142E+01 -		23	3			56	
	3	5.4254E-03	1.0000E+00	1.4771E+00	1.8877E+00	2.9374E+01	3.6024E+01		24			1	43	
	4	5.8735E-03	1.0001E+00	1.4962E+00	1.8449E+00	3.4745E+01	4.2337E+01	1	49			13	19	

Test Case 4

								New Fuel Types						
OF	CYC	FCC	EOC KEFF	MAX(RPF2)	MAX(RPF3)	MAX(EXP2)	MAX(EXP3)	1	2	3	4	6	7	8
1.5872E-01	2	6.9479E-03	1.0048E+00	1.4963E+00	1.8759E+00	2.3993E+01	2.9849E+01 -		43	2		2	43	
	3	6.2191E-03	1.0000E+00	1.4808E+00	1.8619E+00	2.8924E+01	3.5054E+01	2	54	2		2	25	
	4	5.9395E-03	1.0000E+00	1.4993E+00	1.8921E+00	3.1279E+01	3.6718E+01	1	46	12		11	9	2

D.2 – Ordered Sampling with Constant Sampling Probabilities PSA Best Solutions

Test Case 1

								New Fuel Types						
OF	CYC	FCC	EOC KEFF	MAX(RPF2)	MAX(RPF3)	MAX(EXP2)	MAX(EXP3)	1	2	3	4	6	7	8
1.5195E-01	2	6.4873E-03	1.0001E+00	1.4950E+00	1.8736E+00	2.4645E+01	3.0425E+01	-	32	1		1	48	
	3	5.8823E-03	1.0001E+00	1.4825E+00	1.8617E+00	2.9420E+01	3.6148E+01		30	5		3	37	
	4	6.0259E-03	1.0001E+00	1.4978E+00	1.8493E+00	3.3766E+01	3.9859E+01	1	63	5		18	1	

Test Case 2

								New Fuel Types						
OF	CYC	FCC	EOC KEFF	MAX(RPF2)	MAX(RPF3)	MAX(EXP2)	MAX(EXP3)	1	2	3	4	6	7	8
1.5235E-01	2	6.5961E-03	1.0003E+00	1.4911E+00	1.8668E+00	2.4221E+01	3.0078E+01	-	38	6		3	38	
	3	5.7742E-03	1.0001E+00	1.4929E+00	1.9029E+00	2.9722E+01	3.5963E+01	1	14	1		9	47	
	4	6.0550E-03	1.0001E+00	1.3764E+00	1.6581E+00	3.3523E+01	3.9911E+01		72			18		

Test Case 3

								New Fuel Types						
OF	CYC	FCC	EOC KEFF	MAX(RPF2)	MAX(RPF3)	MAX(EXP2)	MAX(EXP3)	1	2	3	4	6	7	8
1.5379E-01	2	6.6082E-03	1.0033E+00	1.4776E+00	1.8635E+00	2.4023E+01	2.9997E+01	-	18			1	60	1
	3	6.1873E-03	1.0000E+00	1.4929E+00	1.8669E+00	2.9587E+01	3.6261E+01		88	2			1	
	4	5.7446E-03	1.0000E+00	1.4881E+00	1.8746E+00	3.2882E+01	3.9644E+01		3	4		6	55	

Test Case 4

								New Fuel Types						
OF	CYC	FCC	EOC KEFF	MAX(RPF2)	MAX(RPF3)	MAX(EXP2)	MAX(EXP3)	1	2	3	4	6	7	8
1.6496E-01	2	7.1811E-03	1.0009E+00	1.4885E+00	1.8517E+00	2.3221E+01	2.8790E+01	-	1	81	16	4		
	3	6.9384E-03	1.0000E+00	1.4993E+00	1.8781E+00	2.5905E+01	3.0994E+01		2	69	11	4	11	
	4	5.6477E-03	1.0000E+00	1.4967E+00	1.8808E+00	3.0237E+01	3.6391E+01		2	14		9	46	

D.3 – Random Sampling with Constant Sampling Probabilities PSA Best Solutions

Test Case 1

								New Fuel Types						
OF	CYC	FCC	EOC KEFF	MAX(RPF2)	MAX(RPF3)	MAX(EXP2)	MAX(EXP3)	1	2	3	4	6	7	8
1.4941E-01	2	6.6131E-03	1.0002E+00	1.4850E+00	1.9265E+00	2.4921E+01	3.1010E+01 -		6			16	59	
	3	5.5215E-03	1.0001E+00	1.4964E+00	1.9042E+00	3.0532E+01	3.8333E+01	1	25			2	42	
	4	5.8917E-03	1.0000E+00	1.4993E+00	1.8942E+00	3.3362E+01	3.9533E+01	2	17			20	38	

Test Case 2

								New Fuel Types						
OF	CYC	FCC	EOC KEFF	MAX(RPF2)	MAX(RPF3)	MAX(EXP2)	MAX(EXP3)	1	2	3	4	6	7	8
1.4718E-01	2	6.4022E-03	1.0016E+00	1.4913E+00	1.8973E+00	2.4715E+01	3.0470E+01 -	4	2			1	69	
	3	5.8959E-03	1.0020E+00	1.4970E+00	1.8682E+00	3.0293E+01	3.6816E+01		43			11	26	
	4	5.4106E-03	1.0000E+00	1.4944E+00	1.9047E+00	3.4750E+01	4.1606E+01		4	16		5	39	

Test Case 3

								New Fuel Types						
OF	CYC	FCC	EOC KEFF	MAX(RPF2)	MAX(RPF3)	MAX(EXP2)	MAX(EXP3)	1	2	3	4	6	7	8
1.5543E-01	2	6.4011E-03	1.0016E+00	1.4923E+00	1.8693E+00	2.4158E+01	3.0305E+01 -	1	16	5		2	54	
	3	6.4084E-03	1.0000E+00	1.4959E+00	1.8405E+00	2.8547E+01	3.4576E+01		87		1	5		1
	4	6.0393E-03	1.0001E+00	1.4948E+00	1.8697E+00	3.0987E+01	3.7937E+01	1	29			7	41	

Test Case 4

								New Fuel Types						
OF	CYC	FCC	EOC KEFF	MAX(RPF2)	MAX(RPF3)	MAX(EXP2)	MAX(EXP3)	1	2	3	4	6	7	8
1.5943E-01	2	6.4965E-03	1.0002E+00	1.4945E+00	1.8809E+00	2.4434E+01	3.0303E+01 -	1	34	1		1	46	
	3	6.5308E-03	1.0001E+00	1.4763E+00	1.8147E+00	2.9369E+01	3.5769E+01		61			5	24	
	4	6.3525E-03	1.0001E+00	1.4912E+00	1.8546E+00	2.9287E+01	3.5166E+01		74	3		11	3	1

D.4 – All Sampling Types with Variable Sampling Probabilities PSA Best Solutions

Test Case 1

								New Fuel Types						
OF	CYC	FCC	EOC KEFF	MAX(RPF2)	MAX(RPF3)	MAX(EXP2)	MAX(EXP3)	1	2	3	4	6	7	8
1.4564E-01	2	6.4753E-03	1.0014E+00	1.4823E+00	1.8725E+00	2.4789E+01	3.0587E+01 -	10	1	2		1	64	1
	3	5.5444E-03	1.0000E+00	1.4709E+00	1.8492E+00	2.9602E+01	3.6792E+01	4	1	11		2	48	
	4	5.4977E-03	1.0000E+00	1.4991E+00	1.8874E+00	3.4756E+01	4.1166E+01	1	13	5		11	39	

Test Case 2

								New Fuel Types						
OF	CYC	FCC	EOC KEFF	MAX(RPF2)	MAX(RPF3)	MAX(EXP2)	MAX(EXP3)	1	2	3	4	6	7	8
1.5385E-01	2	7.1617E-03	1.0008E+00	1.4989E+00	1.9044E+00	2.3522E+01	2.9188E+01 -		4	2		44	42	1
	3	5.9149E-03	1.0001E+00	1.4854E+00	1.8544E+00	2.8869E+01	3.6337E+01	4	14	9		1	45	
	4	5.2461E-03	1.0000E+00	1.4902E+00	1.8959E+00	3.4555E+01	4.0660E+01		18	1		16	33	

Test Case 3

								New Fuel Types						
OF	CYC	FCC	EOC KEFF	MAX(RPF2)	MAX(RPF3)	MAX(EXP2)	MAX(EXP3)	1	2	3	4	6	7	8
1.4937E-01	2	6.6870E-03	1.0042E+00	1.4974E+00	1.8778E+00	2.4443E+01	3.0148E+01 -		23	3			56	
	3	5.4254E-03	1.0000E+00	1.4754E+00	1.8907E+00	2.8903E+01	3.6103E+01		24			1	43	
	4	5.8920E-03	1.0000E+00	1.4915E+00	1.8794E+00	3.4498E+01	4.0999E+01	2	34			25	21	

Test Case 4

								New Fuel Types						
OF	CYC	FCC	EOC KEFF	MAX(RPF2)	MAX(RPF3)	MAX(EXP2)	MAX(EXP3)	1	2	3	4	6	7	8
1.5862E-01	2	6.9479E-03	1.0048E+00	1.4965E+00	1.8754E+00	2.3995E+01	2.9851E+01 -		43	2		2	43	
	3	6.2201E-03	1.0000E+00	1.4818E+00	1.8696E+00	2.8881E+01	3.4999E+01	2	53	3		3	24	
	4	5.9239E-03	1.0000E+00	1.4995E+00	1.8716E+00	3.1750E+01	3.7212E+01	1	51	15		6	7	1

D.5– CRP Search Test Case

Test Case 1

								New Fuel Types						
OF	CYC	FCC	EOC KEFF	MAX(RPF2)	MAX(RPF3)	MAX(EXP2)	MAX(EXP3)	1	2	3	4	6	7	8
4.4598E+00	2	7.2913E-03	1.0014E+00	1.5748E+00	2.0613E+00	2.4541E+01	2.9381E+01	-				1	83	
	3	5.4792E-03	1.0001E+00	1.4922E+00	1.8892E+00	2.8874E+01	3.4871E+01	20	11		1		42	
	4	5.8899E-03	1.0001E+00	1.4972E+00	1.9058E+00	3.4961E+01	4.2633E+01		8			11	53	

Appendix E – Loading Pattern Plots for Best Solutions not Presented in the Text

E.1 – All Sampling Types with Constant Sampling Probabilities PSA Best Solutions

Test Case 1

2nd Cycle Optimized

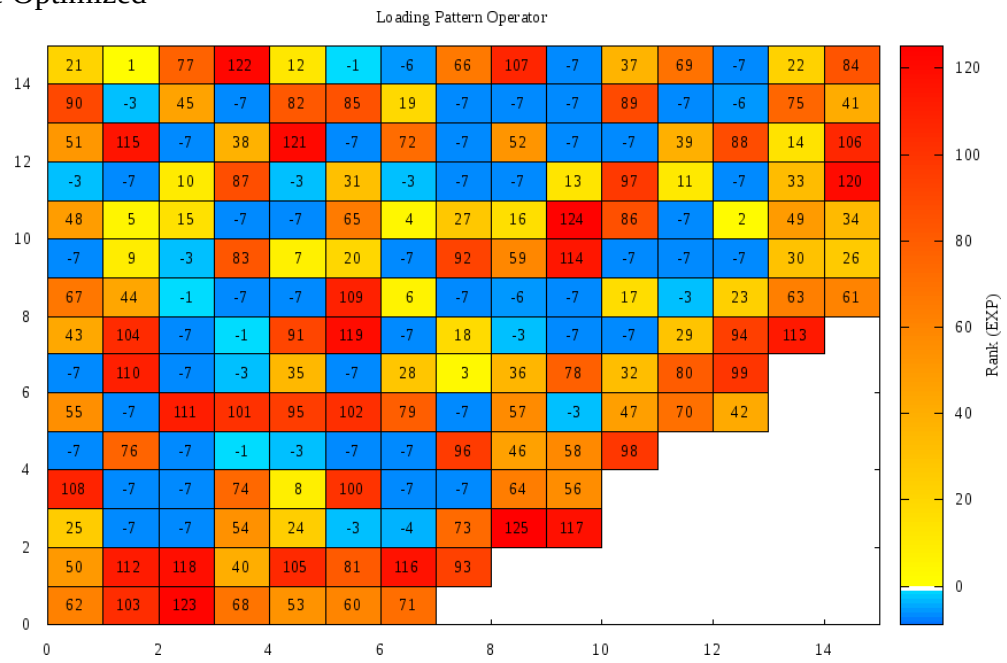

3rd Cycle Optimized

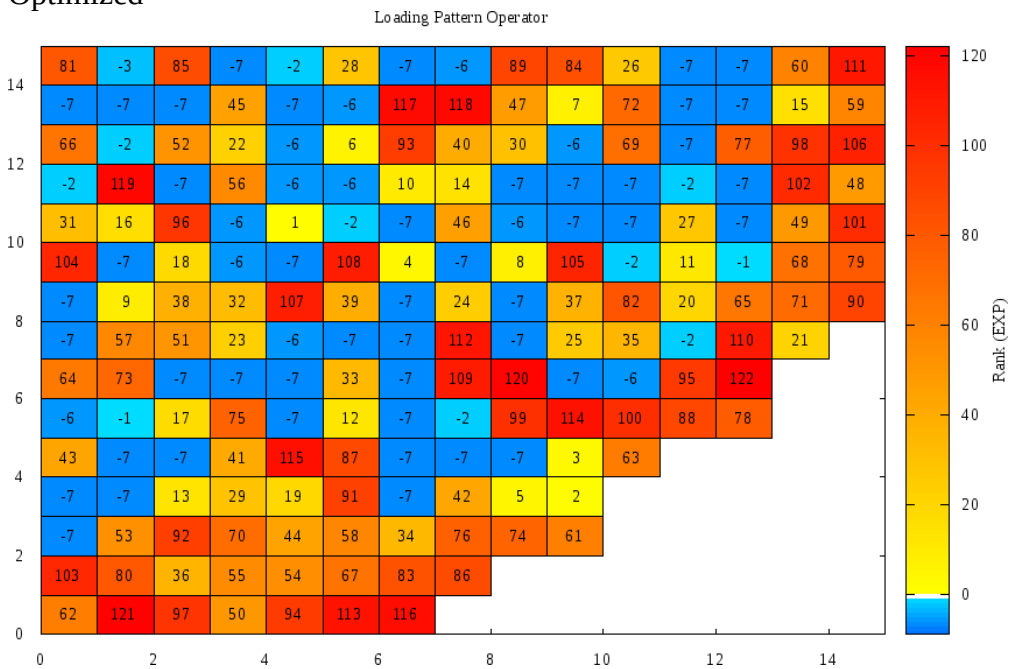

Test Case 2

2nd Cycle Optimized

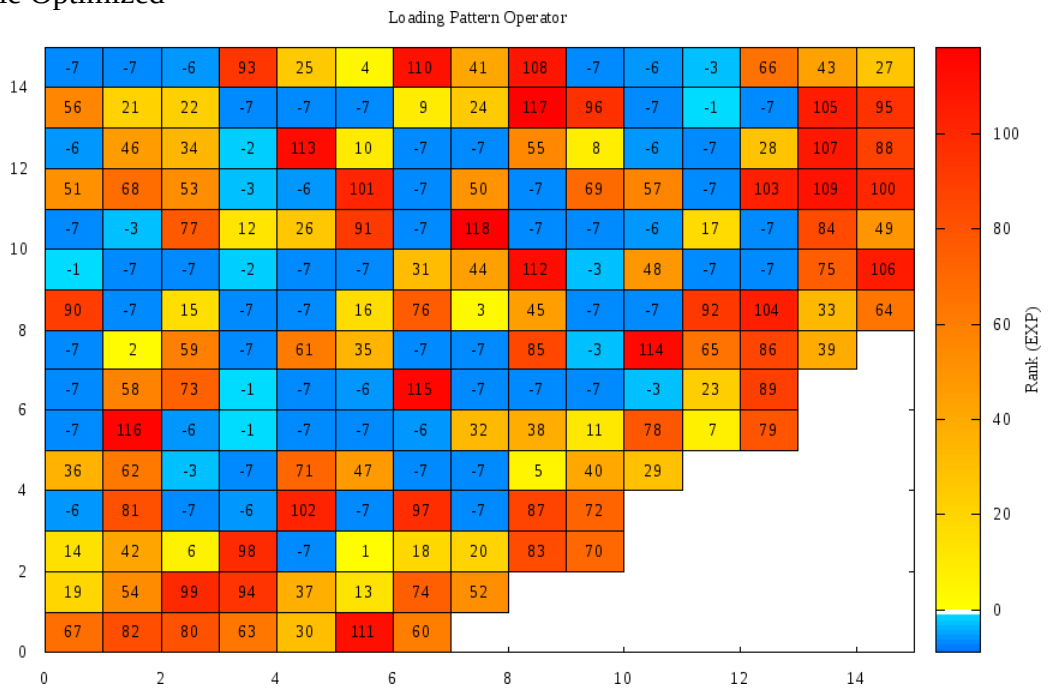

3rd Cycle Optimized

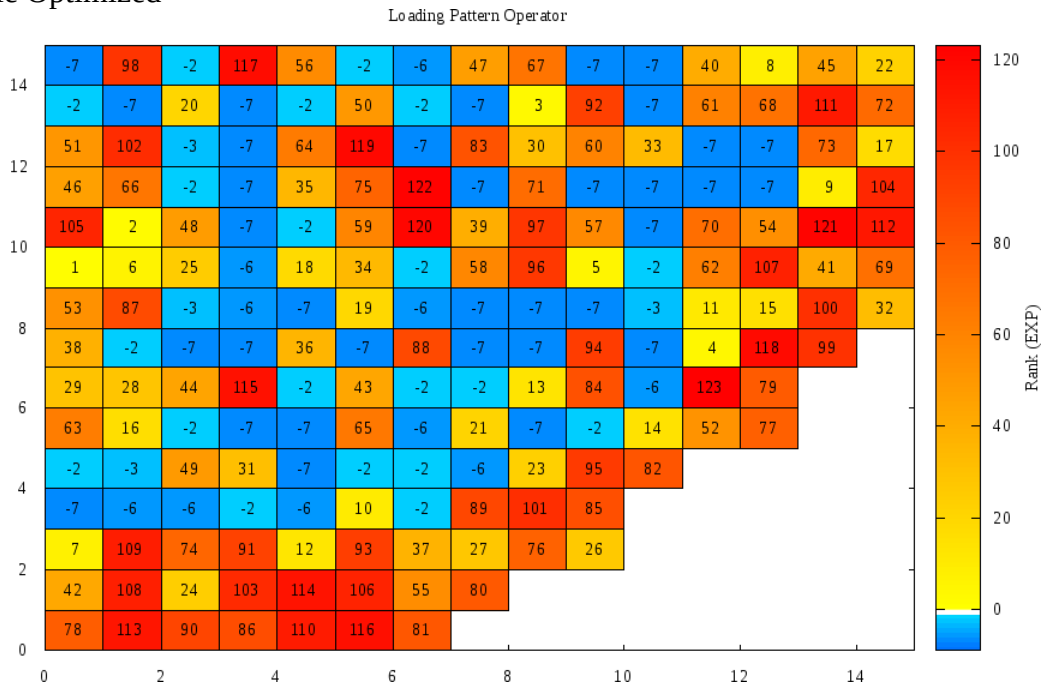

Test Case 3

2nd Cycle Optimized

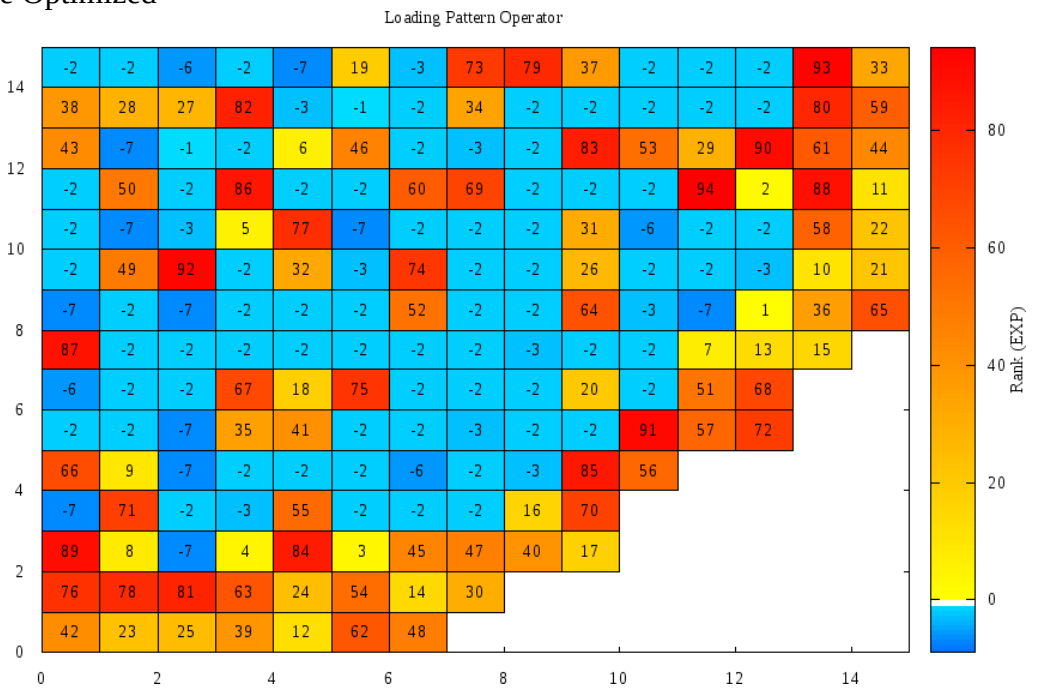

3rd Cycle Optimized

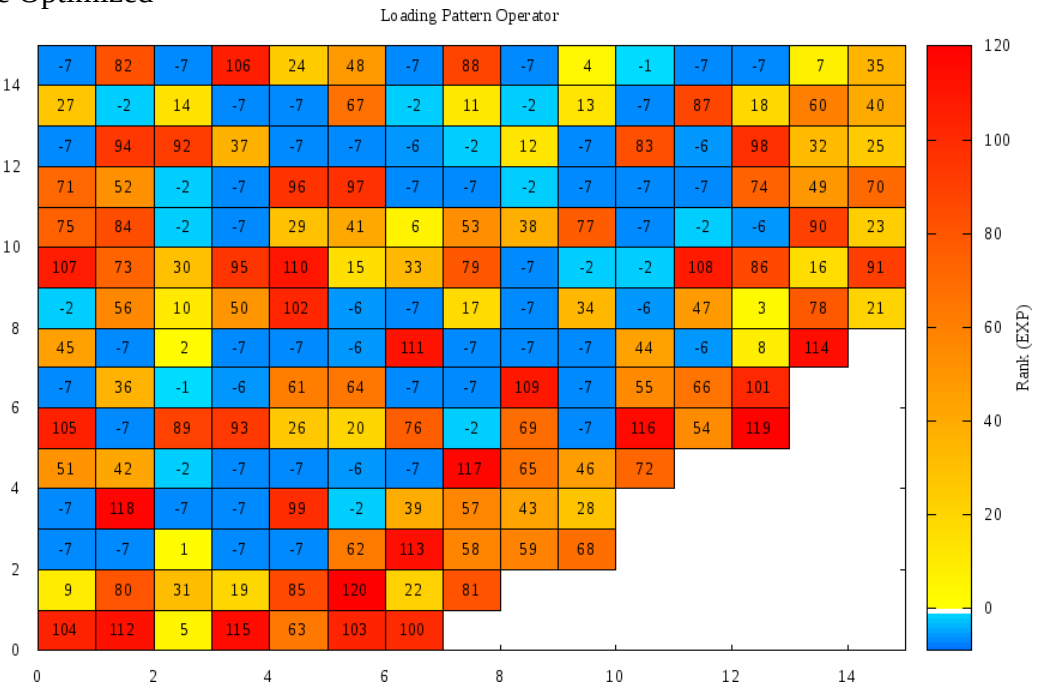

Test Case 4

2nd Cycle Optimized

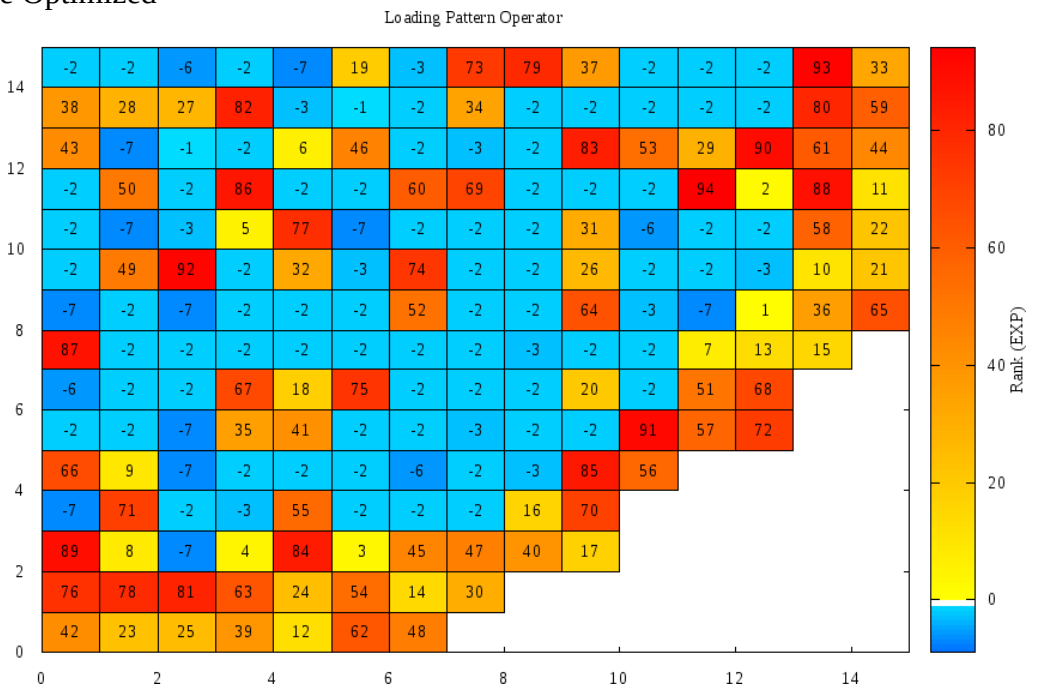

3rd Cycle Optimized

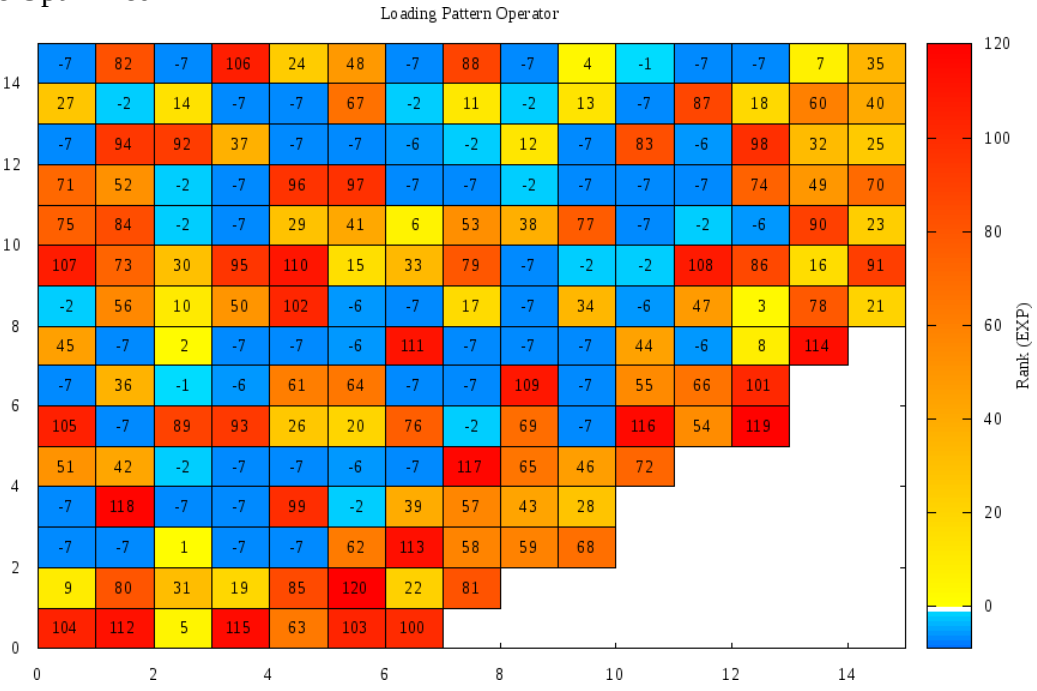

E.2 – Ordered Sampling with Constant Sampling Probabilities PSA Best Solutions

Test Case 1

1st Cycle Optimized

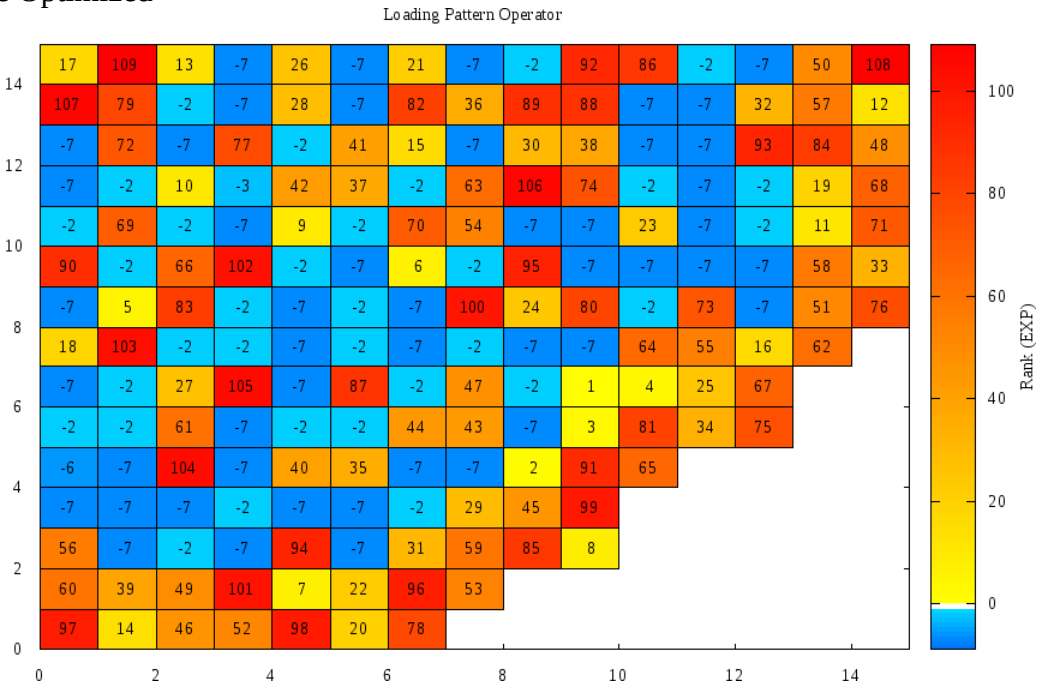

2nd Cycle Optimized

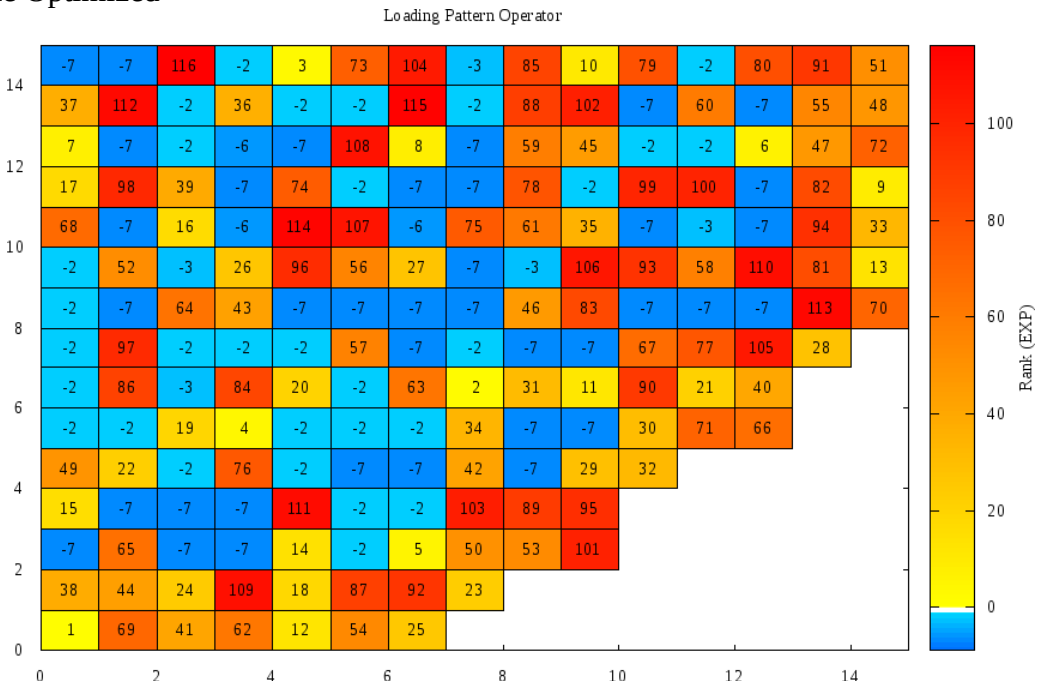

3rd Cycle Optimized

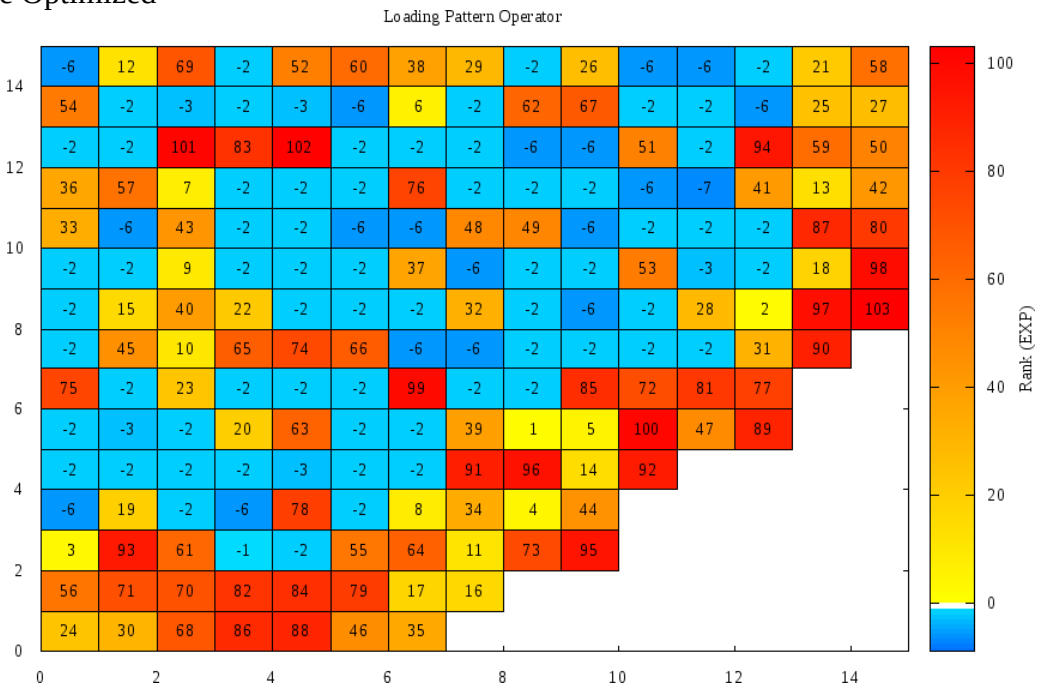

Test Case 2

1st Cycle Optimized

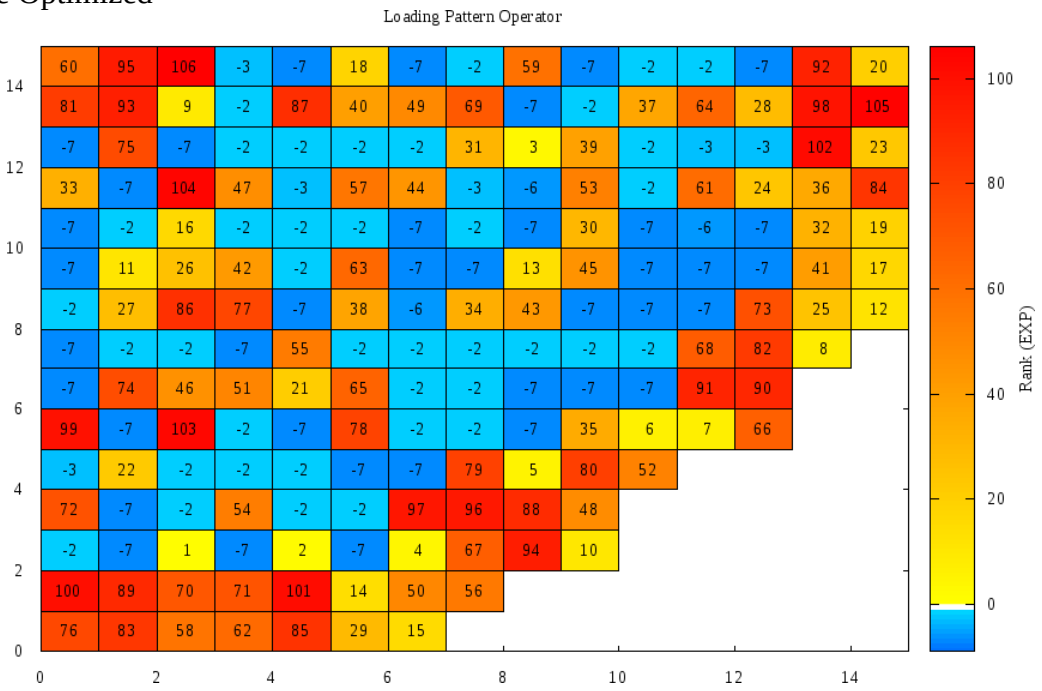

2nd Cycle Optimized

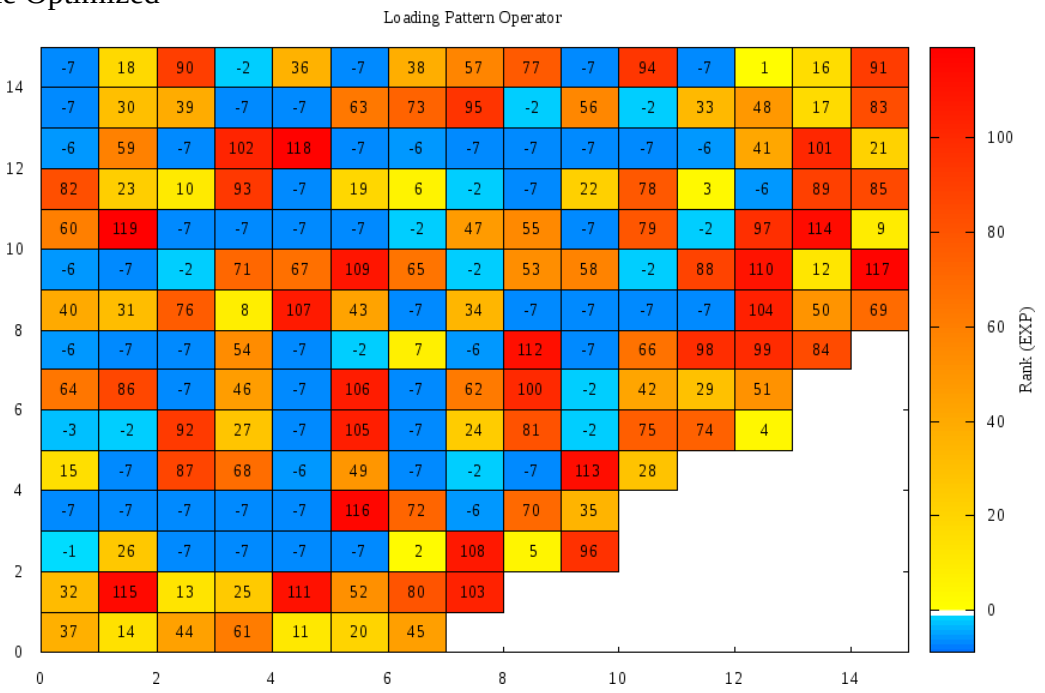

3rd Cycle Optimized

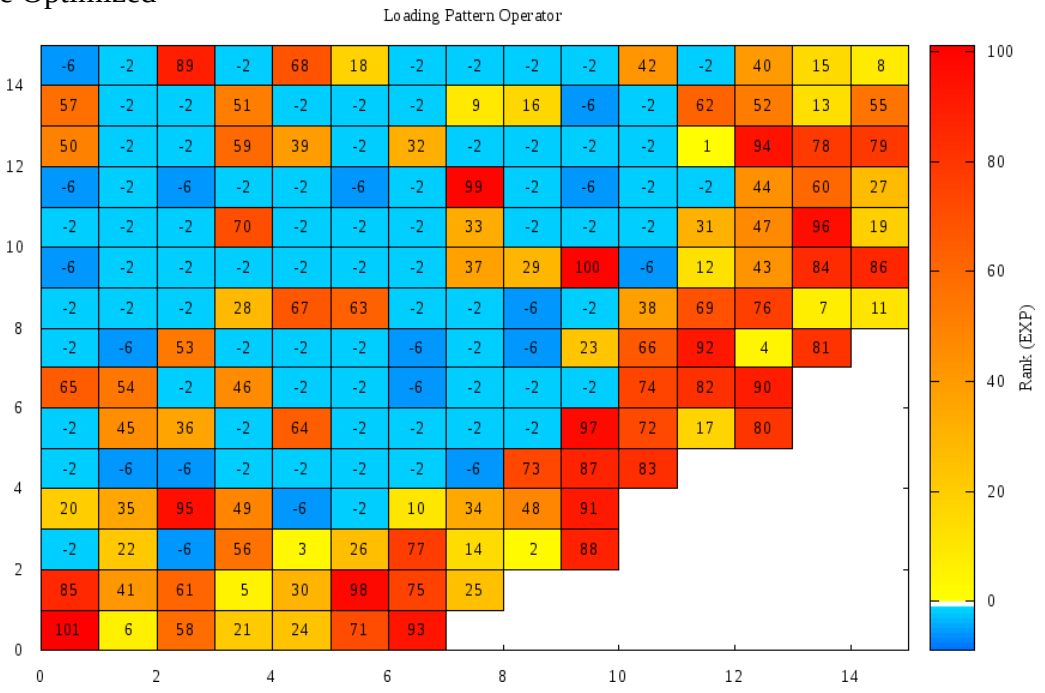

Test Case 3

1st Cycle Optimized

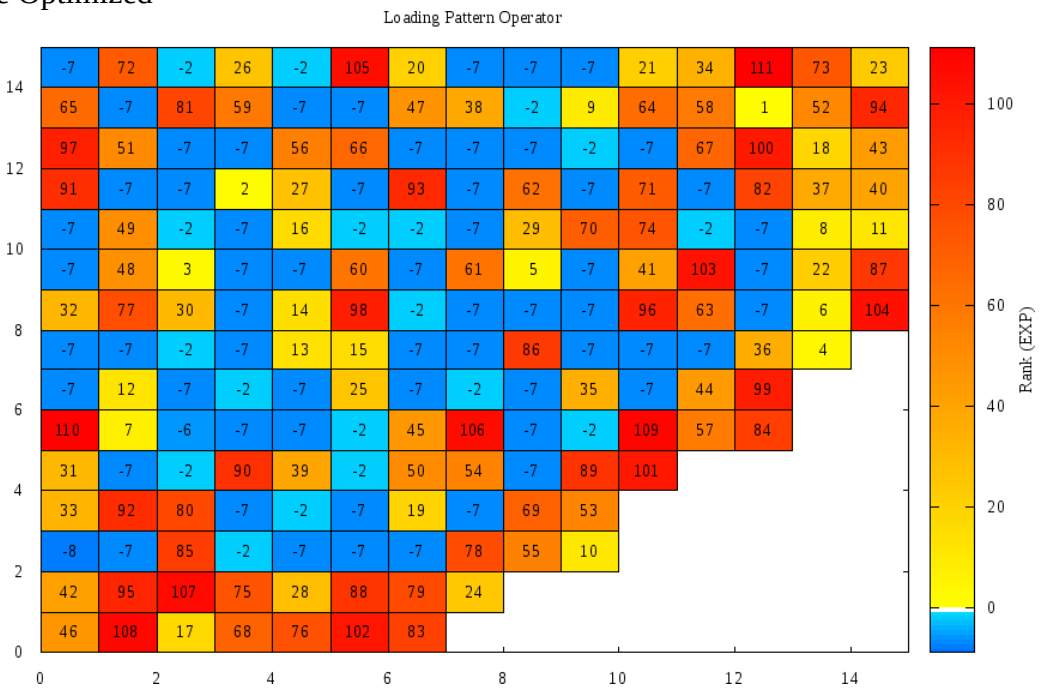

2nd Cycle Optimized

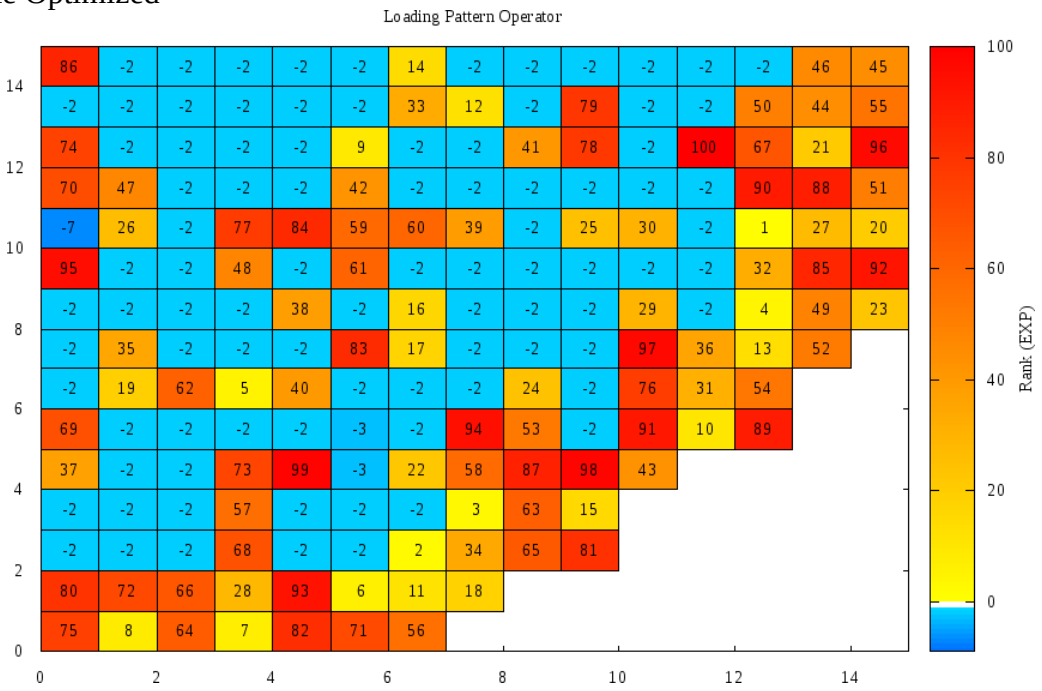

3rd Cycle Optimized

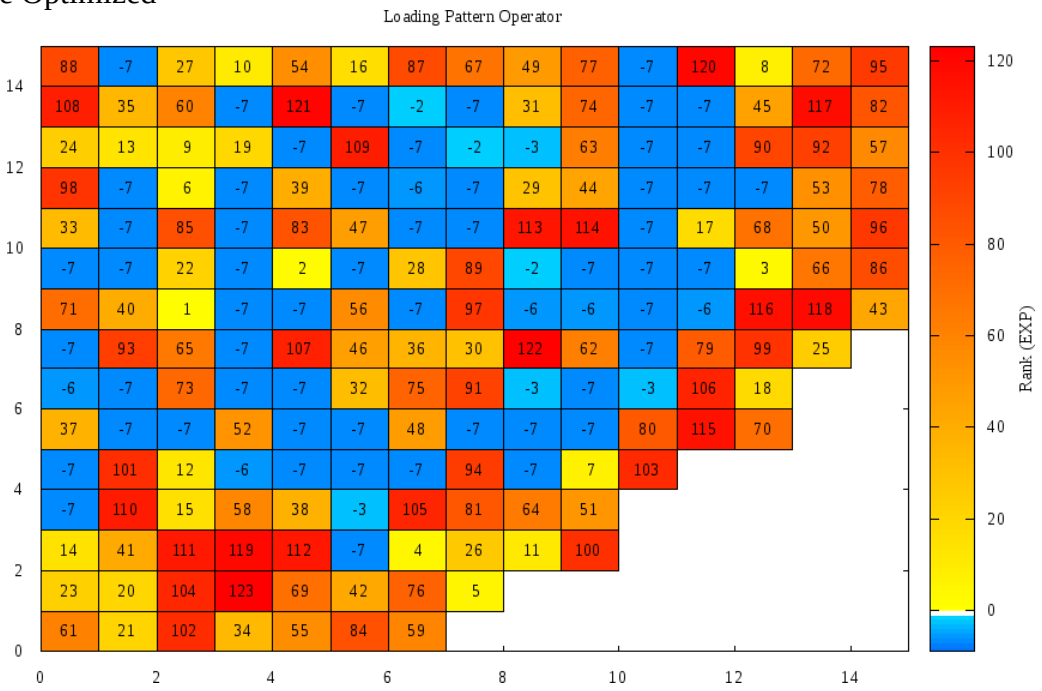

Test Case 4

1st Cycle Optimized

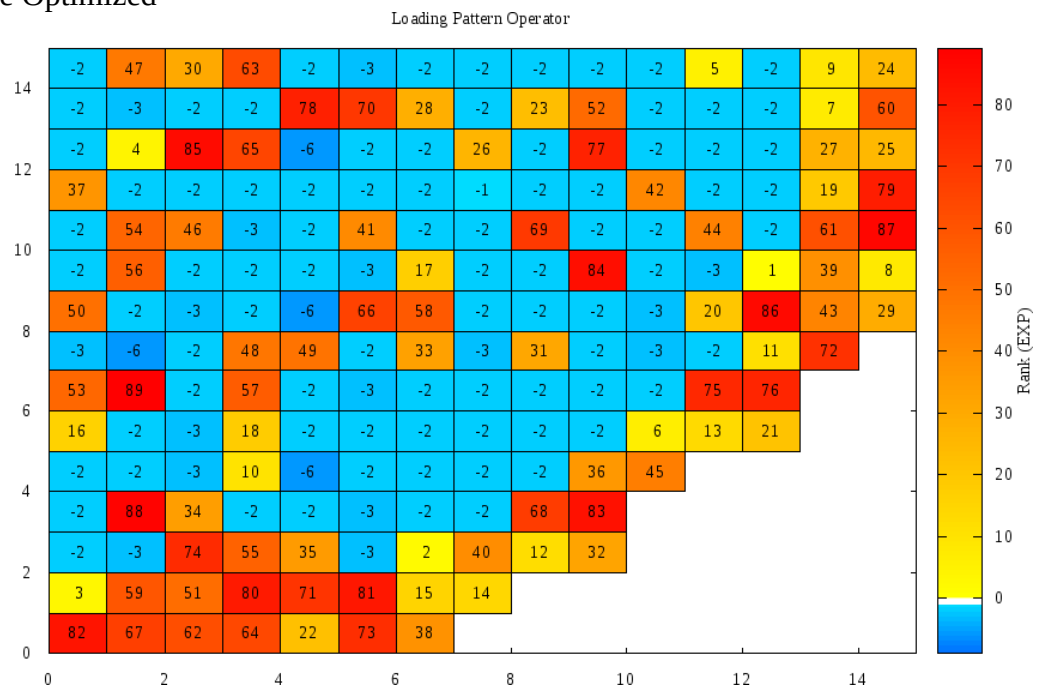

2nd Cycle Optimized

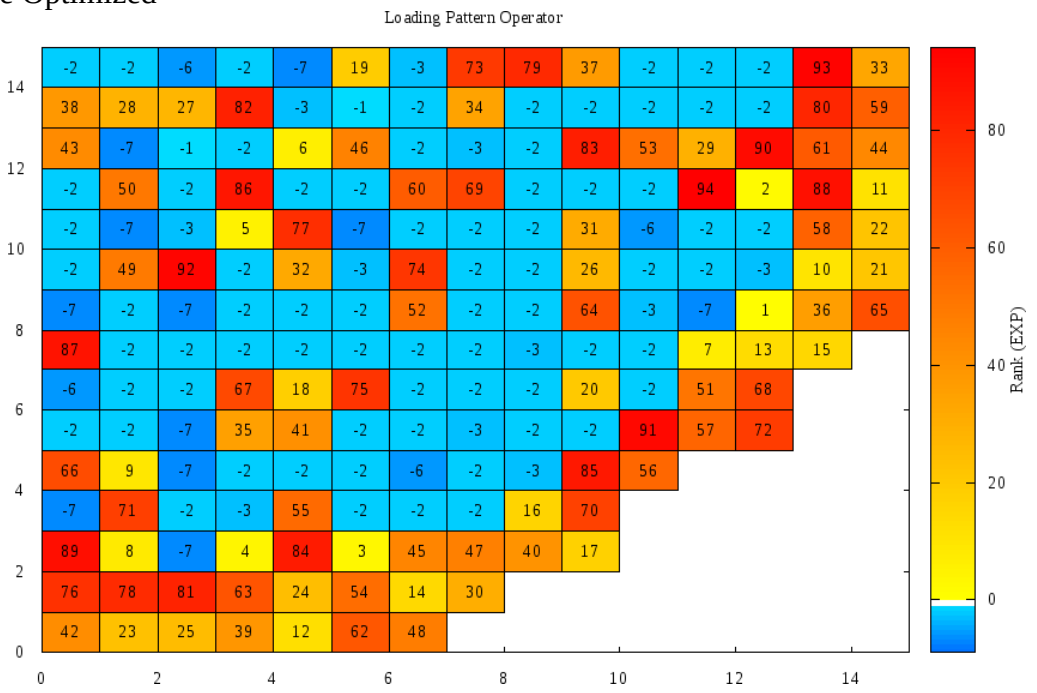

3rd Cycle Optimized

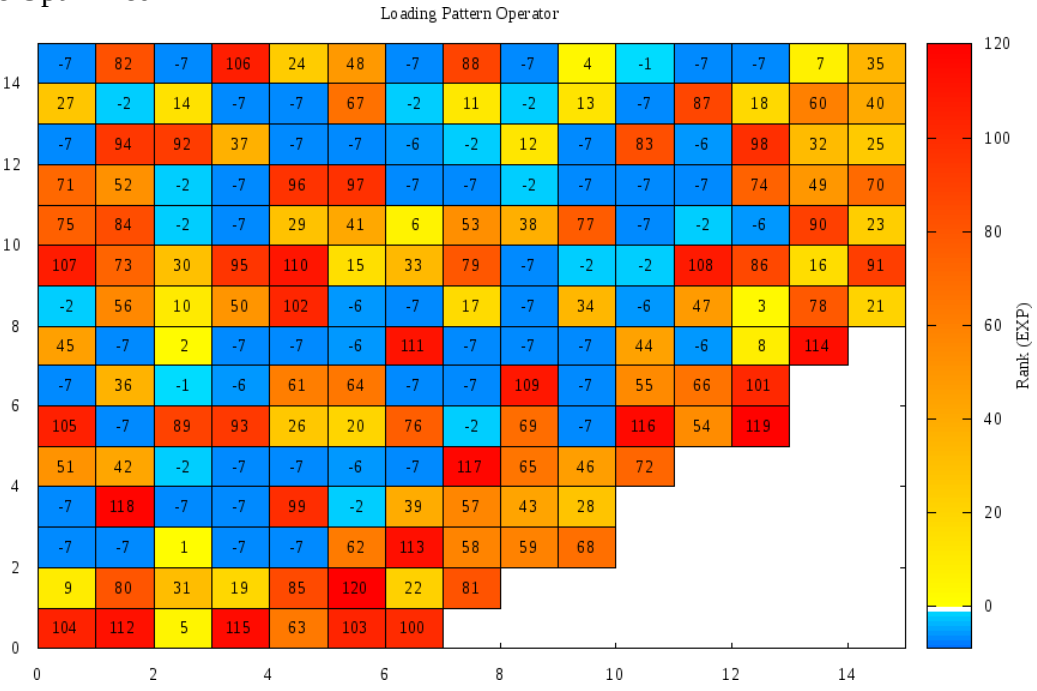

E.3 – Random Sampling with Constant Sampling Probabilities PSA Best Solutions

Test Case 1

1st Cycle Optimized

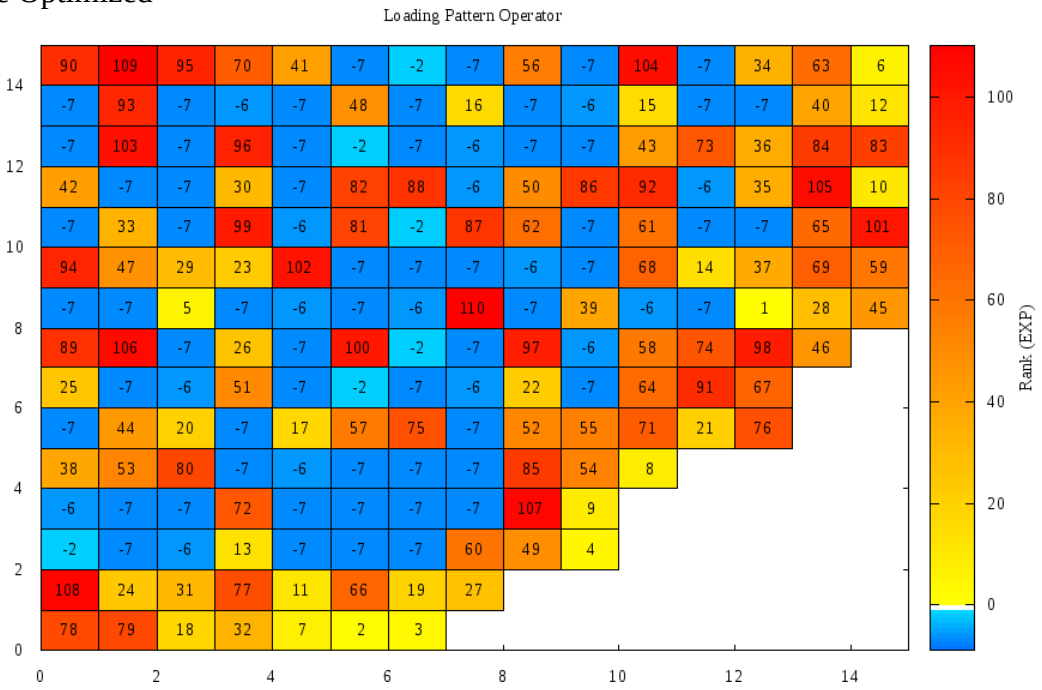

2nd Cycle Optimized

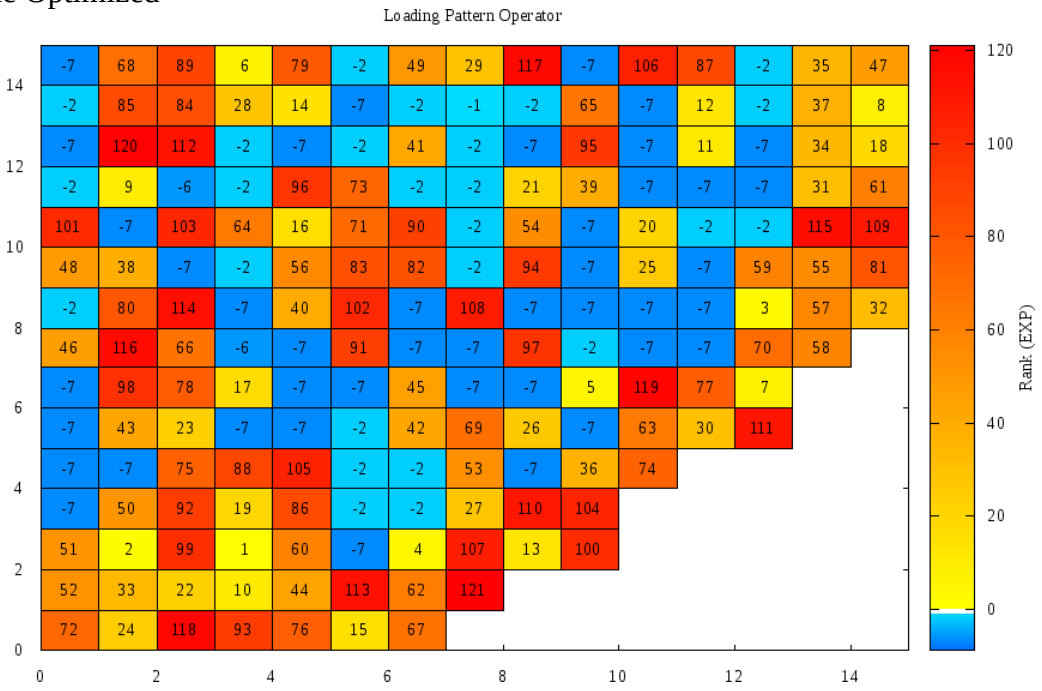

3rd Cycle Optimized

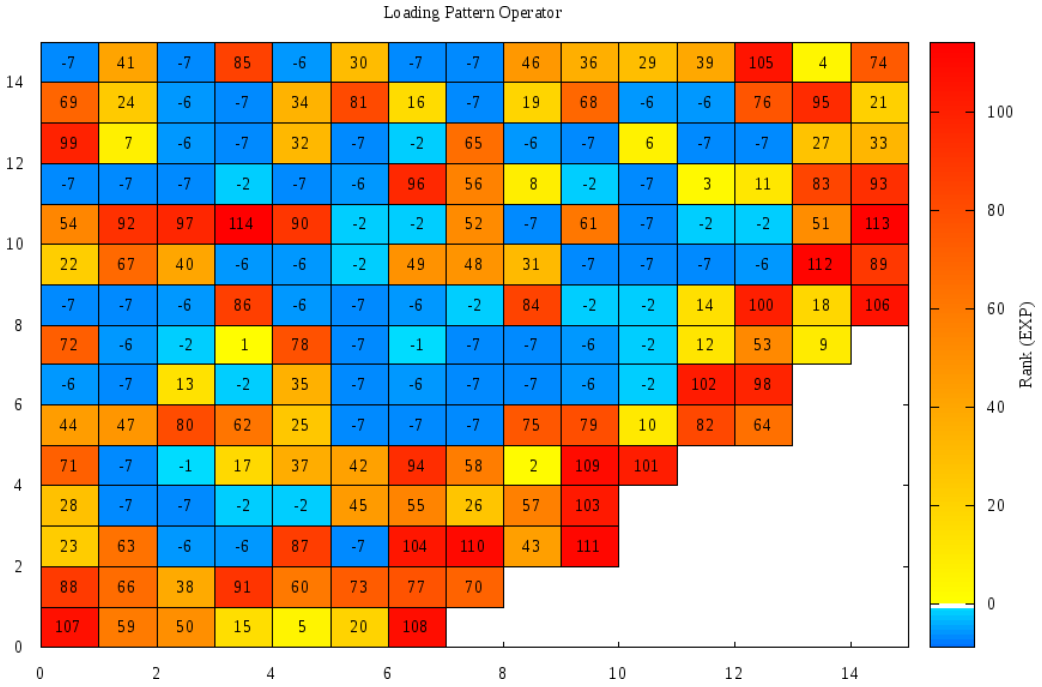

Test Case 2

1st Cycle Optimized

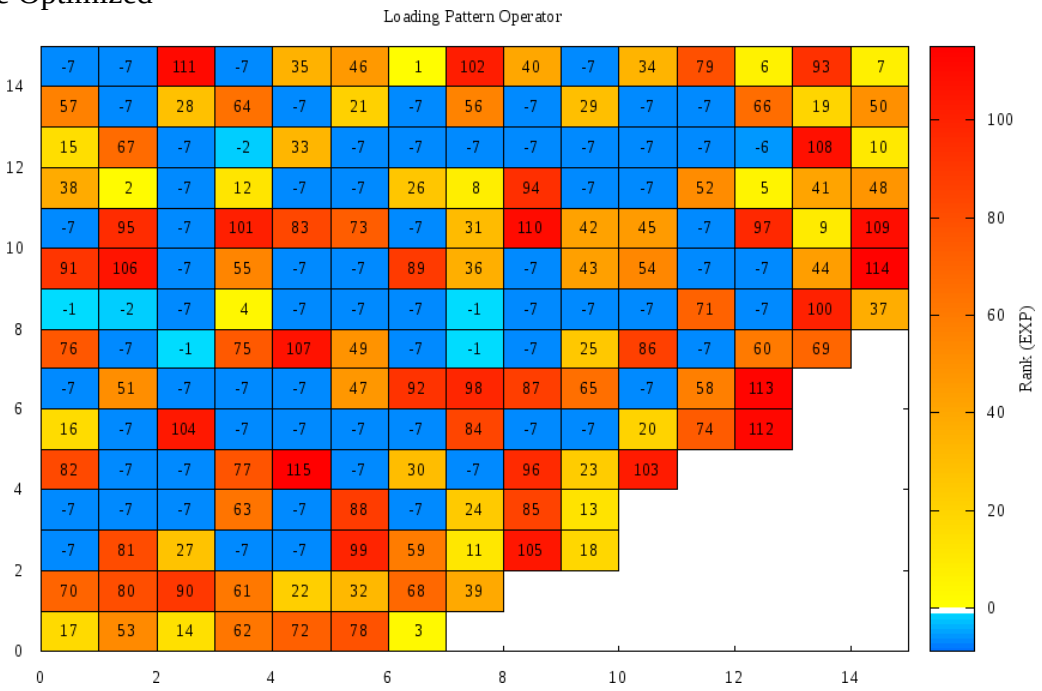

2nd Cycle Optimized

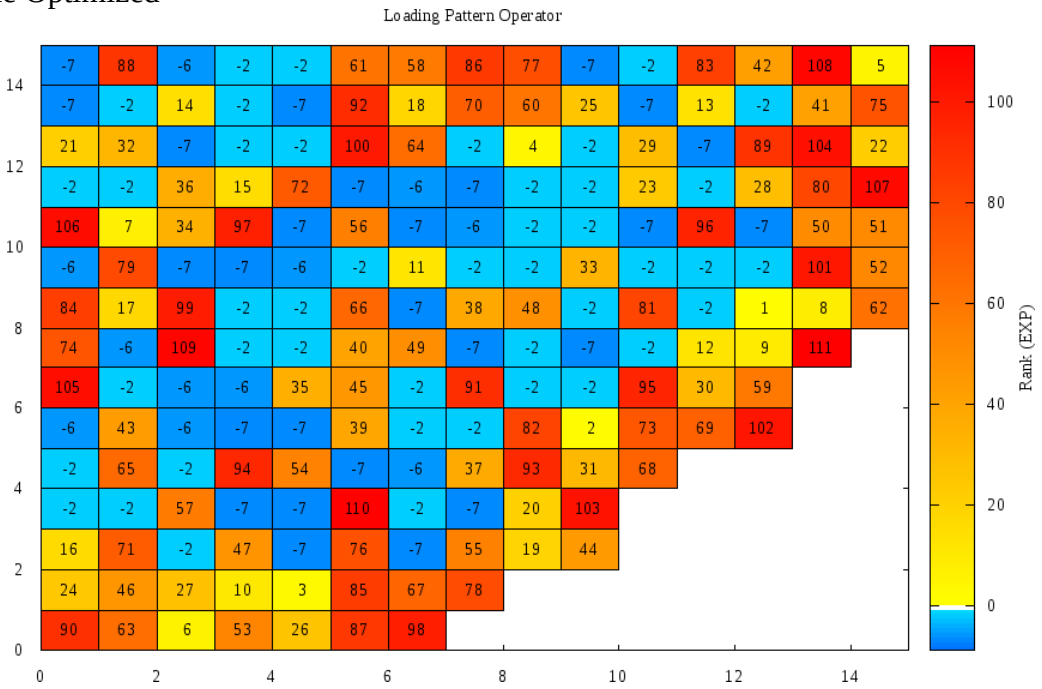

3rd Cycle Optimized

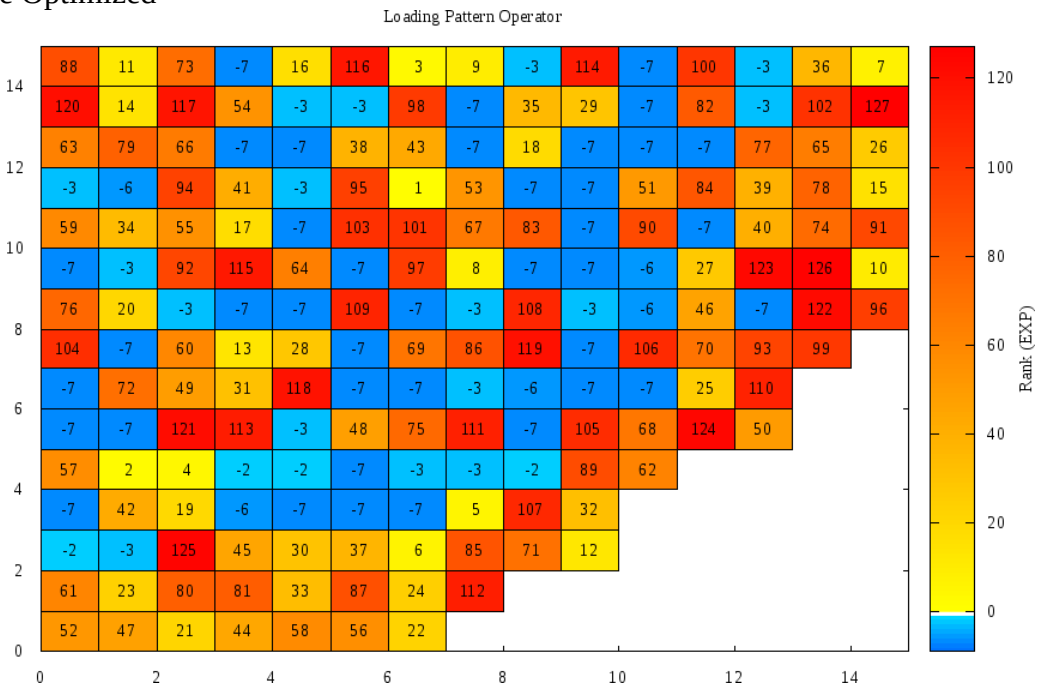

Test Case 3

1st Cycle Optimized

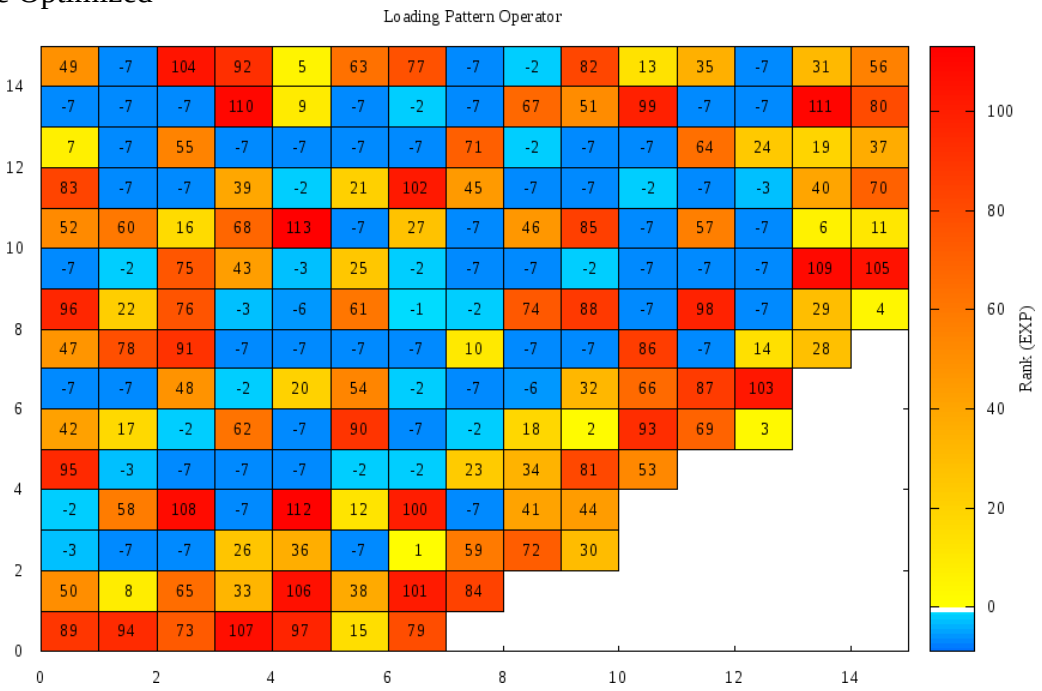

2nd Cycle Optimized

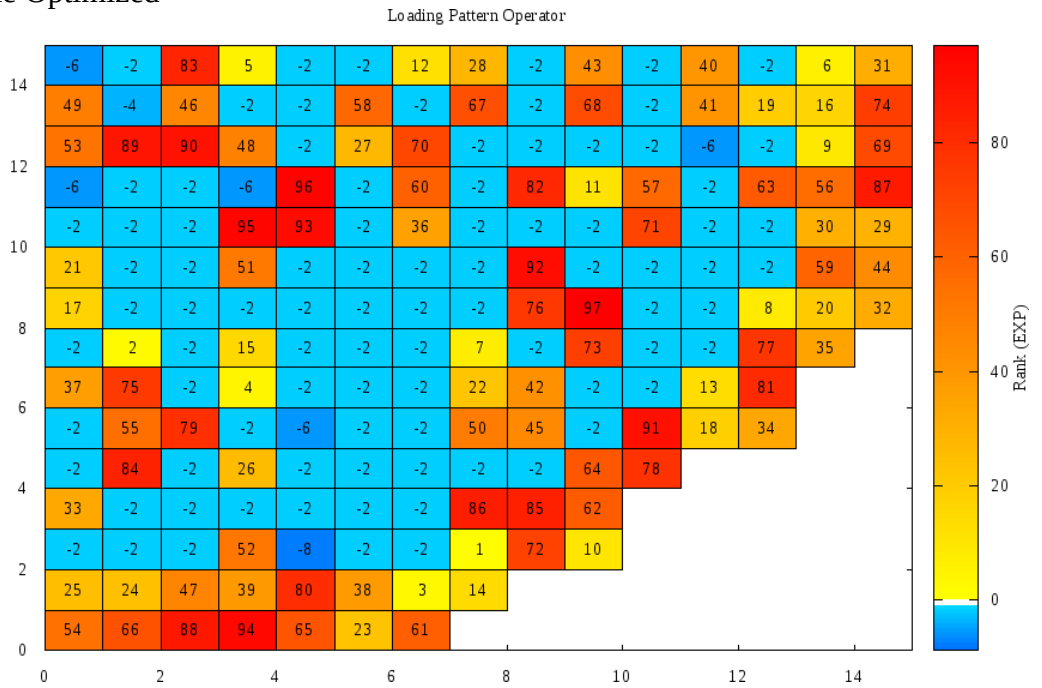

3rd Cycle Optimized

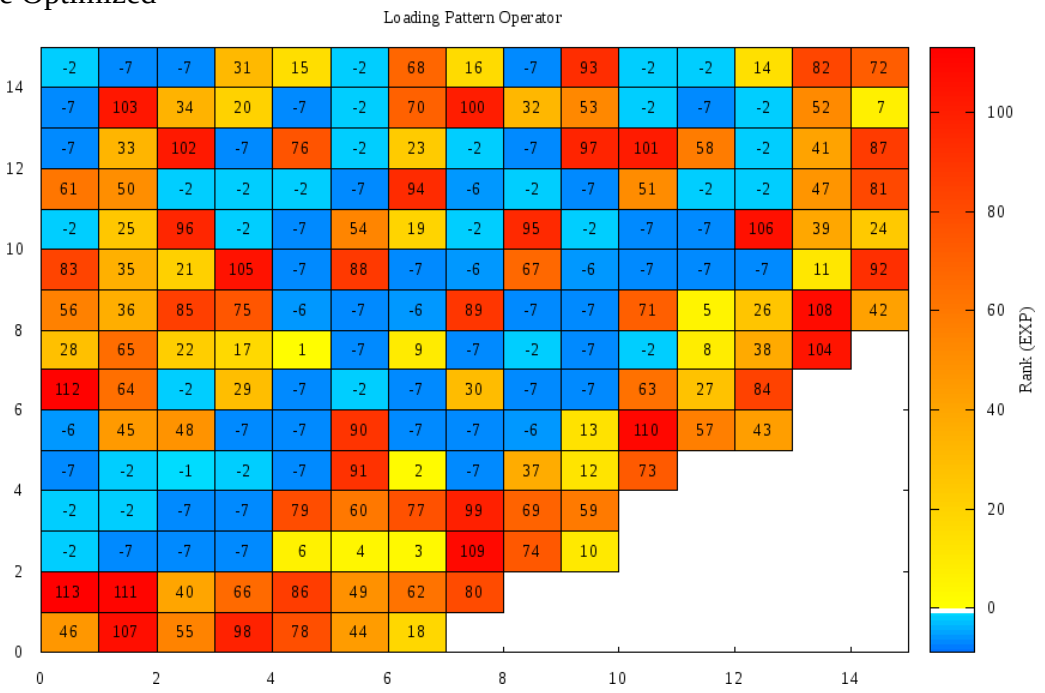

Test Case 4

1st Cycle Optimized

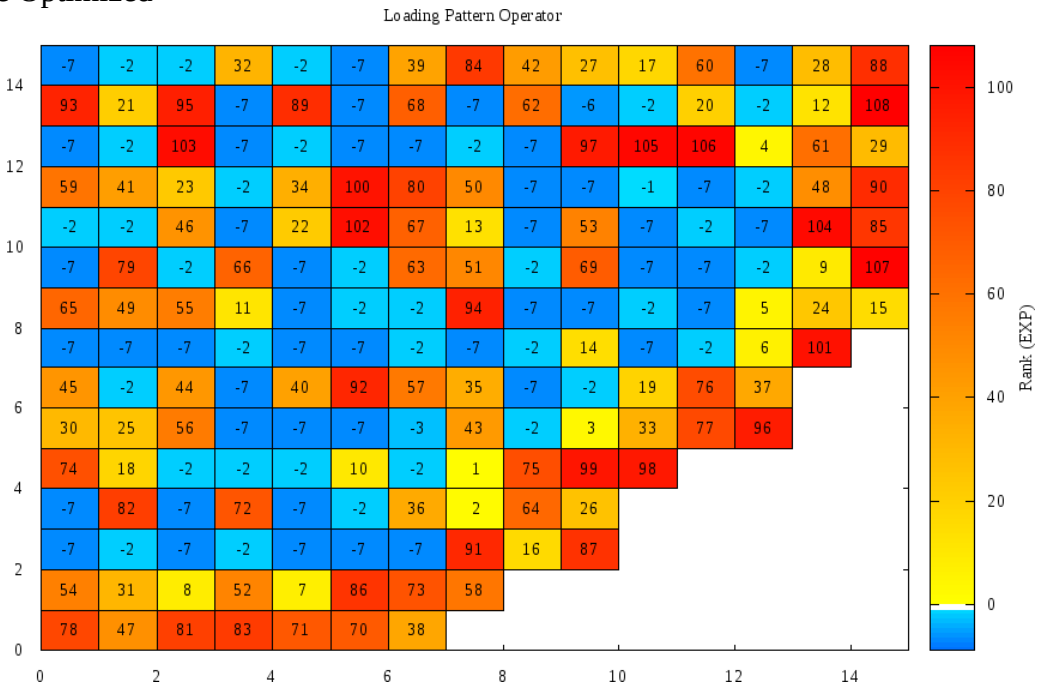

2nd Cycle Optimized

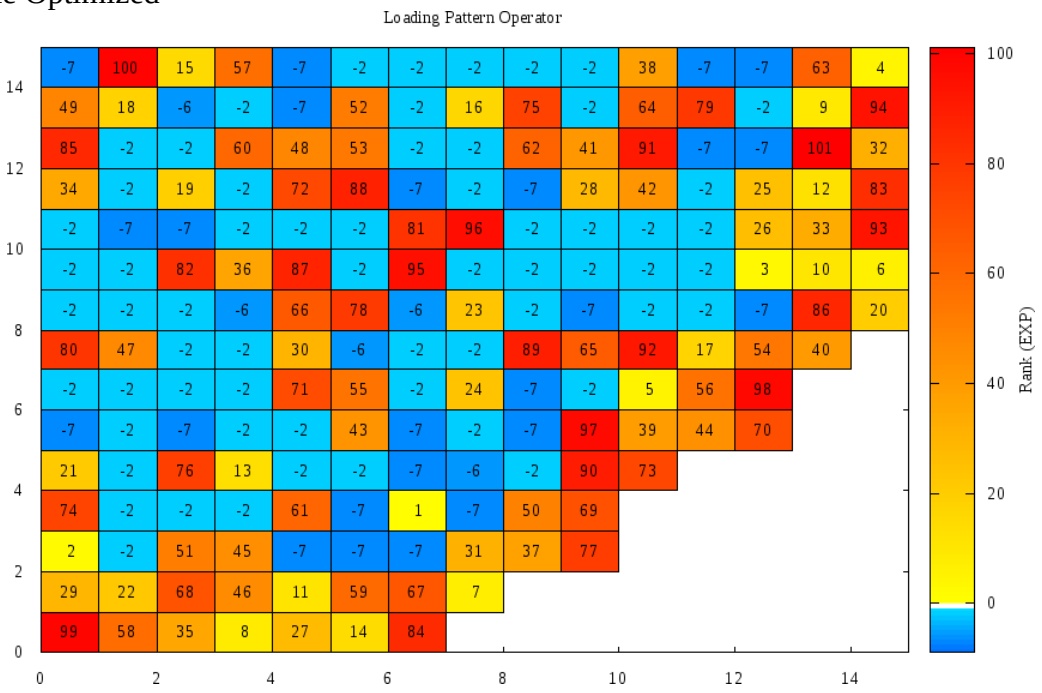

3rd Cycle Optimized

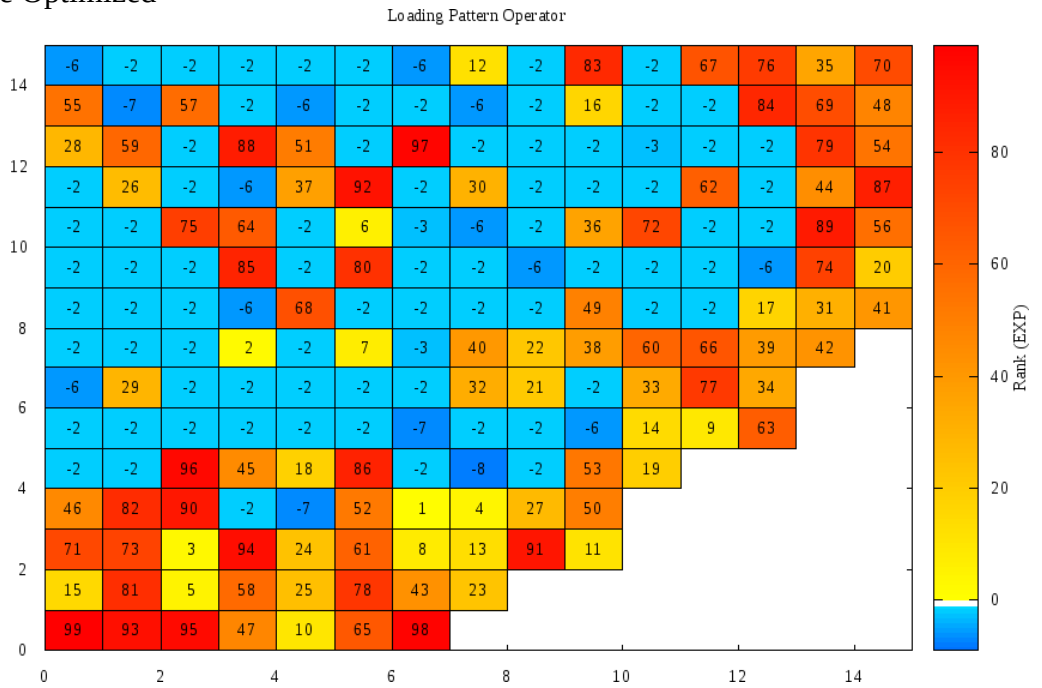

E.4 – All Sampling Types with Variable Sampling Probabilities PSA Best Solutions

Test Case 1

1st Cycle Optimized

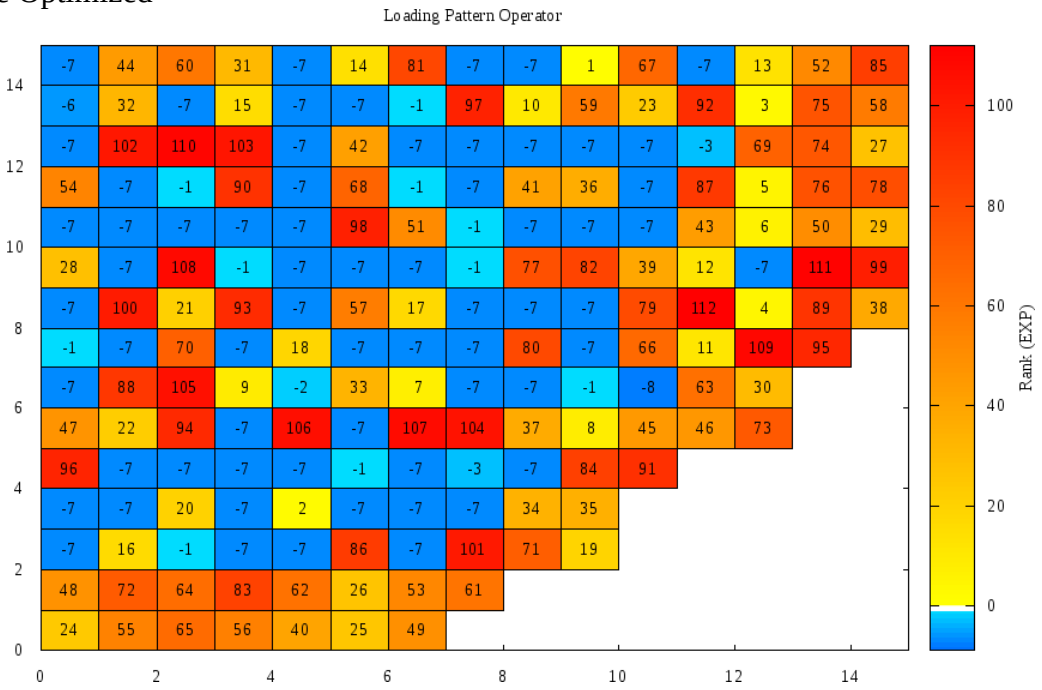

2nd Cycle Optimized

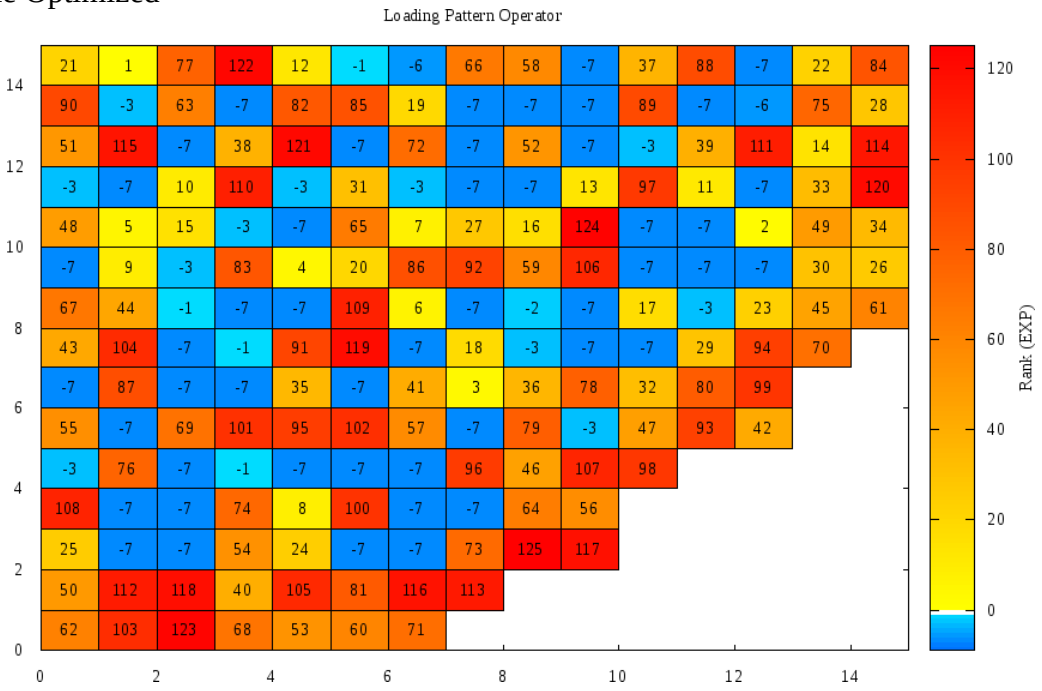

3rd Cycle Optimized

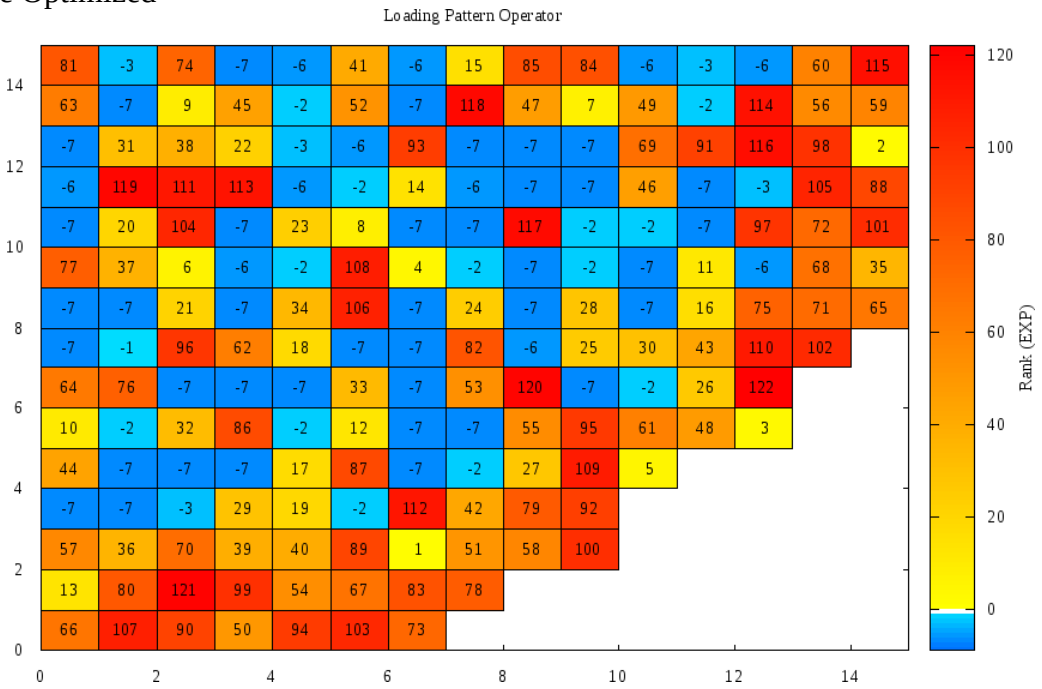

Test Case 2

1st Cycle Optimized

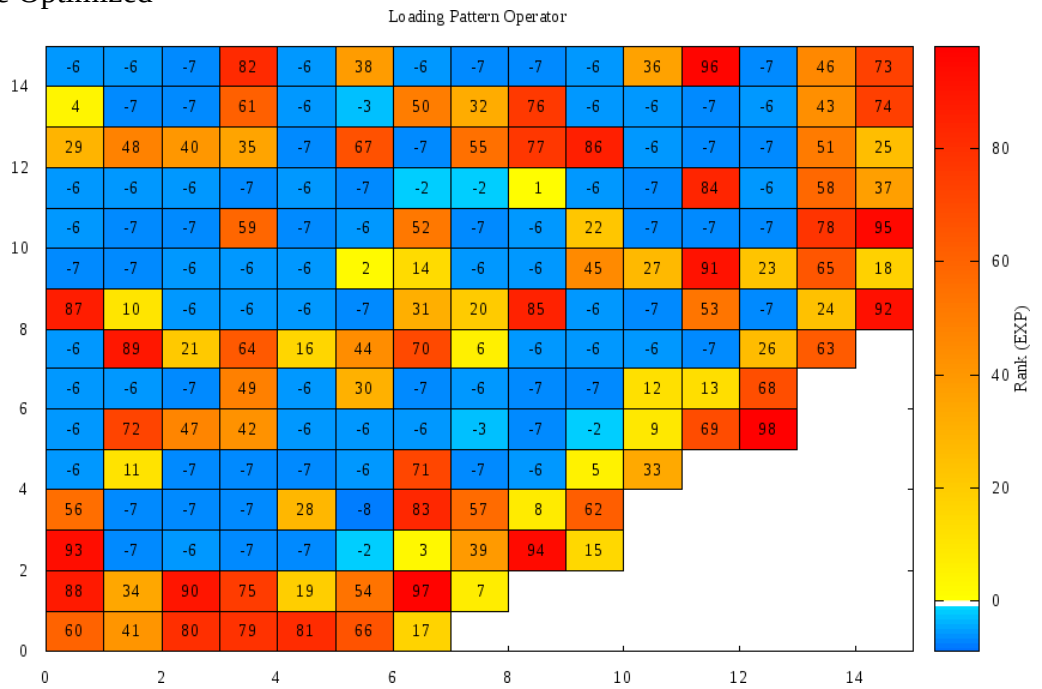

2nd Cycle Optimized

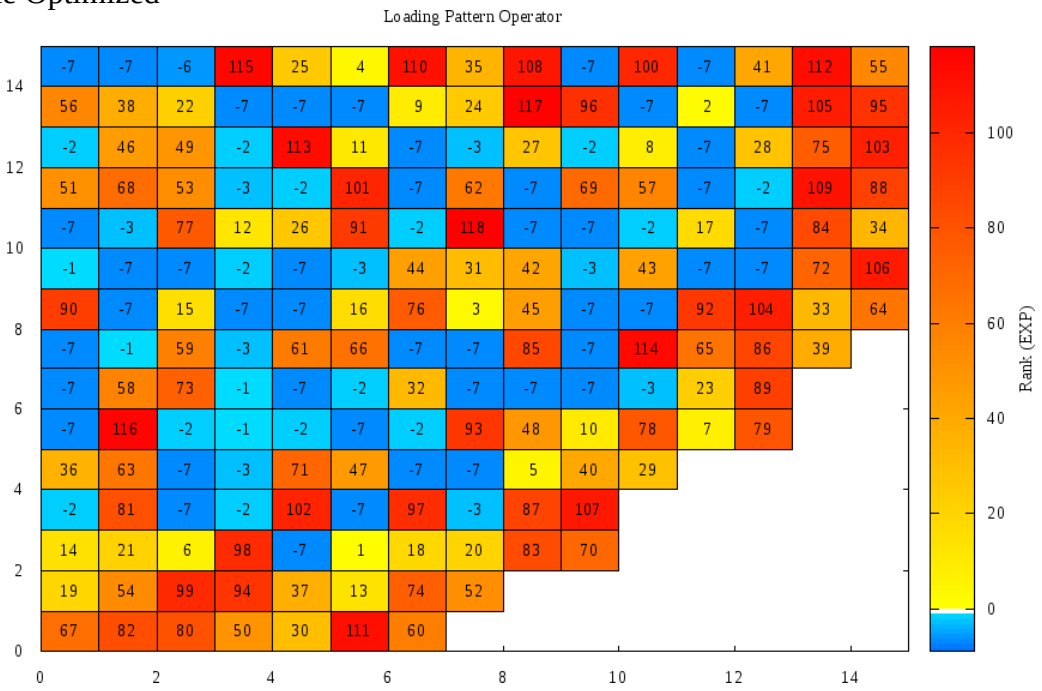

3rd Cycle Optimized

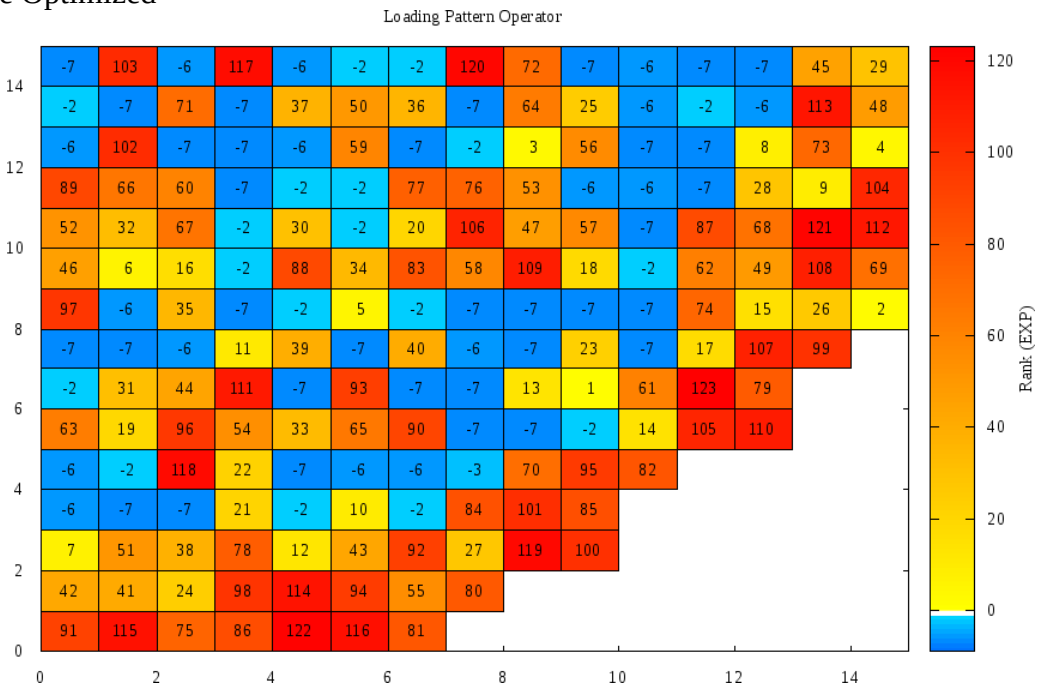

Test Case 3

1st Cycle Optimized

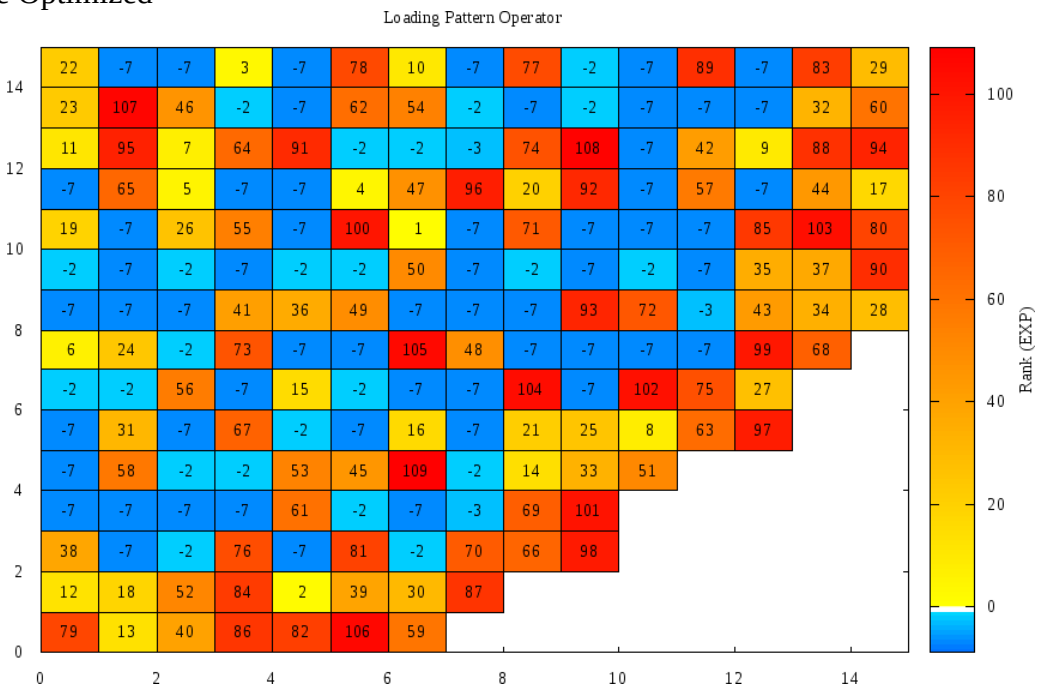

2nd Cycle Optimized

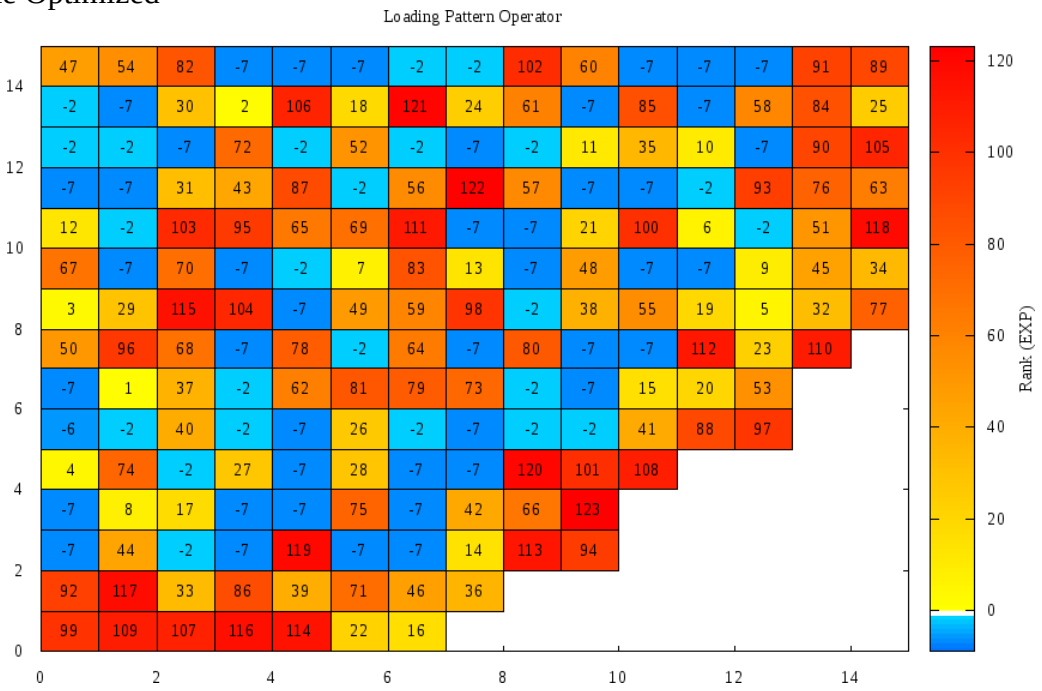

3rd Cycle Optimized

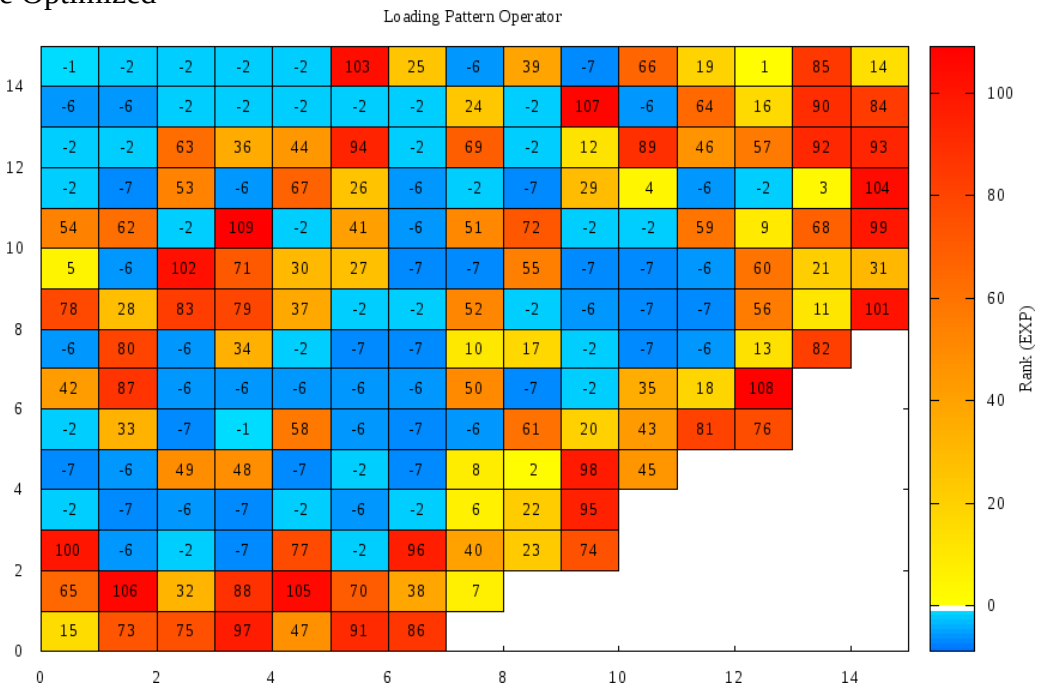

Test Case 4

1st Cycle Optimized

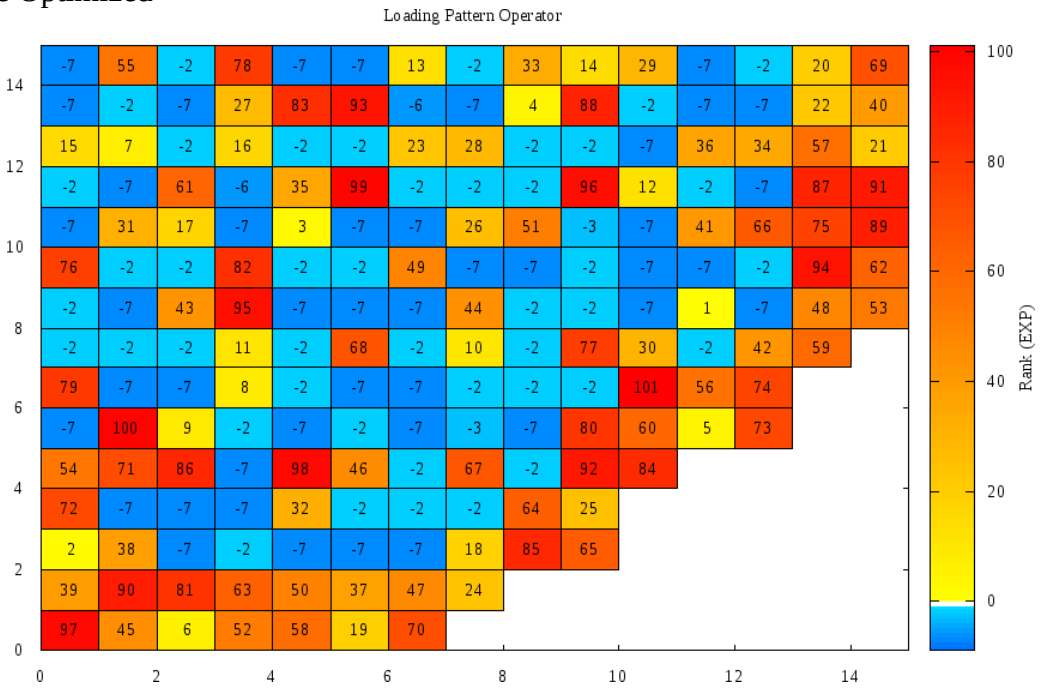

2nd Cycle Optimized

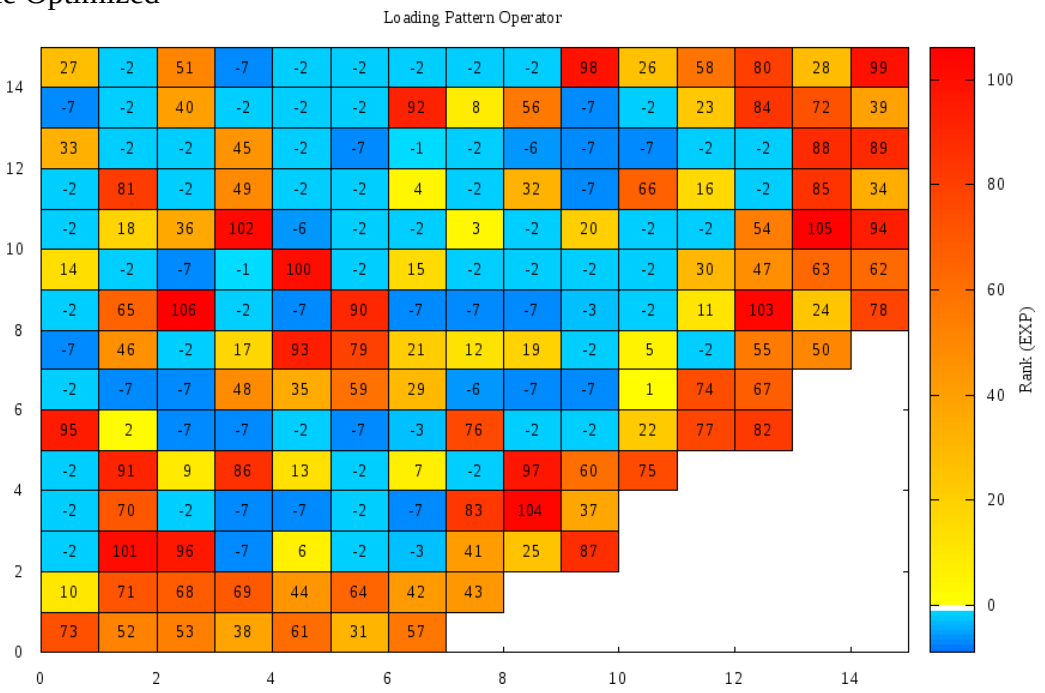

3rd Cycle Optimized

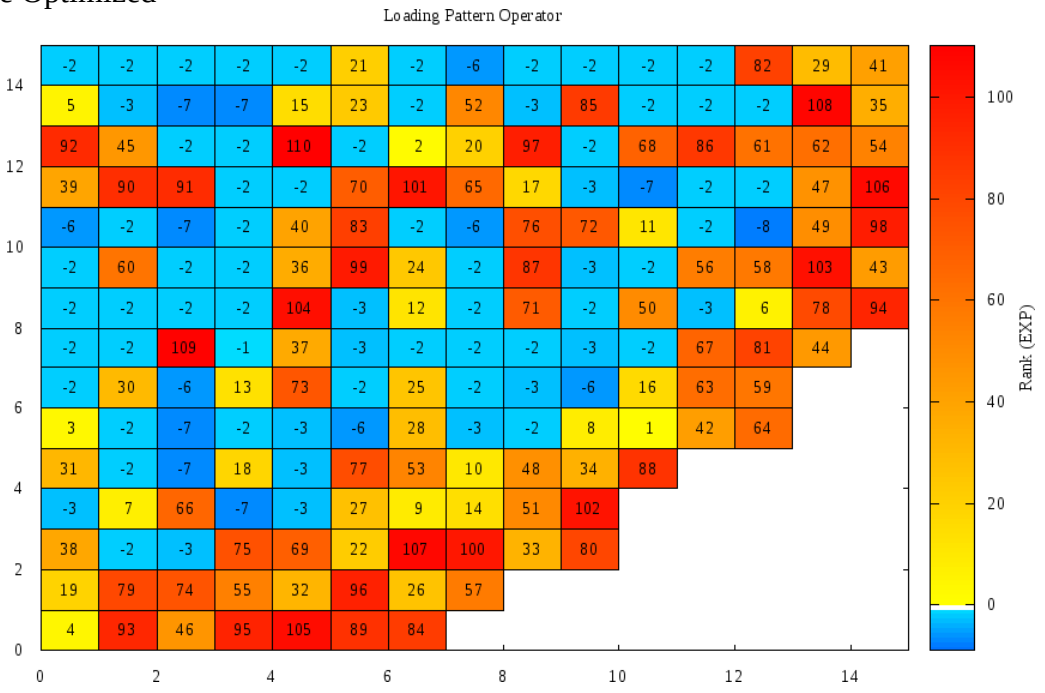

E.5 – CRP Search, All Sampling Types with Variable Sampling Probabilities Best Solutions

Test Case 1

1st Cycle Optimized

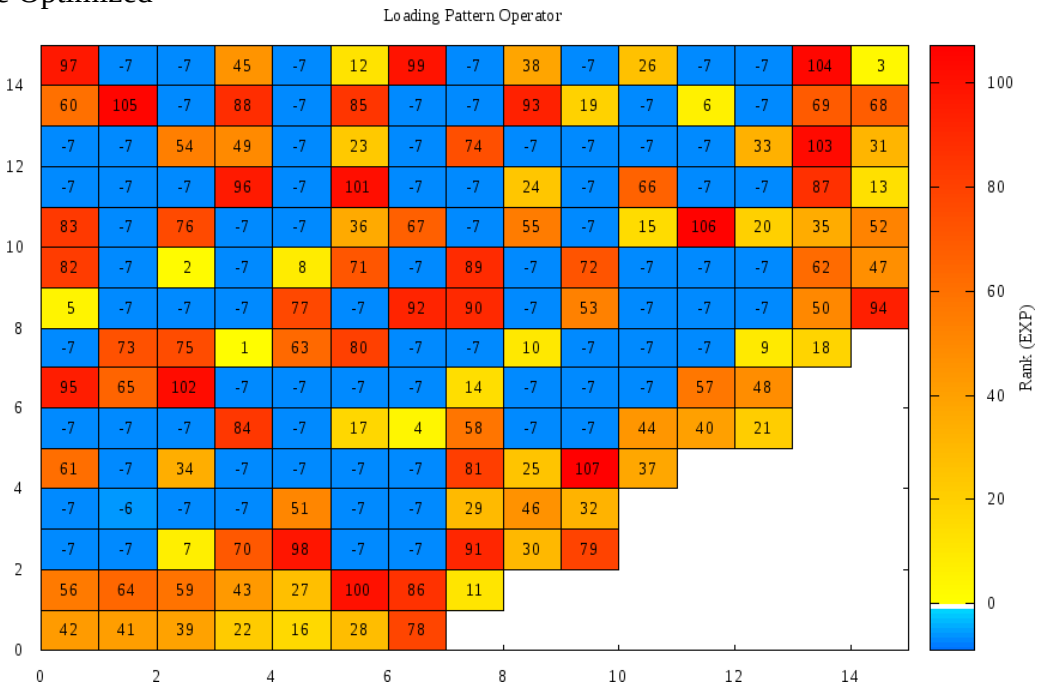

2nd Cycle Optimized

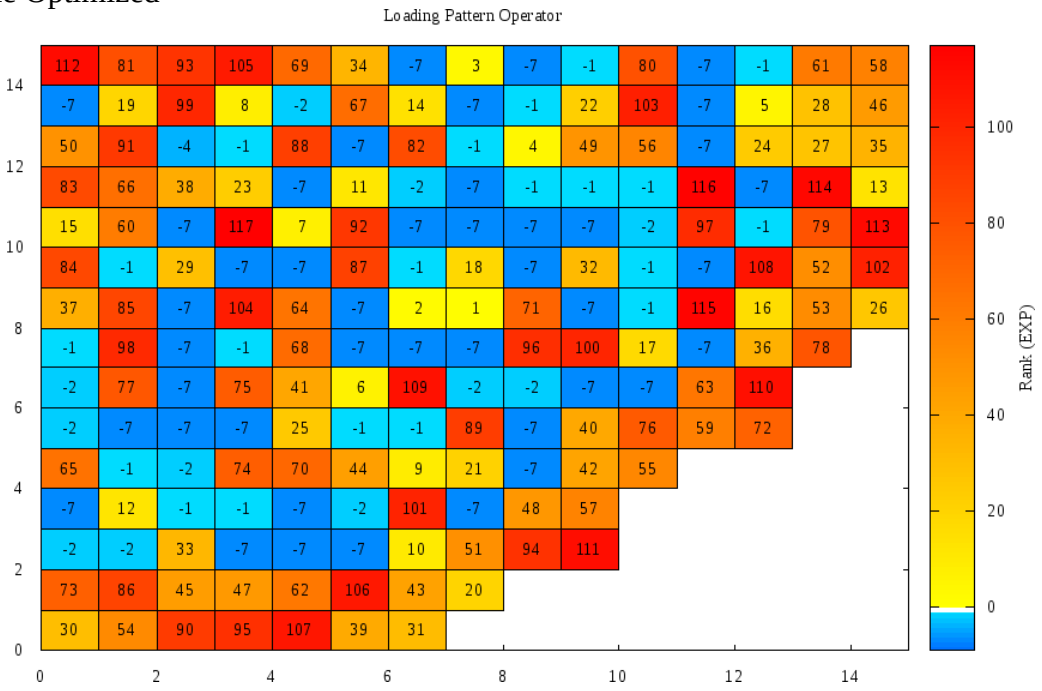

3rd Cycle Optimized

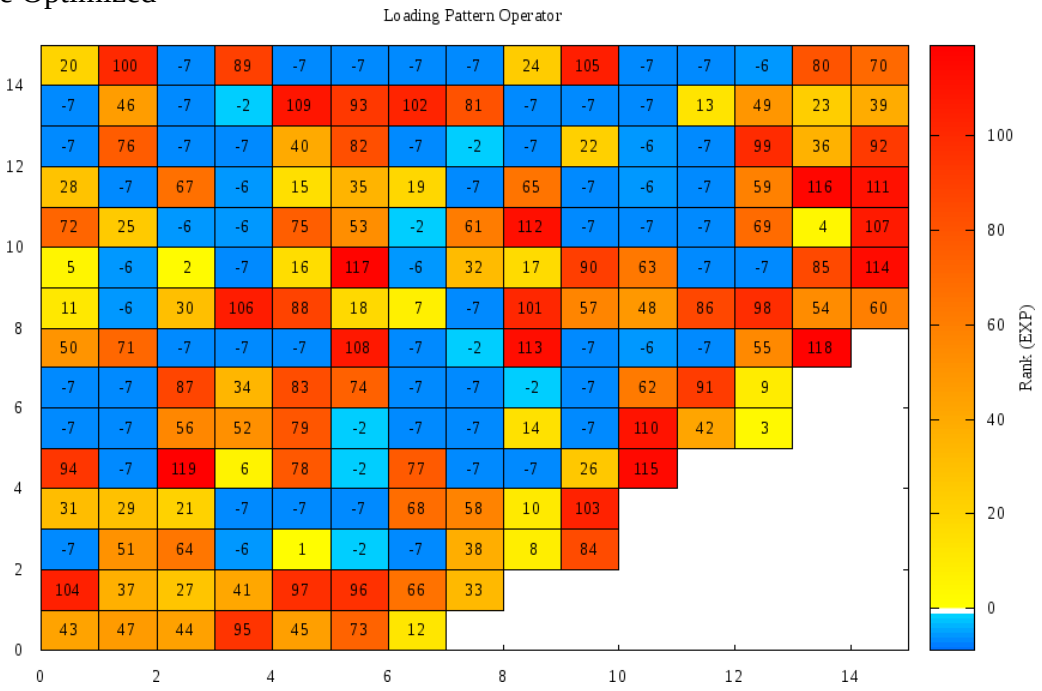

Vita

Keith E. Ottinger was born in Nashville, TN in 1985. He later moved to Lenoir City, TN where he graduated from Lenoir City High School in 2003. He then went to college at the University of Tennessee, Knoxville where he studied Nuclear Engineering and graduated summa cum laude with a Bachelor of Science degree in Nuclear Engineering in May 2007. After receiving his bachelor's degree he attended North Carolina State University, where he earned a Master of Science degree in Nuclear Engineering in May 2009. After graduating from NCSU he worked for Studsvik Scandpower for over a year before returning to the University of Tennessee, Knoxville to pursue a Doctor of Philosophy degree in Nuclear Engineering.